RADIATION FROM Ne II, Ar II, Kr II AND Xe II PRODUCED BY ELECTRON IMPACT

B.F.J. LUIJKEN

RADIATION FROM Ne II, Ar II, Kr II AND Xe II

PRODUCED

BY

ELECTRON IMPACT

S T E L L I N G E N

1. De verklaring, die Walker en St.John geven voor de door hen bij de beschieting van Ne en Ar met electronen gevonden onderlinge verschillen in excitatiefunctie van het $3p^4P_{5/2}$-niveau in Ne II en het $4p^4P_{5/2}$-niveau in Ar II, is onjuist.

   K.G. Walker and R.M. St.John, VII ICPEAC, Amsterdam, North-Holland Publ.Comp., Amsterdam, 720 (1971).

2. In Ar II blijken die configuratie-interacties het sterkst te zijn waarbij twee electronen een verandering van hun baanimpulsmoment ℓ ondergaan en wel zodanig dat voor het ene electron $\Delta\ell = +1$ en voor het andere $\Delta\ell = -1$. Er dient onderzocht te worden of deze regel algemene geldigheid heeft.

   Dit proefschrift, hoofdstuk IV.

3. Het uitgangsvermogen van een watergekoelde molecuullaser kan worden vergroot door de keuze van een kleine wanddiameter, ook al gaat dit ten koste van een minder verliesvrije omsluiting van het mode-volume. De diffractieverliezen worden dan gecompenseerd door de intensievere koeling van het gasmengsel, waardoor de inversie wordt vergroot.

   C. Freed, Appl.Phys.Lett. 18, 458 (1970).
   H.J. Sequin, J. Tulip and B. White, Can.J.Phys. 49, 2731 (1972).

4. De door Martin gebruikte methode om de laagste niveau's van de tweevoudig geïoniseerde spectra van de zeldzame aarden te bepalen kan tot onjuiste voorspellingen leiden.
   W.C. Martin, JOSA, 61, 12, 1682 (1971).

5. De bestaande empirische formules om de energie-afhankelijke botsingsdoorsneden te berekenen zijn in het algemeen niet in staat om gelijktijdig zowel voor energieën, waarvoor de Bethe-benadering wel als niet geldig is, de werkzame doorsneden juist te beschrijven.
   H.W. Drawin, Zeitschr.f.Phys. 164, 513 (1961).
   M.R.H. Rudge and S.B. Schwartz, Proc.Phys.Soc. 88, 563 (1966).

6. Bij gebruik van een omladingsbron om een bundel snelle alkali-atomen te verkrijgen, kan niet zonder meer worden aangenomen dat de kinetische energie van deze atomen correspondeert met de aangelegde versnelspanning. Men dient de energie van de uittredende neutralen te ijken over een groot energiegebied.
   K. Lacmann and D.R. Herschbach, Chem.Phys.Lett. 6, 106 (1970).

7. Het publiceren van numerieke waarden voor vele 3 j-, 6 j- en 9 j-symbolen is niet zinvol.

8. Alvorens te discussiëren over de wenselijkheid de toelatingsleeftijd tot de kleuterschool te verlagen tot 3 jaar dient meer diepgaand onderzoek verricht te worden naar de invloed van de peuterspeelgroep op de sociale, verstandelijke en emotionele ontwikkeling van peuters.
   W. Bruyel en A.F.W. van Meurs, NIK-berichten 7, 44 (1970).

9. Van een evenredige vertegenwoordiging van belanghebbenden bij een goede kwaliteit van het oppervlaktewater in de besturen van waterschappen, waar deze met de uitoefening van de wet op de waterverontreiniging belast zijn, is geen sprake.

10. In verband met de dreigende algehele milieuvervuiling verdient het aanbeveling de omvang van proefschriften tot een minimum te beperken.

B.F.J. Luyken,
24 mei 1972.

RADIATION FROM Ne II, Ar II, Kr II AND Xe II

PRODUCED

BY

ELECTRON IMPACT

PROEFSCHRIFT

TER VERKRIJGING VAN DE GRAAD VAN DOCTOR IN DE WISKUNDE EN NATUURWETENSCHAPPEN AAN DE RIJKS-UNIVERSITEIT TE LEIDEN, OP GEZAG VAN DE RECTOR MAGNIFICUS DR. W.R.O. GOSLINGS, HOOGLERAAR IN DE FACULTEIT DER GENEESKUNDE VOLGENS BESLUIT VAN HET COLLEGE VAN DEKANEN TE VERDEDIGEN OP WOENSDAG 24 MEI 1972 TE KLOKKE 14.15 UUR

DOOR

BOUDEWIJN FREDERIK JOHANNES LUIJKEN

GEBOREN TE HAARLEM IN 1942

PROMOTOR: PROFESSOR DR. J. KISTEMAKER

This work has been done under supervision of

Dr. F.J. de Heer

CO-REFERENT: Dr. P.E. Noorman

Aan: Mirjam
Caroline
Sandra
Jan Willem

CONTENTS

CHAPTER I

GENERAL INTRODUCTION

Among the abundance of experimental and theoretical investigations in the field of atomic collisions in foregoing years, relatively few attention has been paid to the formation of excited ionic states in the case of electron-atom collisions [1-5]. In this work an investigation, experimental as well as theoretical, of the optical spectra resulting from collisions between electrons and the noble gas atoms Ne, Ar, Kr and Xe is described. An important part of the total radiation flux with wavelengths between the far ultraviolet and about 8000 Å in the visible region originates from singly charged excited ions. Assuming the correctness of the shell model in atomic-structure theory, two fundamentally different processes may be distinguished, leading to the formation of an excited ionic state in an electron-atom collision:

$$e + X(ns^2np^6) \rightarrow e + X^{+*}(nsnp^6) + e \qquad (1)$$

and

$$e + X(ns^2np^6) \rightarrow e + X^{+*}(ns^2np^4ml) + e \qquad (2)$$

where X stands for an arbitrary noble-gas atom. In process (1) simply one ns-electron is ejected and an excited ion is left, which in all cases emits radiation in the far ultraviolet when the hole in the ns-subshell is filled up by an electron from the np-shell. In process (2) the excited ion is formed via a two-electron transition; one np electron is ejected and simultaneously another one is excited to a higher orbital. The visible as well as ultraviolet radiation originates from the decay of the ml electron to a lower orbital. A systematic investigation of these two processes seems justified in connection to different fields of physics, such as:

1) astrophysics,
2) the physics of the higher earth atmosphere,
3) laser physics.

The cross section for both processes for incoming electrons of energy

between threshold and 1000 eV is of the order of 10^{-18} cm^2 and the understanding of the relevant mechanisms at the collision process may ultimately give an answer to the question why the cross sections of these two completely different types of excitation nevertheless are of the same order of magnitude.

To get a deeper insight into this problem it is preferable to investigate some intrinsic physical properties of these excited states, such as for instance the coupling of the angular momenta of the electrons involved, or the intermediate coupling composition of the wave functions of the relevant states. From these data one can derive the transition probability for a particular transition or the lifetime of an excited state.

For instance in the case of:

$$e + X(ns^2np^6\ {}^1S_o) \rightarrow e + X^{+*}(nsnp^6\ {}^2S_{1/2}) + e \qquad (1)$$

we have, excluding the possibility of configuration interaction, essentially a one-electron problem in the $^2S_{1/2}$ state, and consequently no coupling problem.

But the other process is more complicated. In an LS coupling notation we have:

$$e + X(ns^2np^6\ {}^1S_o) \rightarrow e + X^{+*}(ns^2np^4\ \overline{L}\overline{S}\ ml\ LSJ) + e \qquad (2)$$

Here in the final state the four np electrons couple their orbital- and spin angular momenta to a core state, designed with the core quantum numbers $\overline{L}$ and $\overline{S}$ and the jumping ml electron couples with this core state to a LSJ state. J is the quantum number specifying the total angular momentum.

Besides the study of the coupling scheme and the intermediate coupling composition of the wave functions, we have also to study the phenomenon of configuration interaction or electron correlation, which could play an important role at two electron transitions, such as in process (2).

In chapter II the experimental procedure is described for the determination of cross sections for process (1) in the case of Ne, Ar, Kr and Xe. In chapters III and IV theoretical calculations have been given of transition probabilities and radiative lifetimes for upper states of Ne II, Ar II, Kr II and Xe II, formed by process (2). In chapter V measurements of branching ratios of these transitions are given, in order to compare experimental data with the theoretical results obtained.

REFERENCES

[1]) Electronic Cross-Sections and Macroscopic Coefficients I - Hydrogen and Rare Gases, by P. Laborie, J.M. Rocard, J.A. Rees, Dunod Paris, 1968.

[2]) Compilation of Low Energy Electron Collision Cross Section Data, Part II, Line and Level Excitation, by L.J. Kieffer, Jila Information Center Report no. 7, University of Colorado, Boulder, Colorado.

[3]) Abstracts of papers of the VIIth ICPEAC, volume II, pages 709 - 727, Eds. L.M. Branscomb et al., Amsterdam, North-Holland Publishing Company, Amsterdam, 1971.

[4]) I.D. Latimer and R.M. St.John, Phys.Rev. A 1 (1970) 1612.

[5]) P.N. Clout and D.W.O. Heddle, J.Phys. B 4 (1971) 483.

CHAPTER II

THE ROLE OF THE OUTER S-SHELL IN SINGLE IONIZATION OF Ne, Ar, Kr AND Xe BY ELECTRON IMPACT

B.F.J. Luyken, F.J. de Heer and R.Ch. Baas

FOM-Instituut voor Atoom- en Molecuulfysica, Amsterdam, Nederland

Synopsis

An optical study is made of the excitation of the $nsnp^6\ ^2S_{\frac{1}{2}}$ ionic level in Ne, Ar, Kr and Xe by electron impact, observing the vacuum ultraviolet radiation, originating from the $nsnp^6\ ^2S_{\frac{1}{2}} \rightarrow ns^2np^5\ ^2P_{\frac{1}{2},3/2}$ transitions. This process has been studied for impact energies between the threshold and 20 keV. Cross sections for the excitation of the $nsnp^6\ ^2S_{1/2}$ level have been determined and are compared with existing theoretical work. The attention has been focused in particular on high impact energies, where the Born and Bethe approximations are valid and where a comparison with photoionization work is possible. The contribution of the $nsnp^6\ ^2S_{1/2}$ excitation to the single ionization has been found to be 12 per cent for Ne, but about 1 per cent for Ar, Kr and Xe. The smallness of this fraction for the latter three cases and the difference with the Ne case is consistent with theoretical calculations of McGuire, and Mansom and Cooper. The role of configuration interaction is considered. It will be demonstrated that the first excited level, designed by $nsnp^6\ ^2S_{1/2}$, cannot be interpreted uniquely as simply a hole in the s-shell. As a consequence the $s^2p^6 \rightarrow sp^6\varepsilon p$ oscillator strength is partly transferred to $s^2p^6 \rightarrow s^2p^4d\ \varepsilon p$ transitions.

1. *Introduction.* Single ionization of noble gas atoms by electron impact occurs chiefly by the removal of an outer-shell electron*; except

* NOTE: We shall omit further on the indication "outer" in outer shell, unless another shell is meant.

for He, we have to consider both a p- and an s-electron. So far many experiments have been done on total ionization cross sections for electron impact (see for instance ref. 1). However, in these experiments no distinction has been made between these two different channels. Electron-energy loss measurements [2] and photoionization experiments [3], including photo-electron spectroscopy [4], indicate that the contribution of the s-shell is small as compared to that of the p-shell.

Several theoretical calculations exist on ionization cross sections, where the contributions of different shells are explicitly taken into account. They may be divided into three classes: binary encounter [5], quantum mechanical (Born approximation) [6,7,8,9] and semi-empirical calculations [10]. The binary encounter treatment is based upon the assumption that the incident particle interacts with only one target particle (electron or nucleus) at a time, disregarding the mutual interaction between the atomic electrons and the nucleus during the collision. The quantum mechanical calculations use a single electron model for the target atom, with an unrelaxed core. The semi-empirical formulae are partly based upon scaling rules, taking the ionization cross section for a subshell proportional to the number of electrons in that shell, and inversely proportional to the corresponding binding energy of the electrons. Unfortunately, the results of all these calculations differ widely from each other and no uniform picture is obtained concerning the relative importance of the s-shell in the ionization process.

Besides, calculations on photoionization (reviewed by Fano and Cooper [11])) point towards a relatively small contribution of the s-shell in the ionization process, just as in the photoionization experiments mentioned before. The purpose of this work is to disentangle the contributions from the s- and p-shell to the single ionization cross section for electron impact by means of an experiment on the ejection of the s-electron. Ejection of such an electron leaves the atom in an excited ionic state with subsequent photon emission to the ionic ground state. The reactions for ejection of s- and p-electrons are:

$$e + X(s^2p^6\ {}^1S_0) \rightarrow e + X^{+*}\ (sp^6\ {}^2S_{1/2}) + \varepsilon\ell \qquad (1a)$$

$$X^{+*}\ (sp^6\ {}^2S_{1/2}) \rightarrow X^{+}(s^2p^5\ {}^2P_{3/2,1/2}) + h\nu \qquad (1b)$$

and

$$e + X(s^2p^6\ {}^1S_0) \rightarrow e + X^{+}(s^2p^5\ {}^2P_{3/2,1/2}) + \varepsilon'\ell'\ , \qquad (2)$$

where X stands for a noble gas atom and $\varepsilon\ell$ and $\varepsilon'\ell'$ are the relevant quantum numbers of the ejected electron (ε stands for the kinetic energy of the ejected electron and ℓ for its orbital angular momentum). In the case of an s-electron ejection, a spectral doublet results because of the fine structure splitting of the ^2P ground state. The corresponding wavelengths for the noble gases of interest are given in table I.

TABLE I

Wavelengths of the $nsnp^6\ ^2S \rightarrow ns^2np^5\ ^2P$ transitions in Ne II, Ar II, Kr II and Xe II

ion	$nsnp^6\ ^2S_{1/2} \rightarrow ns^2np^5\ ^2P_{1/2}$	$nsnp^6\ ^2S_{1/2} \rightarrow ns^2np^5\ ^2P_{3/2}$
	λ(Å)	λ(Å)
Ne	462.39	460.73
Ar	932.05	919.78
Kr	964.96	917.43
Xe	1244.76	1100.43

In our experiment we measure the intensity of the photon emission (1b), which, in the absence of cascade from higher excited levels and configuration interaction, is a direct measure for the s-shell ionization cross section, because other decay processes (as for instance a Coster-Kronig transition), are energetically impossible.

The energy of the incident electrons is varied between threshold and 20 keV. The attention has been focused in particular on incoming electrons of relatively high energies (> 2 keV) for two reasons: firstly to investigate at what impact energy the Born and Bethe approximations become valid and secondly to correlate the results with optical oscillator strengths.

In two abstracts [12,13]) preliminary results of optical experiments of our group were reported on the s-shell ionization of Ne, Ar, Kr and Xe by electron impact. In consultation with our group, some overlapping and complementary work was undertaken by van Raan et al. [14]), partly published in an abstract. We also mention the related experimental work of Lawrence [15]), who measured relative cross sections for Ar between threshold and 1100 eV.

2. *Apparatus.* An extensive description of the apparatus has been given in refs. 16 and 17. In short we shall repeat the main points (see also fig. 1). An electron beam, produced by an electron gun mounted

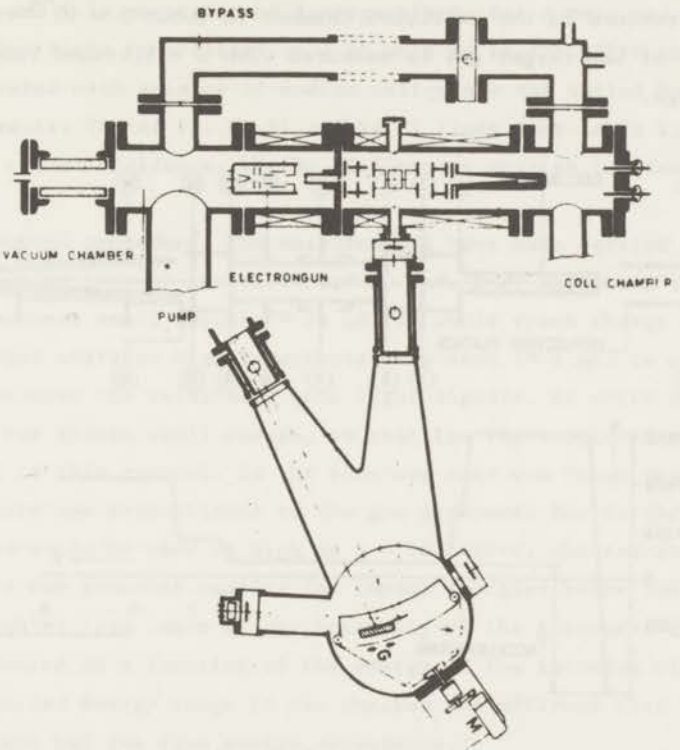

Fig. 1 - Schematical view of the apparatus used for measuring excitation cross sections.

in a vacuum chamber, is accelerated and enters the collision chamber, containing a Faraday cage to measure the electron beam current. The vacuum and collision chamber are separated by a slit body for collimating the beam and maintaining a large gas pressure difference between the two chambers. An axial magnetic field is used for the alignment of the electron beam. Besides, an electrode system is mounted in the collision chamber and a special electric potential distribution (see ref. 16) is applied to suppress disturbing effects, such as those of secondary electrons, in the measurements (see fig. 2). The vacuum chamber is connected with an oil diffusion pump (650 ℓ/s) with a water cooled chevron baffle. A differential pumping system is used; gas is introduced into the collision chamber by means of a needle valve, flows

through the slit body into the vacuum chamber, where it is pumped away. The differential pumping system enables us to maintain a pressure difference of about a factor of 100 between the two chambers. The background pressure in the collision chamber is about 2×10^{-6} torr. The pressure of the target gas is measured with a calibrated Veeco ionization gauge.

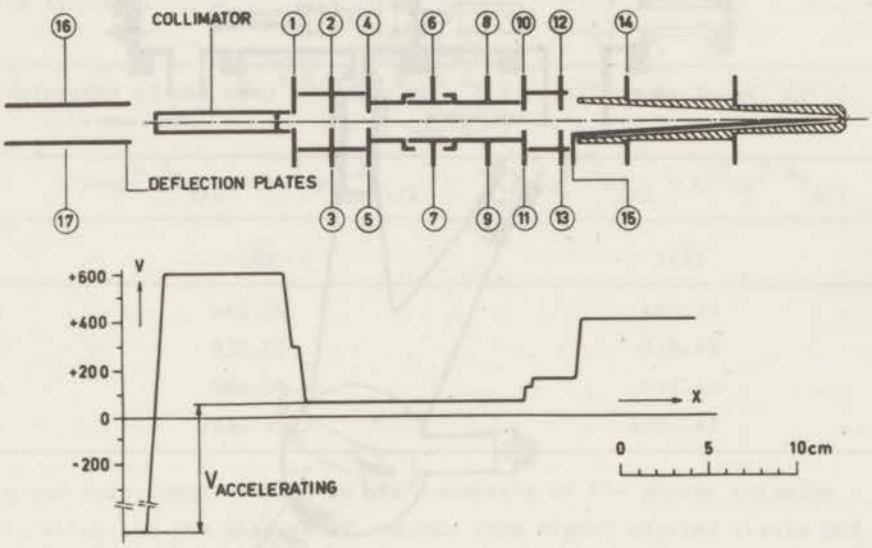

Fig. 2 - Upper part: cross section of the electron system, parallel to the electron beam; the following potentials were applied: collimator: + 200 V; 1 : + 100 V; 2 : + 120 V; 3 : + 40 V; 4, 6 and 8 : 0 V; 5, 7, 9 : 0 V; 10 : + 120 V; 11 : + 40 V; 12 : + 150 V; 13 : + 100 V; 14 : + 400 V; 15 : + 200 V. Lower part: potential distribution along the axis of the electron system.

The light, emitted from the target gas, is observed at 90° to the electron beam axis by means of a vacuum monochromator [17]. This is a 1 meter radius monochromator, which can be used both at normal and grazing incidence and covers the wavelength region of about 200 to 2500 Å. The instrument has a MgF_2 coated grating of Bausch and Lomb (56 × 96 mm and 1200 grooves per mm), movable along a Rowland circle, on which also both the entrance- and exit slit are situated.

The entrance slit serves as a pumping resistance to allow differential pumping with a 650 ℓ/s oil-diffusion pump (with freon baffle) and to avoid the use of a window at the entrance slit. The inverse dispersion is 8.3 Å/mm and f is about 14 and 7 respectively for normal and grazing incidence. The light is detected in a DC mode by an EMI 6256S photomultiplier, covered with a layer of sodium salicylate and cooled by Siemens Peltier elements. The Ar II, Kr II and Xe II lines (see table I) were measured at normal incidence, the Ne II lines at grazing incidence.

3. *Experimental procedure.* The measurements have been carried out for electron energies between threshold and 20 keV. Near threshold the currents used were small enough (≈ 25 μA) to avoid space charge effects, while at larger energies higher currents were used (≈ 1 mA) in order to be able to measure the relatively weak light signals. At every energy the current was chosen small enough, so that the light intensity was proportional to this current. In the same way care was taken that the light intensity was proportional to the gas pressure. For Ne and Ar, gas pressures could be used as high as 5×10^{-3} torr, whereas for Kr and Xe this limit was somewhat smaller for impact energies below 100 eV.

Of each doublet (see table I) the intensity of the strongest component has been measured as a function of the energy of the incoming electrons. Only in a limited energy range it was checked and affirmed that the other component had the same energy dependence.

Between 1 and 20 keV, the energy dependence of the intensity has been determined by means of a continuous energy scanning and below 1 keV a point-wise scanning has been made. In both cases the signal of the photomultiplier is electronically divided by the electron beam current and plotted as a function of energy on an X-Y recorder. During the energy-dependent measurements the gas pressure was measured by means of a calibrated Veeco ionization gauge connected with a digital voltmeter. After having carried out the light intensity measurements for a spectral line, we calculate the corresponding emission cross section in the usual way from the equation:

$$\sigma_{em} = \frac{4\pi}{\omega} \frac{S(\omega)}{(I/e)NLk(\lambda)} \qquad (3)$$

where $S(\omega)$ is the output signal of the monochromator corresponding to an incoming radiation intensity from a solid angle ω, I is the electron

beam current, N is the density of the target gas following from the pressure measurement, L is the observation length along the electron beam, and $k(\lambda)$ is the quantum yield of the monochromator at a wavelength λ, that is the output signal of the monochromator per incoming photon.

Because no simple radiation standard is available in the vacuum ultraviolet region, we were not able to determine the quantum yield of the monochromator below 1000 Å. Therefore we determined only relative emission cross sections in that wavelength region, which follow directly from the quotient S/I, because the other quantities in eq. (3) are constant during an energy dependent scanning of the intensity.

Absolute emission cross sections have been obtained by normalizing our relative values at 300 eV on the absolute cross sections of ref. 14, where the same spectral lines were measured, except the Xe II spectral line at 1245 Å. For Xe II, both at 1100 Å and 1245 Å, we also determined absolute cross sections, using the intensity calibration method of ref. 18 (at 1100 Å these absolute cross sections are 1.34 times larger than those of ref. 14). In order to get a consistent set of cross section data we shall only present (see sec. 4.1) the cross sections normalized on those of ref. 14 at 300 eV. Only in the case of Xe II for 1245 Å we use our own branching ratio $\sigma(1245\ \text{Å})/\sigma(1100\ \text{Å}) = 0.119$. The accuracy of the absolute values is mainly determined by the accuracy of the determination of the quantum yield. The cross sections of ref. 14 have an uncertainty of about 25%, except for Ne where only 50% is claimed. The accuracy in the energy dependence of the relative emission cross section is estimated to be smaller than a few percent.

No corrections need to be made for the polarization of the radiation in eq. (2). Because the upper state of the doublets is a ^2S term, the radiation will be unpolarized and consequently the emission is isotropic. Cascade from higher excited states into the ^2S term is possible. This could be investigated for Ar only. As cascade transitions the spectral lines at 1560 Å and 1575 Å would be the most prominent ones; however, they gave only a few percent contribution to the $^2S_{\frac{1}{2}}$ excitation of Ar II and therefore have been neglected. It is assumed that corresponding cascade transitions in the other noble gases can be neglected too.

4. *Results and discussion.*

4.1. General. In table II we have given our cross sections for the excitation of the $nsnp^6\ ^2S_{\frac{1}{2}}$ level (taken equal to the sum of our $nsnp^6\ ^2S_{\frac{1}{2}} \rightarrow ns^2np^5\ ^2P_{\frac{1}{2},3/2}$ emission cross sections) in Ne II, Ar II, Kr II and Xe II,

TABLE II

Absolute excitation cross sections for the $nsnp^6\ ^2S_{\frac{1}{2}}$ levels in Ne, Ar, Kr and Xe, obtained by adding the $nsnp^6\ ^2S_{\frac{1}{2}} - ns^2np^5\ ^2P_{\frac{1}{2},3/2}$ cross sections. The cross sections are normalized on those of Van Raan et al. [14] at 300 eV. Only for Xe (see text) the normalization was obtained in a slightly different way. Our own absolute data for Xe are not presented; they are 1.34 times higher than those presented here and we found that $\sigma(1245\ \text{Å})/\sigma(1100\ \text{Å}) = 0.119$ (see text).

E	σ in 10^{-18} cm^2			
	Ne	Ar	Kr	Xe
23.39 eV				0.0
27.51			0.0	
29.23		0.0		
30		0.26	2.20	9.02
32		1.25	4.36	10.3
34		2.93	6.33	11.2
36		4.95	8.06	11.8
38		6.71	8.96	11.9
40		8.17	9.37	11.8
42		9.42		
44		10.2		
45			9.64	
46		10.5		
48		10.7		
48.5	0.0			
50	0.20	10.8	9.42	11.4
55		10.5		
60	1.22	10.1	9.06	11.0
70	2.24	9.25	8.87	10.8
80	3.18	8.90	8.73	10.6
90	4.24	8.60	8.46	10.8
100	5.17	8.30	8.14	10.7
120	6.76	7.26	7.60	10.3
140	7.51	6.95	7.10	9.70
160	8.04	6.66	6.65	9.30
180	8.27	6.40	6.23	8.75
200	8.29	6.15	5.82	8.34
300	7.82	4.99	4.65	6.61
400	7.09	4.22	3.83	5.53
500	6.27	3.66	3.29	4.73
600	5.62	3.23	3.04	4.17
700	5.21	2.88	2.59	3.64
800	4.89	2.65	2.37	3.34
900	4.58	2.43	2.16	3.06

TABLE II (continued)

E	σ in 10^{-18} cm^2			
	Ne	Ar	Kr	Xe
1 keV	4.30	2.24	1.99	2.81
1.2	3.81	1.91	1.73	2.41
1.4	3.42	1.68	1.53	2.10
1.6	3.05	1.51	1.39	1.85
1.8	2.77	1.38	1.24	1.70
2.0	2.57	1.29	1.13	1.54
3.0	1.86	0.943	0.790	1.09
4.0	1.49	0.732	0.602	0.83
5.0	1.29	0.608	0.470	0.68
6.0	1.10	0.521	0.413	0.59
8.0	0.855	0.385	0.339	0.47
10.0	0.705	0.323	0.272	0.39
12.0	0.606	0.273	0.230	0.33
14.0	0.518	0.236	0.195	0.280
16.0		0.199	0.173	
18.0		0.182	0.158	
20.0		0.165	0.150	

These results are compared with theory in the next sections: Firstly we compare the experimental results for impact energies between 0.1 and 20 keV with the Born and Bethe approximation. For these relatively high impact energies also a comparison with photoionization calculations is made. Secondly the role of configuration interaction in the excitation process of the $nsnp^6\ ^2S_{1/2}$ level is discussed and thirdly our experimental results are compared at relatively low impact energies, for threshold up till 1 keV, with the binary encounter theory, semi-empirical formulae and the Born approximation.

4.2. Analysis of the results at high impact energies with the Born- and Bethe approximation.

4.2.1. Theory. In the Born approximation the cross section for ionization of an $n\ell$-electron to an $\varepsilon\ell'$ continuum orbital, $(\sigma_{n\ell})$, is presented by the next equation:

$$\sigma(n\ell) = 8\pi R\, E_{el}^{-1} \int_{K_{min}}^{K_{max}} \left| < n\ell^N\ ^1S_0 \| \sum_k e^{i\vec{K}.\vec{r}_k} \| n\ell^{N-1}\ \varepsilon\ell'\ LSJ > \right|^2 K^{-3}\, dK \qquad (4)$$

where $\vec{K}$ is the momentum transfer to an atomic $n\ell$-electron, $\vec{r}_k$ is the position operator of the k's electron, R is the Rydberg energy and $E_{el} = \frac{1}{2} mv^2$, v being the velocity of the incident electron and m the electron rest mass; the sum over k extends over all N electrons of the $n\ell$-subshell; the matrix element contains the ground state and the final state of the atom in the ionization process, where L, S and J are respectively the orbital-, the spin- and the total angular momentum of the final state. A summation over final magnetic sublevels M has already been incorporated in (4).

At sufficiently high impact energies equation (4) can be replaced by the Bethe equation:

$$\sigma(n\ell) = 4\pi a_o^2\, R\, E_{el}^{-1}\, M^2(n\ell)\, \ell n\, c\, E_{el} \qquad (5)$$

where a_o is the first Bohr radius and c a constant. $M^2(n\ell)$ is defined by:

$$M^2(n\ell) = \int_{I(n\ell)}^{\infty} \frac{df}{d\varepsilon}(n\ell \rightarrow \varepsilon\ell')\, \frac{R}{\varepsilon}\, d\varepsilon \qquad (6)$$

where $\frac{df}{d\varepsilon}(n\ell \rightarrow \varepsilon\ell')$ is the differential optical oscillator strength

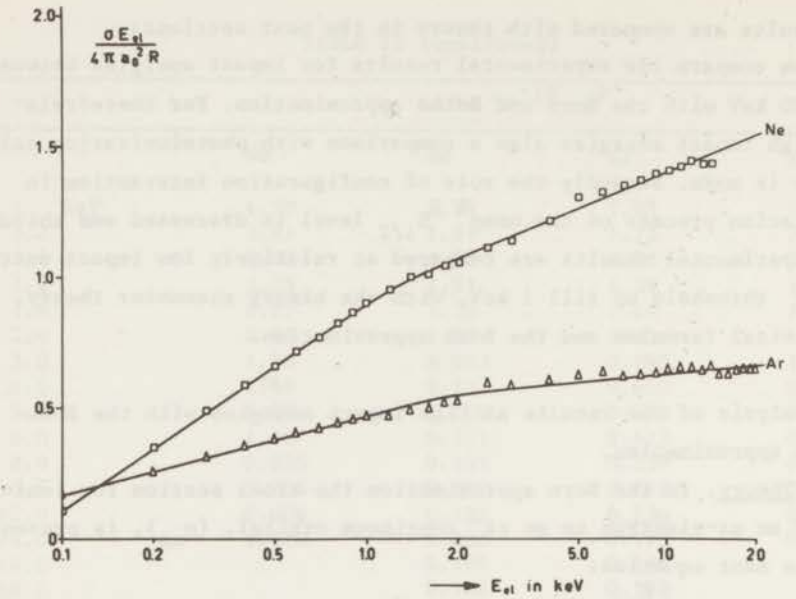

Fig. 3 - Bethe-plots of our measured $ns np^6\ ^2S_{\frac{1}{2}}$ cross section for Ne and Ar.

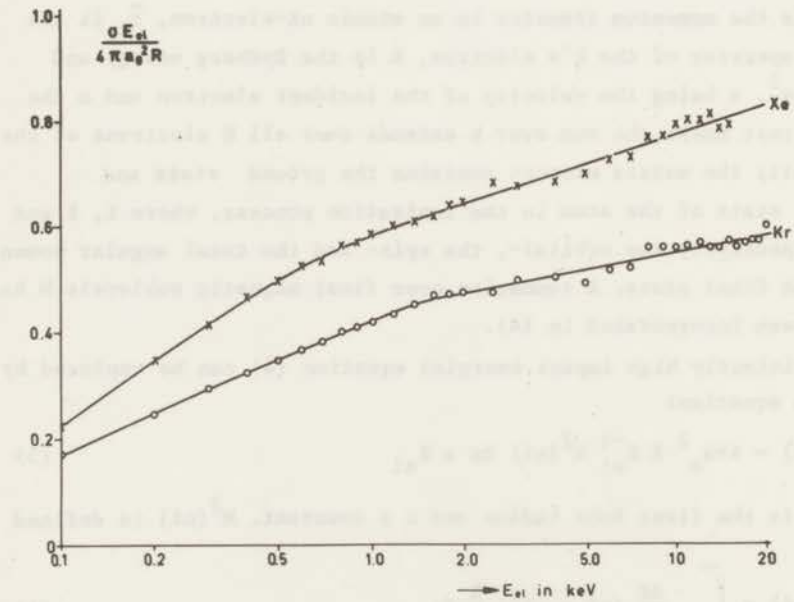

Fig. 4 - Bethe-plots of our measured $ns np^6\ ^2S_{\frac{1}{2}}$ cross section for Kr and Xe.

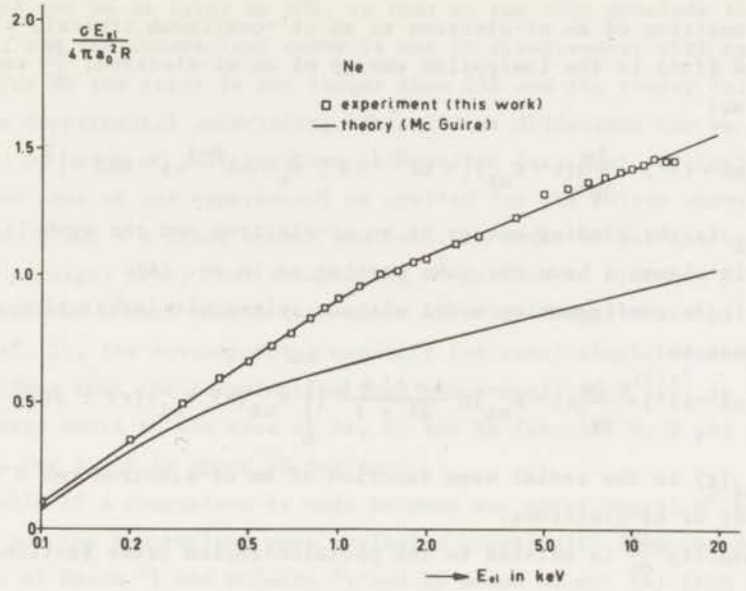

Fig. 5 - Bethe-plot of our measured $2s2p^6\ ^2S_{\frac{1}{2}}$ cross section for Ne (points) compared with the results of the Born approximation of McGuire (solid line).

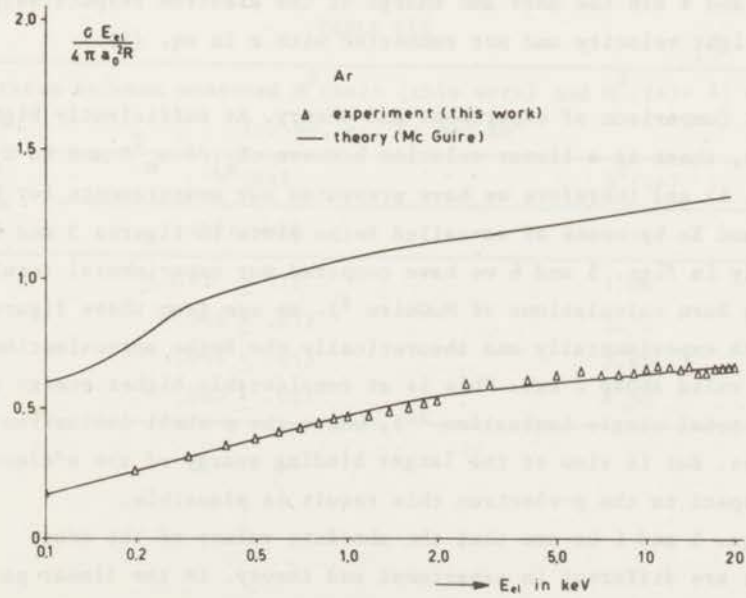

Fig. 6 - Bethe-plot of our measured $3s3p^6\ ^2S_{\frac{1}{2}}$ cross section for Ar (points) compared with the results of the Born approximation of McGuire (solid line).

for a transition of an nℓ-electron to an εℓ'-continuum orbital, ℓ' = ℓ ± 1 and I(nℓ) is the ionization energy of an nℓ-electron; $\frac{df}{d\varepsilon}$ can be defined as:

$$\frac{df}{d\varepsilon}(n\ell \rightarrow \varepsilon\ell') = \frac{2m}{3\hbar^2}(\varepsilon - E_{n\ell}) \left| < n\ell^N \, {}^1S \| \sum_k \vec{r}_k \| n\ell^{N-1} \varepsilon\ell' \; LSJ > \right|^2 \qquad (7)$$

where $E_{n\ell}$ is the binding energy of an nℓ-electron and the symbols in the matrix elements have the same meaning as in eq. (4).

In a single configuration model without spin-orbit interaction eq. (7) reduces to:

$$\frac{df}{d\varepsilon}(n\ell \rightarrow \varepsilon\ell') = \frac{2m}{3\hbar^2}(\varepsilon - E_{n\ell}) N \frac{\ell + \ell' + 1}{2\ell + 1} \left[\int_0^\infty R_{n\ell}(r) \, R_{\varepsilon\ell'}(r) \, r \, dr \right]^2 \qquad (8)$$

where $R_{n\ell}(r)$ is the radial wave function of an nℓ-electron and N is the number of nℓ-electrons.

The quantity $\frac{df}{d\varepsilon}$ is related to the photoionization cross section, σ_{ph}, by:

$$\frac{df}{d\varepsilon} = \frac{mc}{\pi e^2 h} \sigma_{ph} \qquad (9)$$

where m and e are the mass and charge of the electron respectively; c is the light velocity and not connected with c in eq. (5).

4.2.2. Comparison of experiment and theory. At sufficiently high energies, there is a linear relation between $\sigma E_{el}/4\pi a_o^2 R$ and $\ell n \, E_{el}$ (see eq. 5) and therefore we have presented our measurements for Ne, Ar, Kr and Xe by means of so-called Bethe plots in figures 3 and 4. Similarly in figs. 5 and 6 we have compared our experimental results with the Born calculations of McGuire [8]. We see from these figures that both experimentally and theoretically the Bethe approximation (5) becomes valid above 2 keV. This is at considerably higher energy than for the total single ionization [20], where the p-shell ionization dominates. But in view of the larger binding energy of the s-electron with respect to the p-electron this result is plausible.

In figs. 5 and 6 we see that the absolute values of the cross sections are different in experiment and theory. In the linear part above 2 keV, they differ approximately by a constant factor, meaning that in eq. (5) there is a difference in $M^2(n\ell)$, but that ℓn c is almost the same.

For Ne the error in the absolute value of the experimental cross

sections can be as large as 50%, so that we can only conclude that above 2 keV the theoretical curve is not in disagreement with experiment. For Ar the error is not larger than 25% and the theory falls beond the experimental uncertainty. This latter difference can be explained by means of configuration interaction (see next section).

In the case of our experiment, we applied for the points above 2 keV in figs. 3 and 4 a least square analysis, in order to get the best fit with a straight line, thus determining $M^2(ns)$ and $\ell n\ c$ in eq. 5. The thus obtained $M^2(ns)$ values (see table III) are compared with $M^{2(1+)}$ (see ref. 2), the corresponding quantity for total single ionization. It is clear that the contribution from the s-shell to $M^{2(1+)}$ is relatively small in the case of Ar, Kr and Xe (about 1 or 2 per cent), whereas for Ne it is about 12 per cent.

In table IV a comparison is made between our experimental $M^2(ns)$ values and the theoretical ones evaluated graphically from the Born results of Peach [6]) and McGuire [8]) and by means of eq. (6) from the $\frac{df}{d\varepsilon}(ns \rightarrow \varepsilon p)$ values of Manson and Cooper [19]). The integration has been carried out graphically. It is clear from table IV that the results of Peach are in serious disagreement with our measurements*.

TABLE III

Comparison between measured $M^2(ns)$- (this work) and $M^2(1+)$- [2]) values for Ne, Ar, Kr and Xe

atom	$M^2(ns)$	$M^2(1+)$
	this work	from ref. 2
Ne	0.22 ± .11	1.86
Ar	.048 ± .012	3.72
Kr	.048 ± .012	3.95
Xe	.083 ± .021	4.50

* NOTE: The data of McGuire for $M^{2(1+)}(ns+np)$, 1.90 for Ne and 3.40 for Ar, are relatively the closest to the $M^2(1+)$ data of ref. 2 (see table III).

The very large difference between the results of Peach [6], Omidvar [7] and Gaudin and Botter [9] (the latter authors have obtained for Ne practically the same results as Peach) at one side and the results of McGuire [8] and Manson and Cooper [19] on the other side, is due to the use of different final state wave functions. Peach, Omidvar and Gaudin and Botter describe the outgoing electron as moving in a simple hydrogenic potential, generated by an effective charge equal to unity, while McGuire and Manson and Cooper use a Herman-Skillman potential.

TABLE IV

Theoretical $M^2(ns)$ values of Peach, McGuire and Manson and Cooper, compared with our experimental values

atom	$M^2(ns)$			
	Peach [6]	McGuire [8]	Manson and Cooper [18]	experiment (this work)
Ne	0.58	0.14	-	0.22 ± 0.11
Ar	1.04	0.08	0.07	0.048 ± 0.012
Kr	-	-	-	0.048 ± 0.012
Xe	-	-	0.04	0.083 ± 0.021

Fano and Cooper [11] have explained the relatively low $M^2(ns)$ values for Ar, Kr and Xe with the results of Manson and Cooper [19]. Their calculations indicate, that the radial factor in eq. (8) for Ar has a zero point just below the threshold I(3s), and consequently for small ε values the radial factor is small and grows with increasing ε smoothly to a maximum. This effect has a large influence on $M^2(3s)$, because its value is generated for an important part at small ε values, due to the factor $1/\varepsilon$ in (6). For Ne the zero point presumably occurs at lower energy with respect to the threshold for s ionization than for Ar (and for Kr and Xe), just as it occurs at lower energy for Li than for Na [11].

Conclusively in this section it has been demonstrated that our measured $M^2(ns)$ value for Ne is not in disagreement with the theoretical one of McGuire [8]. For Ar we did not obtain agreement with the Born calculation of McGuire and the photoionization calculation of Manson and Cooper [19], but this discrepancy will be explained in the next section

by means of configuration interaction. The discrepancy in Xe between experiment and theory cannot be explained, because not enough is known about configuration interaction in this element.

4.3. The role of configuration interaction. As is known from the Ar II analysis [21] the $3s3p^6\ ^2S_{1/2}$ state is strongly perturbed by the $3s^23p^4(^1D)3d\ ^2S_{\frac{1}{2}}$ state. In chapter IV we demonstrate how in the multi-configuration model the expansion of the wave function of the $3s3p^6\ ^2S_{\frac{1}{2}}$ on a basis of fourteen components has been obtained. We have applied the same procedure to Ne II too. Both for Ne II and Ar II the wave function expansion of the $nsnp^6\ ^2S_{\frac{1}{2}}$ state is given in table V. Comparing these two wave functions it is clear that the mixing in the case of Ne is much smaller than in the case of Ar.

TABLE V

Wave function expansion of the $nsnp^6\ ^2S_{1/2}$ state in Ne II and Ar II

eigenvector component	expansion coefficient	
	Ne II (n=2)	Ar II (n=3)
$ns^2np^4(^3P)nd\ ^4D_{1/2}$	-	+ .00000
$ns^2np^4(^3P)nd\ ^4P_{1/2}$	-	- .00860
$ns^2np^4(^3P)nd\ ^2P_{1/2}$	-	+ .00479
$ns^2np^4(^1D)nd\ ^2P_{1/2}$	-	- .00148
$ns\ np^4(^1D)nd\ ^2S_{1/2}$	-	- .55573
$ns\ np^6\ \ ^2S_{1/2}$	+ .99346	+ .78764
$ns^2np^4(^3P)\ (n+1)d\ ^4D_{1/2}$	+ .00000	+ .00002
$ns^2np^4(^3P)\ (n+1)d\ ^4P_{1/2}$	- .00064	- .00335
$ns^2np^4(^3P)\ (n+1)d\ ^2P_{1/2}$	+ .00045	+ .00181
$ns^2np^4(^1D)\ (n+1)d\ ^2P_{1/2}$	- .00001	- .00056
$ns^2np^4(^1D)\ (n+1)d\ ^2S_{1/2}$	- .11422	- .26416
$ns^2np^4(^3P)\ (n+1)s\ ^4P_{1/2}$	-	- .00107
$ns^2np^4(^3P)\ (n+1)s\ ^2P_{1/2}$	-	+ .00077
$ns^2np^4(^1S)\ (n+1)s\ ^2S_{1/2}$	-	+ .02991

A consequence of this large mixing in Ar II is the relatively long lifetime of this state. In chapter IV we demonstrate that in the single configuration model the theoretical lifetime is a factor of 20 shorter. This mixing of the wave function has also consequences for the oscillator strength of $3s^2 3p^6 \rightarrow 3s3p^6\ \varepsilon p$ transitions. When we substitute the wave function expansion for the residual ionic $3s3p^6\ ^2S_{1/2}$ state of Ar II in eq. (7), it is clear that only one non-zero matrix element results; only the $3s3p^6\ ^2S_{1/2}$ eigenvector component contributes to the oscillator strength and we get:

$$\frac{df}{d\varepsilon}(3s^2 3p^6 \rightarrow 3s3p^6 \varepsilon p) = \frac{2m}{3\hbar^2}(\varepsilon - E_{3s}) \left| .78764 < 3s^2 3p^6\ ^1S_o \| \sum_k \vec{r}_k \| 3s3p^6 (^2S_{\frac{1}{2}}) \varepsilon p\ ^1P_1 > \right|^2 \qquad (10)$$

Compared to the case of a single configuration model, a reduction of about 40% in the oscillator strength for $3s^2 3p^6 \rightarrow 3s3p^6\ \varepsilon p$ transitions is found. Substituting expression (10) into eq. (6), it is clear that the $3s^2 3p^6 \rightarrow 3s3p^6\ \varepsilon p$ transitions contribute only 60% to $M^2(3s)$. The remaining 40% is, as a consequence of the mixing, transferred to $3s^2 3p^6 \rightarrow 3s^2 3p^4 (^1D) nd\varepsilon p$ (n=3, 4, ...) transitions, which latter states all have a $3s3p^6\ ^2S_{1/2}$ eigenvector component in their wave function expansion. In a single configuration treatment (unmixed wave functions) these transitions would be forbidden because they are two electron transitions. Consequently, it now becomes clear that our measured M^2 for $3s^2 3p^6 \rightarrow 3s3p^6 \varepsilon p$ transitions only partly represents the true $M^2(3s)$. We just have the relation:

$$M^2(3s^2 3p^6 \rightarrow 3s3p^6 \varepsilon p) = (.78764)^2\ M^2(3s) = 0.048 \qquad (11)$$

where $M^2(3s^2 3p^6 \rightarrow 3s3p^6 \varepsilon p)$ represents our measured M^2 value.

From (11) it follows that $M^2(3s) = .077$, which value is in very good agreement with the theoretical values of McGuire and of Manson and Cooper (see table IV).

Another consequence of this transfer of oscillator strength is, that we may expect to find also the ionic spectral lines at 543 Å and 547 Å, in our Ar spectrum [22]. These lines correspond to the decay $3s^2 3p^4 (^1D) 3d\ ^2S_{1/2} \rightarrow 3s^2 3p^5\ ^2P_{3/2,1/2}$. They have been found both in our spectrum as well as in that of van Raan et al. [23], but their intensities have not yet been measured accurately. Two difficulties are present: the uncertainty in the quantum yield of the monochromator at

these wavelengths and the overlap with neighbouring lines because of the limited spectral resolution used. An estimation learns that the intensities of the $3s^2 3p^4 (^1D) 3d\ ^2S_{\frac{1}{2}} \rightarrow 3s^2 3p^5\ ^2P_{3/2,\frac{1}{2}}$ lines together is about $\frac{1}{3}$ of that of the intensities of the $3s3p^6\ ^2S_{\frac{1}{2}} \rightarrow 3s^2 3p^5\ ^2P_{3/2,\frac{1}{2}}$ lines together, which is close to a rough theoretical estimation.

A consequence of the strong configuration interaction in Ar II between the $3s3p^6\ ^2S_{\frac{1}{2}}$ state and the $3s^2 3p^4 (^1D) nd\ ^2S_{\frac{1}{2}}$ states is, that the $3s3p^6\ ^2S_{\frac{1}{2}}$ state in fact does not fit in with the physical picture of a hole in the 3s-shell. From the wave function expansion (see table V) it follows, that in Ar II this state also bears properties of the $3s^2 3p^4 (^1D) nd\ ^2S_{\frac{1}{2}}$ states, and consequently the ionization process, we have studied, cannot be identified uniquely as ionization of a 3s-electron, but should be correctly interpreted as "the excitation process", leading to the occupation of the first excited state in Ar II.

The above described configuration interaction and its consequences refer to the residual ion, which is left after the collision and the subsequent ejection of an electron. It is therefore independent of ε, the energy of the ejected electron. We have not studied in this work the additional interaction of the compound state $3s3p^6\ (^2S_{\frac{1}{2}})\varepsilon p\ ^1P_1$ with other atomic or ionic states, which interaction should be ε-dependent. Configuration interaction of this kind has been recognized from the analysis of the $nsnp^6 n'p$ resonances in photoionization [3]. The fact that their profile index q (see ref. 11) in Ar is smaller than unity, shows that as a consequence of inter-channel interaction, spectral repulsion is present just in the vicinity of the 3s threshold, which results in a downward jump in the photo absorption curve at the 3s onset energy. Probably this kind of configuration interaction is of minor importance [11].

For Kr and Xe no numerical data stand to our disposal. It is sure however, that configuration interaction also in these elements plays an important role.

4.4. Cross sections for s-shell ionization from threshold up to 2 keV. In figures 7 and 8 we give our cross section results for Ne, Ar, Kr and Xe as a function of the impact energy. It turns out that the energy behaviour of the Ne 2s shell cross section is similar to that of the total single ionization cross section of noble gases, having

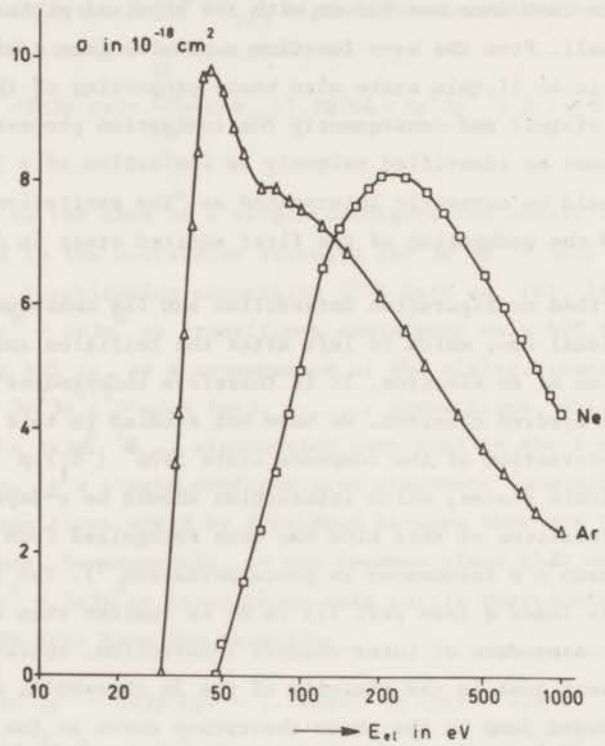

Fig. 7 - Cross sections for the nsnp^6 $^2S_{\frac{1}{2}}$ level in Ne and Ar as a function of the impact energy E_{el}.

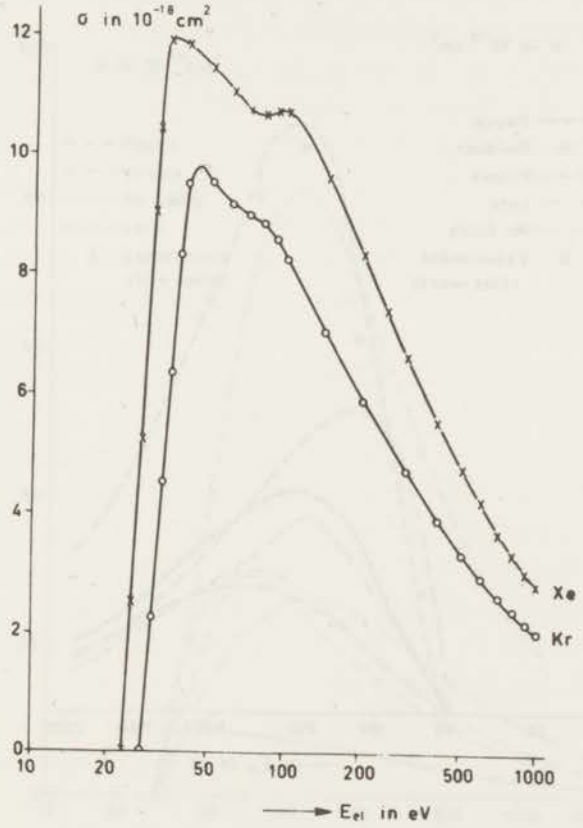

Fig. 8 - Cross sections for the $nsnp^6\ ^2S_{\frac{1}{2}}$ level in Kr and Xe as a function of the impact energy E_{el}.

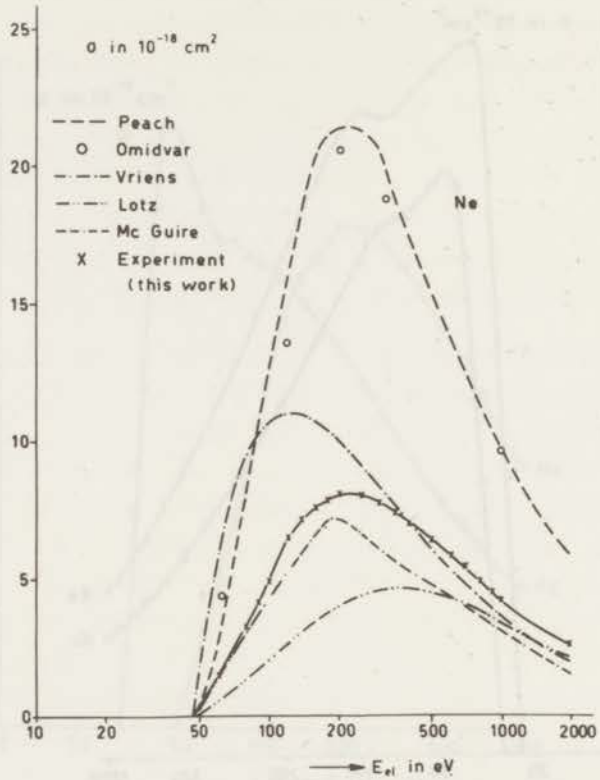

Fig. 9 - Comparison between our measured cross section for the $2s2p^6\ ^2S_{\frac{1}{2}}$ level of Ne II and theoretical results for single ionization of the Born approximations of Peach, Omidvar and McGuire, the binary encounter theory of Vriens and the semi-empirical formula of Lotz.

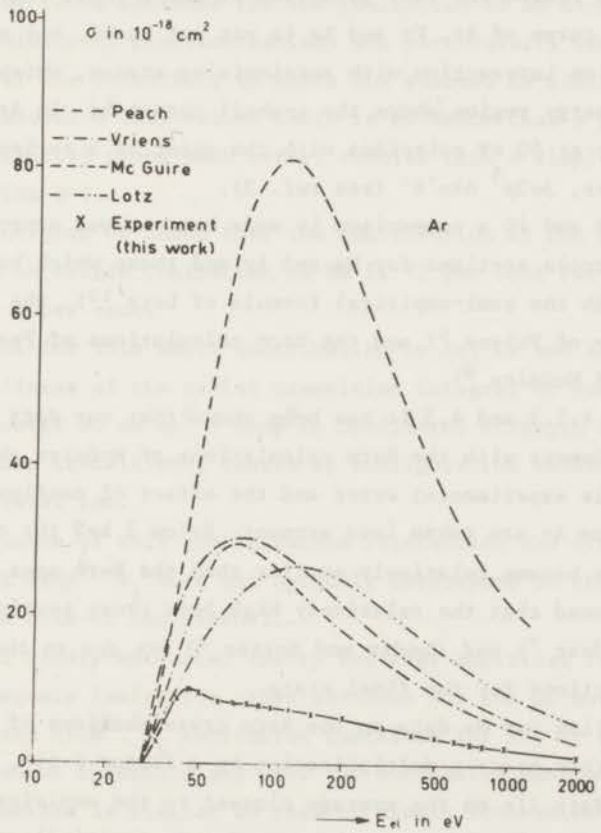

Fig. 10 - Comparison between our measured cross sections for the $3s3p^6\ ^2S_{\frac{1}{2}}$ level of Ar II and theoretical results for single ionization of the Born approximation of Peach and McGuire, the binary encounter theory of Vriens and the semi-empirical formula of Lotz.

one maximum and a not too sharp rise from threshold. For Ar the energy behaviour of the 3s shell cross section is completely different as compared to single ionization. Typical, as also found for Kr and Xe (see fig. 8), is the steep threshold behaviour of the excitation function, reaching a maximum at about 10 to 20 eV above the threshold. Besides, a second maximum is present between 80 and 100 eV in the Ar, Kr and Xe curves. The reason for this behaviour of the s-shell ionization cross section curve of Ar, Kr and Xe is not yet known, but may be due to configuration interaction with autoionizing states, which are present in the energy region above the s-shell threshold. In Ar for instance the dip at 50 eV coincides with the onset of a series of autoionizing states, $3s3p^5\ n\ell n'\ell'$ (see ref. 3).

In figures 9 and 10 a comparison is made between our experimental s-ionization cross sections for Ne and Ar and those which have been calculated with the semi-empirical formula of Lotz [10]), the binary encounter theory of Vriens [5]) and the Born calculations of Peach [6]), Omidvar [7]) and McGuire [8]).

In sections 4.2.2 and 4.3 it has been shown that our data for Ne and Ar are in agreement with the Born calculations of McGuire above 2 keV, if the possible experimental error and the effect of configuration interaction for Ar are taken into account. Below 2 keV the experimental cross sections become relatively smaller than the Born ones. We have already mentioned that the relatively high Born cross sections of Peach [6]), Omidvar [7]) and Gaudin and Botter [9]) are due to the choice of their wavefunctions for the final state.

If we normalize our Ne data on the Born cross sections of McGuire above 2 keV (this means a multiplication by a factor 0.66), then below 2 keV the Ne data lie on the average closest to the empirical curve of Lotz [10]) (see fig. 9). If we do the same for Ar (multiplication factor 1.99), then below 2 keV the cross section remains smaller than all the calculations predict. Though we do not know the effect for configuration interaction in the case of Kr and Xe, the experimental data are relatively small compared to those calculated with the semi-empirical formula of Lotz [10]).

Summary and conclusions. In the case of electrons incident on noble gases, we have measured in how far the first excited ion level, designed as $nsnp^6\ ^2S_{\frac{1}{2}}$, is populated by observing the $nsnp^6\ ^2S_{\frac{1}{2}} \rightarrow ns^2np^5\ ^2P_{\frac{1}{2},3/2}$.

The results and conclusions can be summarized as follows:

The Bethe-, as well as the Born approximation for ionization of an ns-electron are valid for impact energies higher than 2 keV.

Theoretical cross sections for the ionization of an ns-electron (Born approximation, photoionization) are particularly sensitive to the choice of the potential, in which the ejected ns-electron moves. From our measured $M^2(ns)$ values there is evidence that a Herman-Skillman potential gives much better results than a simple hydrogenic potential with Z=1.

At high energies we found that the contribution of the $nsnp^6\ ^2S_{\frac{1}{2}}$ ionic state to single ionization in Ne is 12 per cent but for Ar, Kr and Xe only 1 per cent.

The reasons for this small contribution in Ar, Kr and Xe are:

i) the smallness of the radial transition integral at small ε values;
ii) the transfer of $ns^2np^6 \rightarrow nsnp^6\varepsilon p$ oscillator strength to $ns^2np^6 \rightarrow ns^2np^4md\varepsilon p$ transitions, caused by configuration interaction within the residual ion.

As a consequence of this configuration interaction the first excited ionic states $nsnp^6\ ^2S_{\frac{1}{2}}$ does not uniquely correspond to the physical picture of a hole in the ns-shell.

In general binary-encounter theory and semi-empirical formulae do not give adequate ionization cross sections for the ns-shell.

The measured $nsnp^6\ ^2S_{\frac{1}{2}}$ excitation functions for Ar, Kr and Xe are steep just above threshold and have two successive maxima. The Ne excitation function is similar to that of single ionization.

Acknowledgements. We are grateful to Dr. M.J. van der Wiel and Dr. A. Tip for valuable comments and suggestions.

This work is part of the research program of the Stichting voor Fundamenteel Onderzoek der Materie (Foundation for Fundamental Research on Matter) and was made possible by financial support from the Nederlandse Organisatie voor Zuiver-Wetenschappelijk Onderzoek (Netherlands Organization for the Advancement of Pure Research).

REFERENCES

[1]) L.J. Kieffer and G.H. Dunn, Rev.Mod.Phys. 38, 1 (1966).

[2]) M.J. van der Wiel, Th.M. El-Sherbini and L. Vriens, Physica 42, 411 (1969);
Th.M. El-Sherbini, M.J. van der Wiel and F.J. de Heer, Physica 48, 157 (1970).

[3]) K. Codling, R.P. Madden and D.L. Ederer, Phys.Rev. 155, 1, 26 (1967).
R.P. Madden, D.L. Ederer and K. Codling, Phys.Rev. 177, 1, 136 (1969).

[4]) J.A.R. Samson, Phys.Rev. 173, 80 (1968).

[5]) L. Vriens, Proc.Phys.Soc. 89, 13 (1966).

[6]) G. Peach, J.Phys. B: .Mol.Phys. 3, 328 (1970); and addendum, to be published (1971).

[7]) K. Omidvar and H.L. Kyle, VIIth ICPEAC, Amsterdam, North-Holland Publ.Comp. Amsterdam, 890 (1971).

[8]) McGuire, private communication.

[9]) A. Gaudin and R. Botter, C.R.Acad.Sc.Paris, 265 (1967).

[10]) W. Lotz, Zeitschr. für Phys., 206, 205 (1967).

[11]) U. Fano and J.W. Cooper, Rev.Mod.Phys., 40, 441 (1968).

[12]) B.F.J. Luyken, F.J. de Heer and L. Vriens, VIth ICPEAC, Boston, M.I.T. Press (1969).

[13]) B.F.J. Luyken, R.C. Baas and F.J. de Heer, VIIth ICPEAC, Amsterdam. North-Holland Publ.Comp., Amsterdam, 726 (1971).

[14]) A.F.J. van Raan, J.P. de Jongh and J. van Eck, VIIth ICPEAC, Amsterdam, North-Holland Publ.Comp., Amsterdam, 704 (1971).

[15]) G.M. Lawrence, VIth ICPEAC, Boston, MIT Press, 278 (1969).

[16]) H.R. Moustafa Moussa and F.J. de Heer, Physica 40, 517 (1969).

[17]) H.R. Moustafa Moussa and F.J. de Heer, Physica 36, 646 (1967).

[18]) F.J. de Heer and J.D. Carrière, J.chem.Phys. 55, 3829 (1971).

[19]) S.T. Manson and J.W. Cooper, Phys.Rev. 165, 1 (1968).

[20]) B.L. Schram, Physica 32, 197 (1966).

[21]) L. Minnhagen, Arkiv Fysik, 25, 203 (1963).

[22]) A.R. Striganov and N.S. Sventitskii, Tables of Spectral Lines of Neutral and Ionized Atoms, IFI/PLENUM, New York - Washington (1968).

[23]) A.F.J. van Raan, J.P. de Jongh and J. van Eck, private communication.

CHAPTER III

TRANSITION PROBABILITIES AND RADIATIVE LIFETIMES FOR Ne II

B. F. J. LUYKEN

FOM-Instituut voor Atoom- en Molecuulfysica, Amsterdam, Nederland

Received 9 September 1970

Synopsis

Transition probabilities for $2s^22p^43s$–$2s^22p^43p$ and $2s^22p^43p$–$2s^22p^43d$ transitions in Ne II have been calculated in intermediate coupling. Configuration interactions have been taken into account in contrast to existing calculations, showing a relevant influence on some transition probabilities. A comparison is made with previous calculations and experimental data. Lifetimes of the 3p states are given.

1. *Introduction.* In the field of atomic collisions much attention is paid to the excitation of noble gas atoms, studied by optical measurements. Especially the formation of the singly-charged ion spectra of these atoms is important. A systematic study of the excitation process, requires the knowledge of accurate dipole transition probabilities for spontaneous emission between the various configurations of the ions. Laserphysics and astrophysics are other branches, which have stimulated more accurate line-strength calculations.

Garstang[1]) performed the first intermediate coupling calculations for Ne II and Koopman[2]) compared his measurements with these calculations. On this basis Wiese *et al.*[3]) composed their Data Compilation (1966) for Ne II. More recent contributions[4–6]) show that some of the previously tabulated line strengths are in need of revision.

This paper reports new calculations on transition probabilities for $2p^43s$–$2p^43p$ and $2p^43p$–$2p^43d$ transitions. In contrast to earlier calculations specific configuration interactions are investigated and some effective operators are included.

To describe the various states in the one-configuration model in intermediate coupling, their wavefunctions are expanded on a pure L–S basis:

$$\Psi_E(J, M) = \sum_i \alpha_i \, |p^4 L_i^c S_i^c; l r\tfrac{1}{2}; L_i S_i J M\rangle, \qquad (1)$$

where J is the total angular momentum of the state of energy E, M the corresponding magnetic quantum number, L_i^c and S_i^c the orbital- and spin

angular momentum of the p^4 core electrons, l^r the orbital angular momentum of the running electron and L_i and S_i the total orbital and spin angular momentum of the pure L–S basis states. The set of expansion coefficients α has to be determined for each level. The transition probability for two states of energy E_l and E_u, where E_u is the energy of the upper state, and with the wavefunctions $\Psi_{E_l}(J_l)$ and $\Psi_{E_u}(J_u)$ is:

$$A(J_l, J_u) = \frac{64\pi^4}{3h\lambda^3(2J_u + 1)} S(J_l, J_u), \tag{2}$$

where $S(J_l, J_u)$ can be given in different forms.

We have, for instance, the length formulation:

$$S_r(J_l, J_u) = \langle \Psi_{E_l}(J_l) \| e\mathbf{r}^{(1)} \| \Psi_{E_u}(J_u) \rangle^2 \tag{3}$$

and the velocity formulation:

$$S_v(J_l, J_u) = \frac{\hbar^4}{m^2} (E_u - E_l)^{-2} \langle \Psi_{E_l}(J_l) \| e\nabla^{(1)} \| \Psi_{E_u}(J_u) \rangle^2. \tag{4}$$

When the wavefunctions, used in (3) and (4), are exact eigen functions of the hamiltonian, both formulations are equivalent.

When (3) is developed, and the summation indices i and j refer to the upper and lower state, respectively, we get:

$$\begin{aligned} S(J_l, J_u) = e^2 \Bigg| & \sum_{i,j} \alpha_i \alpha_j^* \delta(S_i, S_j)\, \delta(L_i^c, L_j^c) \\ & \times [(2J_u + 1)(2J_l + 1)(2L_i + 1)(2L_j + 1)(2l_u^r + 1)(2l_l^r + 1)]^{\frac{1}{2}} \\ & \times (-1)^{S_j + J_u + l_u^r + L_j^c} \begin{Bmatrix} S_j & L_j & J_l \\ 1 & J_u & L_i \end{Bmatrix} \begin{Bmatrix} L_j^c & l_l^r & L_j \\ 1 & L_i & l_u^r \end{Bmatrix} \begin{pmatrix} l_u^r & 1 & l_l^r \\ 0 & 0 & 0 \end{pmatrix} \Bigg|^2 \\ & \times \Big[\int_0^\infty R_{l_u r}(r)\, r R_{l_l r}(r)\, \mathrm{d}r \Big]^2, \end{aligned} \tag{5}$$

where J_u, J_l and l_u^r, l_l^r are, respectively, the total angular momenta, and orbital angular momenta of the running electron for the two states of energy E_u and E_l, and $R_{l_u r}(r)$ and $R_{l_l r}(r)$ the radial wavefunctions of the running electron. The transition probability can be calculated when the expansion coefficients and the radial integral are known. In the many-configuration model the wavefunctions are linear combinations of type (1) functions and formula (5) must be changed accordingly.

2. *Calculation of the wavefunctions.* Energy matrices have been constructed in the L–S coupling scheme for the configurations involved. For the electrostatic part, described with the radial integrals $F^{(k)}$ and $G^{(k)}$, use

is made of the tables of ref. 7, and the spin–orbit part is calculated in the following manner:

The matrix elements of the spin–orbit operator,

$$H_{so} = \zeta_{2p\,2p\ \mathrm{core}} \sum \boldsymbol{l}_i \cdot \boldsymbol{s}_i + \zeta^{r} \boldsymbol{l}^{r} \cdot \boldsymbol{s}^{r},$$

are

$$\begin{aligned}
&(L_1 S_1 J M;\, l^r_{1\frac{1}{2}};\, L^c_1 S^c_1 \,|H_{so}|\, L^c_2 S^c_2;\, l^r_{2\frac{1}{2}};\, L_2 S_2 J M) \\
&\quad = 6\zeta_{2p}\delta(l^r_1, l^r_2)(-1)^{J+S_1+S_2+L_1^c+L_2^c+S_1^c+S_2^c+l_1^r+\frac{1}{2}} \\
&\quad \times [(2L_1+1)\,(2L_2+1)\,(2S_1+1)\,(2S_2+1) \\
&\quad \times (2L^c_1+1)(2L^c_2+1)(2S^c_1+1)(2S^c_2+1)]^{\frac{1}{2}} \\
&\quad \times \begin{Bmatrix} L_2 & S_2 & J \\ S_1 & L_1 & 1 \end{Bmatrix} \begin{Bmatrix} L_1 & 1 & L_2 \\ L^c_1 & l^r_1 & L^c_1 \end{Bmatrix} \begin{Bmatrix} S_1 & 1 & S_2 \\ S^c_2 & \frac{1}{2} & S^c_1 \end{Bmatrix} \\
&\quad \times \begin{Bmatrix} L^c_1 & 1 & L^c_2 \\ 1 & 1 & 1 \end{Bmatrix} \begin{Bmatrix} S^c_1 & 1 & S^c_2 \\ \frac{1}{2} & \frac{1}{2} & \frac{1}{2} \end{Bmatrix} \\
&\quad + (\tfrac{3}{2})^{\frac{1}{2}}\, \zeta_{nl^r}\, \delta(L^c_1, L^c_2)\, \delta(S^c_1, S^c_2)\, \delta(l^r_1, l^r_2)(-1)^{J+L_1+L_2+L_1^c+S_1^c+2S_1+l_1^r+\frac{1}{2}} \\
&\quad \times [(2L_1+1)(2L_2+1)(2S_1+1)(2S_2+1)(2l^r_1+1)(l^r_1+1)\, l^r_1]^{\frac{1}{2}} \\
&\quad \times \begin{Bmatrix} J & S_1 & L_1 \\ 1 & L_2 & S_2 \end{Bmatrix} \begin{Bmatrix} l^r_1 & L_1 & L^c_1 \\ L_2 & l^r_1 & 1 \end{Bmatrix} \begin{Bmatrix} \frac{1}{2} & S_1 & S^c_1 \\ S_2 & \frac{1}{2} & 1 \end{Bmatrix},
\end{aligned} \tag{6}$$

where ζ_{2p} and ζ_{nl^r} are the radial spin–orbit integrals of a 2p core electron and of the running electron, respectively, L^c and S^c the orbital and spin angular momentum of the core, L and S the total orbital and spin angular momentum of the state under consideration and l^r the orbital angular momentum of the running electron. The phase convention used in formula (6) is consistent with formula (5).

The matrix elements of the complete energy matrices depend on the above radial integrals, which are treated as adjustable parameters. The method followed for the determination of these parameters is well known and extensively described by others[8,9]. In short the method is as follows: Estimated parameter values give preliminary energy eigenvalues and eigenfunctions. These eigenvalues are compared with the experimental energy values (ref. 10), and by means of a least-squares adjustment better parameter values are calculated. These new values are used to start the procedure again and this iteration will go on until the parameter values eventually become stationary. Final energy eigenvalues and eigenfunctions are then available. The sucess of the level fitting is expressed by a quantity Δ defined by:

$$\Delta = (\sum_i \Delta_i^2/(N-M))^{\frac{1}{2}}, \tag{7}$$

where Δ_i is the difference between calculated and experimental energy eigenvalue for the ith level, N the total number of levels involved in the least-squares procedure and M the number of free parameters. The actual calculations have been performed on the EL X-8 machine of the "Mathematisch Instituut" at Amsterdam.

3. *Results.* 3.1. $2s^22p^43p$ and $2s^22p^5$ configuration. These configurations are treated together because their interaction, although small, cannot be neglected.

The results of the calculation are listed in the tables I and II. To describe the states of these configurations use has been made of the following parameters. E is the average energy of the $2p^43p$ configuration and S that of the $2p^5$ configuration relative to E. $F_2(2p, 2p)$ and $F_2(2p, 3p)$ are direct Slater integrals and $G_0(2p, 3p)$ and $G_2(2p, 3p)$ exchange integrals. Note that subscripted parameters are used, as defined in ref. 11, instead of superscripted ones. The spin–orbit interaction is expressed by ζ_{2p} and ζ_{3p}, defined earlier, and the spin–orbit parameter of the $2p^5$ configuration by ζ'_{2p}.

The direct configuration interaction between the $2p^43p$ and $2p^5$ configurations is described by only one parameter, ϕ, connecting the $2p^4(^3P)\ 3p^2P$ term with the $2p^5\ ^2P$ term. This because the calculations showed that in contrast to ϕ, which takes on a value appreciably different from zero, the other matrix elements, connecting the $2p^4(^1D)\ 3p^2P$ and $2p^4(^1S)3p^2P$ terms with the $2p^5\ ^2P$ term, take on very small values with large uncertainties. Therefore these latter elements were fixed to zero throughout the calculation. This configuration interaction reduces the Δ value somewhat, but the result is still not satisfying. The most natural way to proceed is to build matrices which include more configurations of odd parity, as for instance the sequence $2p^5 + 2p^43p + 2p^44p + 2p^45p + \ldots$. Unfortunately, experimental values for the energy levels with $n > 3$ are not yet available, so it is impossible to explicitly take more configuration interactions into account.

A second possibility, which avoids the construction of gigantic matrices is given by the formalisme of effective operators. These operators, acting within a first-order basis, take into account higher-order effects and relativistic corrections, such as configuration interactions with configurations well separated in energy from the one under consideration[12,13]). For the Ne II case two specific two-particle operators have been examined, resulting, respectively, in the $\alpha L(L + 1)$ and $\beta S(S + 1)$ correction to the diagonal matrix elements. L and S are the orbital and spin angular momentum, α and β are free adjustable parameters. As can be seen from table I, where the obtained parameter and Δ values are listed, the introduction of effective operators by means of the parameters α and β gives a substantial improvement, just as the α correction does for some configurations in Ne I[14]), and the resulting r.m.s. error of 6 cm^{-1} can be considered as an excellent result.

However, this is only the case when the specific $2p^43p$–$2p^5$ interaction is simultaneously taken into account by means of the parameter ϕ. When ϕ is fixed to zero during the calculation and α and β be adjusted freely, the r.m.s. error becomes 167 cm^{-1} and β takes on the value -64 cm^{-1}, a result that has to be rejected.

The theoretical description of the energies of the different core states with the parameter $F_2(2p, 2p)$ seems to break down, because the calculated energies of the $2p^4(^1S)3p\ ^2P_{\frac{1}{2},\frac{3}{2}}$ states are 7000 cm^{-1} too high. This, however, is a general feature for p^2 and p^4 configurations in the first short period[15]). For this reason the levels based on the ^1S core state were systematically excluded from all calculations described in this paper.

In table II calculated and experimental energies and Landé g-values are compared with each other. The composition of each state is given. It appears that break down of LS coupling is not very pronounced for most states of these configurations.

TABLE I

Parameters for the $2p^43p$ and $2p^5$ configuration

Parameter	cm^{-1}			
E	316220 ± 446	316298 ± 404	314897 ± 36	315008 ± 21
S	−316020 ± 210	−315508 ± 200	−314067 ± 21	−314099 ± 8
$F_2(2p, 2p)$	4221 ± 22	4242 ± 20	4167 ± 2	4176 ± 1
$F_2(2p, 3p)$	434 ± 13	430 ± 11	448 ± 1	450 ± 0.4
$G_0(2p, 3p)$	2487 ± 77	2374 ± 81	2606 ± 8	2615 ± 3
$G_2(2p, 3p)$	168 ± 13	155 ± 12	133 ± 1	139 ± 0.8
ζ_{2p}	743 ± 199	724 ± 172	627 ± 14	619 ± 5
ζ_{3p}	−6 ± 174	16 ± 152	36 ± 12	33 ± 5
ζ'_{2p}	522 ± 168	522 ± 142	522 ± 11	522 ± 6
ϕ	–	12175 ± 2518	12714 ± 179	12857 ± 71
α	–	–	87 ± 2	85 ± 0.8
β	–	–	–	23 ± 3
A	237	201	15	6

3.2. $2s^22p^43s$ configuration. The seven levels considered are described with the parameters $F_2(2p, 2p)$ and $G_1(2p, 3s)$, the configuration averaged E and a spin-orbit parameter ζ_{2p}. The results are given in tables III and IV, from which can be concluded that LS coupling is very well obeyed.

3.3. $2s^22p^43d$ configuration. The parameters involved are E, $F_2(2p, 2p)$, $F_2(2p, 3d)$, $G_1(2p, 3d)$, $G_3(2p, 3d)$ and the spin-orbit parameters ζ_{2p} and ζ_{3d}.

The results for this configuration are given in tables V and VI. Because of the strong interaction between the $2s^22p^4(^1D)3d\ ^2S_{\frac{1}{2}}$ and $2s2p^6\ ^2S_{\frac{1}{2}}$ levels (see ref. 10) the former has been excluded from the calculations. Probably due

TABLE II

Eigenvalues, Landé g-values and composition of states in the $2s^22p^43p$ configuration. Values between brackets were excluded from the least-squares adjustment.

Level	E_{theor} (cm^{-1})	E_{exp} (cm^{-1})	g_{theor}	g_{exp}	Percentage composition
$(^1D)^2F_{\frac{7}{2}}$	274413.9	274411.4	1.143	1.14	100% $(^1D)^2F_{\frac{7}{2}}$
$(^3P)^4D_{\frac{7}{2}}$	249109.3	249111.0	1.429	1.43	100% $(^3P)^4D_{\frac{7}{2}}$
$(^1D)^2D_{\frac{5}{2}}$	277341.6	277346.6	1.200	1.20	100% $(^1D)^2D_{\frac{5}{2}}$
$(^1D)^2F_{\frac{5}{2}}$	274375.6	274366.9	0.857	0.86	100% $(^1D)^2F_{\frac{5}{2}}$
$(^3P)^2D_{\frac{5}{2}}$	251012.5	251013.5	1.204	1.20	98% $(^3P)^2D_{\frac{5}{2}}$
$(^3P)^4D_{\frac{5}{2}}$	249443.6	249448.3	1.368	1.37	97% $(^3P)^4D_{\frac{5}{2}}$
$(^3P)^4P_{\frac{5}{2}}$	246194.3	246194.8	1.598	1.60	99% $(^3P)^4P_{\frac{5}{2}}$
$(^1S)^2P_{\frac{3}{2}}$	(312693.7)	305401.0	1.333	1.33	100% $(^1S)^2P_{\frac{3}{2}}$
$(^1D)^2D_{\frac{3}{2}}$	277321.6	277327.9	0.803	0.80	100% $(^1D)^2D_{\frac{3}{2}}$
$(^1D)^2P_{\frac{3}{2}}$	276276.1	276279.1	1.331	1.33	92% $(^1D)^2P_{\frac{3}{2}}$
$(^3P)^2P_{\frac{3}{2}}$	254163.7	254167.4	1.331	1.33	92% $(^3P)^2P_{\frac{3}{2}}$
$(^3P)^4S_{\frac{3}{2}}$	252963.5	252955.9	1.997	—	99% $(^3P)^4S_{\frac{3}{2}}$
$(^3P)^2D_{\frac{3}{2}}$	251521.9	251524.4	0.807	0.80	98% $(^3P)^2D_{\frac{3}{2}}$
$(^3P)^4D_{\frac{3}{2}}$	249695.0	249697.9	1.199	1.20	99% $(^3P)^4D_{\frac{3}{2}}$
$(^3P)^4P_{\frac{3}{2}}$	246421.0	246417.4	1.731	1.73	99% $(^3P)^4P_{\frac{3}{2}}$
$p^5\ ^2P_{\frac{3}{2}}$	0	0	1.333	—	100% $p^5\ ^2P_{\frac{3}{2}}$
$(^1S)^2P_{\frac{1}{2}}$	(312680.0	305410.9	0.667	0.67	100% $(^1S)^2P_{\frac{1}{2}}$
$(^1D)^2P_{\frac{1}{2}}$	276517.2	276514.1	0.667	0.67	92% $(^3P)^2P_{\frac{1}{2}}$
$(^3P)^2P_{\frac{1}{2}}$	254298.1	254294.5	0.742	0.71	87% $(^3P)^2P_{\frac{1}{2}}$
$(^3P)^2S_{\frac{1}{2}}$	252804.5	252800.9	1.925	1.96	94% $(^3P)^2S_{\frac{1}{2}}$
$(^3P)^4D_{\frac{1}{2}}$	249843.6	249842.0	0.004	0.00	100% $(^3P)^4D_{\frac{1}{2}}$
$(^3P)^4P_{\frac{1}{2}}$	246596.8	246600.0	2.662	2.67	100% $(^3P)^4P_{\frac{1}{2}}$
$p^5\ ^2P_{\frac{1}{2}}$	782.0	782.0	0.667	—	100% $p^5\ ^2P_{\frac{1}{2}}$

TABLE III

Parameters for the $2p^43s$ configuration	
Parameter	cm^{-1}
E	287606 ± 10
$F_2(2p, 2p)$	4221 ± 1
$G_1(2p, 3s)$	1613 ± 1
ζ_{2p}	617 ± 4
Δ	5

to interactions with near configurations the influence of far configurations, embodied in the parameters α and β, is not as pronounced as in the $2p^43p$ case. In fact, the spread in the values of α and β leads to the conclusion that these parameters are not relevant here. This is also the case for the parameter ζ_{3d}, which takes on a negative value. Fixing this parameter to zero does not change the final result of the calculation.

TABLE IV

Eigenvalues, Landé g-values and composition of states in the $2s^22p^43s$ configuration. The value between brackets was excluded from the least-squares adjustment.

Level	E_{theor} (cm^{-1})	E_{exp} (cm^{-1})	g_{theor}	g_{exp}	Percentage composition	
$(^1D)^2D_{\frac{3}{2}}$	246397	246396	1.20	1.20	100%	$(^1D)^2D_{\frac{3}{2}}$
$(^3P)^4P_{\frac{5}{2}}$	219135	219133	1.60	1.60	100%	$(^3P)^4P_{\frac{5}{2}}$
$(^1D)^2D_{\frac{5}{2}}$	246398	246400	0.80	0.80	100%	$(^1D)^2D_{\frac{5}{2}}$
$(^3P)^2P_{\frac{3}{2}}$	224089	224089	1.33	1.33	100%	$(^3P)^2P_{\frac{3}{2}}$
$(^3P)^4P_{\frac{3}{2}}$	219643	219650	1.73	1.73	100%	$(^3P)^4P_{\frac{3}{2}}$
$(^3P)^2P_{\frac{1}{2}}$	224701	224701	0.67	0.67	100%	$(^3P)^2P_{\frac{1}{2}}$
$(^3P)^4P_{\frac{1}{2}}$	219954	219949	2.665	2.67	100%	$(^3P)^4P_{\frac{1}{2}}$
$(^1S)^2S_{\frac{1}{2}}$	(284392)	276678	2.00	2.00	100%	$(^1S)^2S_{\frac{1}{2}}$

TABLE V

Parameters for the $2p^43d$ configuration

Parameter	cm^{-1}		
E	344657 ± 65	334540 ± 115	344728 ± 141
$F_2(2p, 2p)$	4256 ± 4	4252 ± 5	4269 ± 10
$F_2(2p, 3d)$	38.7 ± 0.8	38.8 ± 0.8	40.1 ± 0.9
$G_1(2p, 3d)$	78.6 ± 3.7	83.3 ± 5.4	94.8 ± 7.3
$G_3(2p, 3d)$	8.6 ± 1.8	6.1 ± 2.6	9.4 ± 2.9
ζ_{2p}	610 ± 36	615 ± 35	615 ± 32
ζ_{3d}	−4.0 ± 15	−3.1 ± 14	−4.1 ± 13
α	—	5.8 ± 4.8	6.8 ± 4.4
β	—	—	55.7 ± 27
Δ	59	58	53

The r.m.s. error of 53 cm^{-1} is a reasonable result and it seems not to be justified to improve this by considering for instance near configuration interaction. As can be concluded from table VI a marked breakdown of LS coupling occurs for several states. The calculations suggest the interchange of assignment of the $(^3P)^4F_{\frac{7}{2}}$ and $(^3P)^2F_{\frac{7}{2}}$ levels in ref. 10. In spite of this, to avoid confusion the assignments of ref. 10 have been maintained throughout this work.

4. *Calculation of transition probabilities.* By means of the formulae (2) and (5) relative transition probabilities have been calculated by using the angular wavefunctions obtained in the previous sections. To put these relative values on an absolute scale the radial integral in (5) has to be known. Assuming that the influence of configuration interactions on the radial wavefunctions is small, we can use the Coulomb approximation[16]) to calculate the radial integral in (5) for the configurations considered here.

TABLE VI

Eigenvalues and composition of states in the $2s^2 2p^4 3d$ configuration. Value between brackets was included.

Level	E_{theor}	E_{exp}	Percentage composition	
$(^1D)^2G_{\frac{9}{2}}$	305381	305366	100%	$(^1D)^2G_{\frac{9}{2}}$
$(^3P)^4F_{\frac{9}{2}}$	280138	280174	100%	$(^3P)^4F_{\frac{9}{2}}$
$(^1D)^2F_{\frac{7}{2}}$	306679	306689	100%	$(^1D)^2F_{\frac{7}{2}}$
$(^1D)^2G_{\frac{7}{2}}$	305391	305367	100%	$(^1D)^2G_{\frac{7}{2}}$
$(^3P)^2F_{\frac{7}{2}}$	280647	280702	34%	$(^3P)^2F_{\frac{7}{2}}$ + 62% $(^3P)^4F_{\frac{7}{2}}$
$(^3P)^4F_{\frac{7}{2}}$	280228	280264	35%	$(^3P)^4F_{\frac{7}{2}}$ + 65% $(^3P)^2F_{\frac{7}{2}}$
$(^3P)^4D_{\frac{7}{2}}$	279162	279139	96%	$(^3P)^4D_{\frac{7}{2}}$
$(^1S)^2D_{\frac{5}{2}}$	344331	—	100%	$(^1S)^2D_{\frac{5}{2}}$
$(^1D)^2F_{\frac{5}{2}}$	306684	306689	100%	$(^1D)^2F_{\frac{5}{2}}$
$(^1D)^2D_{\frac{5}{2}}$	306311	306245	100%	$(^1D)^2D_{\frac{5}{2}}$
$(^3P)^4P_{\frac{5}{2}}$	281254	281173	81%	$(^3P)^4P_{\frac{5}{2}}$
$(^3P)^2F_{\frac{5}{2}}$	280988	281028	69%	$(^3P)^2F_{\frac{5}{2}}$ + 12% $(^3P)^4P_{\frac{5}{2}}$ + 10% $(^3P)^4F_{\frac{5}{2}}$
$(^3P)^4F_{\frac{5}{2}}$	280780	280800	72%	$(^3P)^4F_{\frac{5}{2}}$ + 23% $(^3P)^2D_{\frac{5}{2}}$
$(^3P)^2D_{\frac{5}{2}}$	280310	280271	59%	$(^3P)^2D_{\frac{5}{2}}$ + 23% $(^3P)^2F_{\frac{5}{2}}$ + 14% $(^3P)^4F_{\frac{5}{2}}$
$(^3P)^4D_{\frac{5}{2}}$	279248	279221	95%	$(^3P)^4D_{\frac{5}{2}}$
$(^1S)^2D_{\frac{3}{2}}$	344309	—	100%	$(^1S)^2D_{\frac{3}{2}}$
$(^1D)^2D_{\frac{3}{2}}$	306336	306265	100%	$(^1D)^2D_{\frac{3}{2}}$
$(^1D)^2P_{\frac{3}{2}}$	305483	305568	100%	$(^1D)^2P_{\frac{3}{2}}$
$(^3P)^2P_{\frac{3}{2}}$	281739	281722	89%	$(^3P)^2P_{\frac{3}{2}}$
$(^3P)^4P_{\frac{3}{2}}$	280981	280992	46%	$(^3P)^4P_{\frac{3}{2}}$ + 32% $(^3P)^4F_{\frac{3}{2}}$ + 20% $(^3P)^2D_{\frac{3}{2}}$
$(^3P)^4F_{\frac{3}{2}}$	280924	280949	52%	$(^3P)^4F_{\frac{3}{2}}$ + 41% $(^3P)^4P_{\frac{3}{2}}$
$(^3P)^2D_{\frac{3}{2}}$	280517	280475	71%	$(^3P)^2D_{\frac{3}{2}}$ + 14% $(^3P)^4F_{\frac{3}{2}}$
$(^3P)^4D_{\frac{3}{2}}$	279352	279326	95%	$(^3P)^4D_{\frac{3}{2}}$
$(^1D)^2P_{\frac{1}{2}}$	305513	305584	100%	$(^1D)^2P_{\frac{1}{2}}$
$(^1D)^2S_{\frac{1}{2}}$	(304853)	306013	100%	$(^1D)^2S_{\frac{1}{2}}$
$(^3D)^2P_{\frac{1}{2}}$	281325	281334	96%	$(^3P)^2P_{\frac{1}{2}}$
$(^3P)^4P_{\frac{1}{2}}$	280736	280770	96%	$(^3P)^4P_{\frac{1}{2}}$
$(^3P)^4D_{\frac{1}{2}}$	279446	279425	97%	$(^3P)^4D_{\frac{1}{2}}$

In table VIIa the results for the quantity $S_r(J_l, J_u)$ are compared with the results of Garstang[1]), Koozekanani[4]) and those following from pure L–S coupling, and with the experimental values of Koopman[2]) and Hodges *et al.*[6]) for 3s–3p transitions. In table VIIb the results for the 3p–3d transitions are given and compared with available experimental values. To avoid confusion, introduced by the change of assignment of some levels in ref. 10, also the wavelengths of the transitions are given. The last column of these tables gives the calculated transition probabilities. Only those transitions, indentified in ref. 10, and having a calculated transition probability of more than 1×10^6 s^{-1} are listed. For simplicity in the notation those states based on a ^{3}P core are unprimed, while those based on a ^{1}D core are primed.

Because the wavefunctions, found in the previous sections, are only approximate eigenfunctions of the hamiltonian, the results are dependent on

TABLE VII-a

$2p^43s$–$2p^43p$ transitions

Transition	Units $e^2a_0^2$							Units s^{-1}
	S_r				S_v	S (experimental)		$A(J_l, J_u)$
	L–S coupling	Garstang	Koozekanani	this work	this work	Hodges	Koopman	this work
$^4P_{\frac{1}{2}}$–$^4D_{\frac{3}{2}}$	26.4	26.5	26.4	26.40	24.77	28.2	27.0	180.11 10^6
$^4P_{\frac{1}{2}}$–$^4D_{\frac{5}{2}}$	5.9	4.45	4.16	4.58	4.20	4.59	5.3	43.07
$^4P_{\frac{3}{2}}$	13.9	15.1	15.3	15.04	14.29	15.3	15.6	134.34
$^4P_{\frac{3}{2}}$–$^4D_{\frac{1}{2}}$	0.66	0.43	0.30	0.40	0.36	0.35	0.83	5.74
$^4P_{\frac{3}{2}}$	7.0	6.45	6.40	6.61	6.18	8.62	7.0	90.77
$^4P_{\frac{3}{2}}$	5.5	6.3	6.35	6.15	5.86	6.19	5.5	81.98
$^4P_{\frac{3}{2}}$–$^4D_{\frac{1}{2}}$	5.5	5.7	5.73	5.67	5.35	5.52	5.6	153.66
$^4P_{\frac{3}{2}}$	1.1	0.93	0.84	0.92	0.85	1.07	1.0	25.69
$^4P_{\frac{5}{2}}$–$^4P_{\frac{3}{2}}$	13.9	15.2	15.6	15.17	17.47	12.67	14.8	101.54
$^4P_{\frac{5}{2}}$	5.9	4.6	4.18	4.63	5.54	6.00	4.0	29.22
$^4P_{\frac{5}{2}}$–$^4P_{\frac{1}{2}}$	5.9	5.5	7.07	6.84	7.75	5.50	7.1	70.41
$^4P_{\frac{5}{2}}$	1.7	2.58	2.03	1.93	2.27	2.43	2.3	18.73
$^4P_{\frac{1}{2}}$	5.5	5.1	4.07	4.43	5.33	5.04	3.7	41.60
$^4P_{\frac{1}{2}}$–$^4P_{\frac{1}{2}}$	5.5	5.65	5.74	5.68	6.60	6.31	5.6	112.58
$^4P_{\frac{1}{2}}$	1.1	0.92	0.85	0.92	1.09	0.94	0.86	17.65
$^4P_{\frac{1}{2}}$–$^4S_{\frac{3}{2}}$	6.6	7.15	5.79	5.95	4.42	5.94	5.25	116.65
$^4P_{\frac{1}{2}}$	4.4	4.05	4.57	4.65	3.53	5.09	4.0	87.02
$^4P_{\frac{1}{2}}$	2.2	1.78	2.64	2.60	2.01	2.90	4.05	47.27
$^2P_{\frac{3}{2}}$–$^2D_{\frac{5}{2}}$	19.8	19.6	19.1	19.61	22.82	20.93	19.5	129.21
$^2P_{\frac{3}{2}}$–$^2D_{\frac{3}{2}}$	2.2	3.14	4.55	3.10	3.47	3.23	2.2	32.45
$^2P_{\frac{3}{2}}$	11.0	10.0	8.48	10.05	11.78	10.61	10.0	98.27
$^2P_{\frac{1}{2}}$–$^2P_{\frac{3}{2}}$	10.0	9.8	7.87	11.69	10.90	11.89	11.0	161.12
$^2P_{\frac{1}{2}}$	2.2	3.08	4.40	3.41	3.31	2.53	2.2	44.17
$^2P_{\frac{1}{2}}$–$^2P_{\frac{1}{2}}$	2.2	3.35	—	1.10	1.02	0.98	1.06	30.81
$^2P_{\frac{3}{2}}$	4.4	3.25	—	6.39	6.16	4.31	5.7	167.80
$^2P_{\frac{3}{2}}$–$^2S_{\frac{1}{2}}$	4.4	3.2	6.13	5.82	5.95	5.69	5.6	139.57
$^2P_{\frac{1}{2}}$	2.2	3.33	0.37	0.83	0.89	1.02	1.09	18.74
$'^2D_{\frac{5}{2}}$–$'^2F_{\frac{7}{2}}$	25.0	25.0	—	25.04	26.91	28.19	22	142.46
$'^2D_{\frac{5}{2}}$–$'^2F_{\frac{5}{2}}$	1.25	1.34	—	1.35	1.46	1.70	1.25	10.20
$'^2D_{\frac{3}{2}}$	17.5	17.4	—	17.43	18.79	17.0	17.5	128.73
$'^2D_{\frac{3}{2}}$–$'^2D_{\frac{5}{2}}$	17.5	17.4	—	17.42	15.34	—	—	177.80
$'^2D_{\frac{3}{2}}$	1.25	1.35	—	1.35	1.19	—	—	13.52
$'^2D_{\frac{3}{2}}$–$'^2D_{\frac{3}{2}}$	1.25	1.50	—	1.75	1.54	—	—	26.69
$'^2D_{\frac{3}{2}}$	11.2	11.0	—	10.77	9.50	—	—	161.28
$'^2D_{\frac{3}{2}}$–$'^2P_{\frac{3}{2}}$	11.2	11.0	—	9.94	9.39	11.27	11.0	137.04
$'^2D_{\frac{3}{2}}$	1.25	1.21	—	1.65	1.56	1.87	1.25	22.34
$'^2D_{\frac{3}{2}}$–$'^2P_{\frac{1}{2}}$	6.3	6.26	—	5.80	5.39	6.55	6.2	160.35
$^2P_{\frac{3}{2}}$–$^4D_{\frac{1}{2}}$	0	0.22	—	0.18	0.24	0.21	—	1.01
$^4P_{\frac{3}{2}}$–$^2D_{\frac{3}{2}}$	0	0.15	—	0.14	0.12	—	—	1.41
$^2P_{\frac{3}{2}}$–$'^2P_{\frac{3}{2}}$	0	—	—	0.96	0.30	—	—	69.30
$^2P_{\frac{3}{2}}$–$'^2P_{\frac{3}{2}}$	0	—	—	0.19	0.06	—	—	13.39
$^2P_{\frac{3}{2}}$–$'^2P_{\frac{3}{2}}$	0	—	—	0.19	0.06	—	—	27.63
$^2P_{\frac{1}{2}}$–$'^2P_{\frac{1}{2}}$	0	—	—	0.40	0.13	—	—	56.83

TABLE VII-b

2p43p–2p43d transitions

Transition	λ (Å)	Units $e^2a_0^2$					Units s^{-1}
		S_r		S_v	S (experimental)		$A(J_l, J_u)$
		L–S coupling	this work	this work	Hodges	Koopman	this work
$^4D_{\frac{7}{2}}$–$^4F_{\frac{9}{2}}$	3218	59.4	59.40	55.74	60.9	62.5	360.73 × 10^6
$^4D_{\frac{7}{2}}$–$^2F_{\frac{7}{2}}$	3164	0	1.99	1.80	—	—	15.88
$^2D_{\frac{3}{2}}$	3367	47.5	22.64	23.26	29.15	20.5	150.05
$^4D_{\frac{3}{2}}$	3199	0	22.38	20.75	15.65	—	173.06
$^4P_{\frac{3}{2}}$	2897	0	0.50	0.38	—	—	5.20
$^4D_{\frac{7}{2}}$–$^4F_{\frac{7}{2}}$	3209	6.8	2.10	1.96	2.71	—	16.11
$^2D_{\frac{3}{2}}$	3418	0	24.62	26.05	—	—	156.01
$^4D_{\frac{3}{2}}$	3244	40.7	20.79	19.82	12.95	24.8	154.06
$^4D_{\frac{7}{2}}$–$^4D_{\frac{7}{2}}$	3329	10.3	12.88	12.93	14.8	12.2	88.31
$^4D_{\frac{3}{2}}$	3367	1.70	0.42	0.43	—	—	2.81
$^4P_{\frac{5}{2}}$	3034	35.6	34.01	28.38	30.1	—	308.00
$^4D_{\frac{7}{2}}$–$^4P_{\frac{5}{2}}$	3118	0.79	0.37	0.33	—	—	4.17
$^2D_{\frac{5}{2}}$	3315	0	0.47	0.47	—	—	4.36
$^4D_{\frac{5}{2}}$	3151	0.18	0.45	0.40	—	—	4.83
$^4P_{\frac{5}{2}}$	2858	10.4	5.49	4.07	2.90	—	79.40
$^2P_{\frac{3}{2}}$	3702	0	4.10	5.09	—	—	27.27
$^4S_{\frac{3}{2}}$	3543	19.8	16.27	18.51	18.9	—	123.48
$^2D_{\frac{3}{2}}$	3372	0	2.48	2.56	4.53	—	21.84
$^4D_{\frac{3}{2}}$	3176	0.02	0.57	0.52	1.02	—	6.00
$^4P_{\frac{3}{2}}$	2876	4.5	5.48	4.11	2.59	—	77.69
$^2D_{\frac{5}{2}}$–$^2F_{\frac{5}{2}}$	3330	2.38	0.43	0.43	—	—	3.94
$^4D_{\frac{5}{2}}$	3166	0	1.12	1.02	—	—	11.91
$^4P_{\frac{5}{2}}$	2870	0	1.21	0.90	—	—	17.32
$^2P_{\frac{3}{2}}$	3722	0	3.01	3.78	—	—	19.70
$^4S_{\frac{3}{2}}$	3561	0	2.83	3.25	—	4.4	21.10
$^2D_{\frac{3}{2}}$	3388	33.2	25.10	26.11	16.1	19.7	217.68
$^4D_{\frac{3}{2}}$	3191	0	1.46	1.35	8.94	—	15.21
$^4P_{\frac{3}{2}}$	2888	0	0.50	0.38	—	—	6.95
$^4D_{\frac{7}{2}}$–$^4F_{\frac{5}{2}}$	3155	0.34	0.17	0.15	—	—	1.83
$^2D_{\frac{5}{2}}$	3356	0	2.21	2.26	—	—	19.74
$^4D_{\frac{5}{2}}$	3189	8.69	3.75	3.46	—	—	39.07
$^2P_{\frac{3}{2}}$	3754	0	7.05	9.00	9.50	3.5	44.97
$^4S_{\frac{3}{2}}$	3590	0	0.50	0.58	—	—	3.63
$^2D_{\frac{3}{2}}$	3415	0	0.21	0.22	—	—	1.80
$^4D_{\frac{3}{2}}$	3214	26.6	21.56	20.18	5.33	—	219.01
$^2D_{\frac{5}{2}}$–$^2D_{\frac{5}{2}}$	3417	8.3	7.55	7.99	—	—	63.84
$^4D_{\frac{5}{2}}$	3243	0	2.31	2.21	—	—	22.92
$^4P_{\frac{5}{2}}$	2934	0	0.52	0.40	—	—	6.89
$^2P_{\frac{3}{2}}$	3830	26.7	14.00	18.61	17.2	8.4	84.10
$^4S_{\frac{3}{2}}$	3660	0	0.97	1.18	—	—	6.68
$^2D_{\frac{3}{2}}$	3478	0.59	5.34	5.85	4.14	2.5	42.84
$^4D_{\frac{3}{2}}$	3270	0	5.32	5.15	2.53	—	51.32

TABLE VII-b (*continued*)

2p⁴3p–2p⁴3d transitions

Transition	λ (Å)	Units $e^2a_0^2$					Units s^{-1}
		S_r		S_v	S (experimental)		$A(J_l, J_u)$
		L–S coupling	this work	this work	Hodges	Koopman	this work
$^4D_{\frac{7}{2}}$–$^4D_{\frac{9}{2}}$	3320	1.70	2.26	2.26	—	—	20.83×10^6
$^4D_{\frac{5}{2}}$	3358	5.13	5.60	5.72	4.91	3.8	49.92
$^4P_{\frac{5}{2}}$	3027	8.02	11.90	9.88	12.89	—	144.69
$^4D_{\frac{3}{2}}$	3386	2.08	0.63	0.65	—	—	5.50
$^4P_{\frac{3}{2}}$	3048	18.71	14.95	12.58	15.8	—	178.22
$^2D_{\frac{5}{2}}$–$^2P_{\frac{3}{2}}$	3255	0.59	0.26	0.25	—	—	3.82
$^2P_{\frac{3}{2}}$	3628	8.25	5.61	6.70	—	2.4	59.50
$^4S_{\frac{3}{2}}$	3475	0	0.10	0.11	—	—	1.24
$^2D_{\frac{3}{2}}$	3311	0.07	0.50	0.49	—	—	6.92
$^2P_{\frac{1}{2}}$	3645	1.65	9.50	11.44	—	—	99.31
$^2S_{\frac{1}{2}}$	3457	13.20	7.85	8.50	—	8.1	96.20
$^2P_{\frac{3}{2}}$–$^4P_{\frac{3}{2}}$	3727	0	1.18	1.49	—	—	11.58
$^4S_{\frac{3}{2}}$	3566	13.20	5.59	6.44	2.82	—	62.41
$^2D_{\frac{3}{2}}$	3393	0	1.64	1.71	—	—	21.34
$^4D_{\frac{1}{2}}$	3195	0.21	3.32	3.07	1.89	—	51.59
$^4P_{\frac{1}{2}}$	2892	1.32	0.29	0.22	—	—	6.08
$^4P_{\frac{5}{2}}$–$^4P_{\frac{3}{2}}$	2873	4.46	1.76	1.32	1.61	—	37.57
$^2P_{\frac{1}{2}}$	3745	0	2.66	3.38	—	—	25.61
$^2S_{\frac{1}{2}}$	3546	0	0.56	0.64	—	—	6.33
$^4D_{\frac{1}{2}}$	3209	0.03	3.94	3.68	2.53	—	60.32
$^4P_{\frac{1}{2}}$	2907	4.13	2.67	2.05	—	—	55.13
$^4D_{\frac{5}{2}}$–$^4F_{\frac{5}{2}}$	3174	0.48	0.28	0.26	—	—	4.50
$^4P_{\frac{5}{2}}$	2876	0	1.55	1.17	—	—	33.02
$^4S_{\frac{3}{2}}$	3571	0	5.63	6.51	3.75	—	62.58
$^4D_{\frac{3}{2}}$	3199	6.65	1.48	1.37	1.36	—	22.83
$^2S_{\frac{1}{2}}$	3552	0	0.33	0.38	—	—	3.72
$^4D_{\frac{1}{2}}$	3214	16.63	11.08	10.36	—	—	168.86
$^4P_{\frac{1}{2}}$	2910	0	2.89	2.22	—	—	59.38
$^2D_{\frac{3}{2}}$–$^2D_{\frac{5}{2}}$	3393	0.59	0.66	0.69	—	—	8.61
$^4P_{\frac{3}{2}}$	2916	0	0.47	0.36	—	—	9.61
$^2P_{\frac{3}{2}}$	3800	2.97	3.99	5.21	3.71	—	36.77
$^4S_{\frac{3}{2}}$	3633	0	1.23	1.47	—	—	12.99
$^2D_{\frac{5}{2}}$	3453	5.35	3.75	4.05	—	2.9	46.10
$^4D_{\frac{3}{2}}$	3248	0	1.60	1.53	—	—	23.61
$^2P_{\frac{1}{2}}$	3818	14.85	6.76	8.93	7.53	3.9	61.46
$^2S_{\frac{1}{2}}$	3612	0	2.44	2.89	—	—	26.22
$^4D_{\frac{1}{2}}$	3263	0	2.70	2.60	—	—	39.29
$^4P_{\frac{5}{2}}$–$^4D_{\frac{7}{2}}$	3017	0.89	1.92	1.59	3.47	—	35.43
$^4D_{\frac{5}{2}}$	3374	2.38	2.30	2.38	1.34	—	30.37
$^4P_{\frac{3}{2}}$	3038	9.50	11.13	9.31	8.87	—	210.00
$^4D_{\frac{1}{2}}$	3391	1.49	0.59	0.61	—	—	7.65
$^4P_{\frac{1}{2}}$	3055	7.43	5.28	4.46	4.53	—	93.73

TABLE VII-b (*continued*)

2p⁴3p–2p⁴3d transitions

Transition	λ (Å)	Units $e^2a_0^2$					Units s^{-1}
		S_r		S_v	S (experimental)		$A(J_l, J_u)$
		L–S coupling	this work	this work	Hodges	Koopman	this work
$^2P_{\frac{3}{2}}$–$^2P_{\frac{1}{2}}$	3680	1.65	1.56	1.92	—	—	31.77×10^6
$^4S_{\frac{3}{2}}$	3523	0	0.10	0.11	—	—	2.29
$^2D_{\frac{3}{2}}$	3354	0.33	0.45	0.45	—	—	11.97
$^2P_{\frac{1}{2}}$	3697	3.30	1.40	1.73	—	—	28.00
$^2S_{\frac{1}{2}}$–$^2P_{\frac{1}{2}}$	3504	6.60	8.34	9.28	8.44	—	196.36
$^4P_{\frac{1}{2}}$	2878	0	0.16	0.12	—	—	6.87
$^4S_{\frac{3}{2}}$–$^4P_{\frac{3}{2}}$	3594	6.60	5.91	6.92	—	6.0	128.85
$^4P_{\frac{3}{2}}$	2910	4.13	4.09	3.14	—	—	167.93
$^4P_{\frac{5}{2}}$	2926	0.83	1.39	1.08	1.38	—	56.09
$^4D_{\frac{7}{2}}$–$^4D_{\frac{5}{2}}$	3363	1.49	1.33	1.36	—	—	35.43
$^4P_{\frac{3}{2}}$	3029	1.49	2.33	1.93	1.69	—	84.71
$^4D_{\frac{5}{2}}$	3379	1.49	1.13	1.17	—	—	29.71
$^4P_{\frac{5}{2}}$	3046	7.43	6.97	5.86	9.15	—	249.67
$'^2F_{\frac{7}{2}}$–$'^2G_{\frac{9}{2}}$	3230	59.40	59.39	56.13	60.77	—	356.95
$'^2F_{\frac{7}{2}}$–$'^2G_{\frac{7}{2}}$	3229	1.70	1.69	1.59	—	—	12.67
$'^2F_{\frac{5}{2}}$	3225	45.83	45.83	43.18	46.98	—	345.76
$'^2F_{\frac{7}{2}}$–$'^2F_{\frac{7}{2}}$	3097	15.27	15.28	13.27	—	—	130.27
$'^2D_{\frac{5}{2}}$	3407	31.68	31.75	33.37	—	—	231.45
$'^2F_{\frac{5}{2}}$–$'^2F_{\frac{5}{2}}$	3092	11.31	11.32	9.80	—	—	129.31
$'^2D_{\frac{3}{2}}$	3388	22.18	21.78	22.64	—	—	189.11
$'^2F_{\frac{7}{2}}$–$'^2D_{\frac{5}{2}}$	3140	2.26	2.19	1.96	—	—	23.88
$'^2D_{\frac{5}{2}}$	3459	19.40	19.03	20.60	—	—	155.27
$'^2D_{\frac{3}{2}}$	3457	1.39	1.21	1.31	—	—	9.89
$'^2P_{\frac{3}{2}}$	3336	12.47	12.34	12.44	—	—	112.23
$'^2F_{\frac{5}{2}}$–$'^2D_{\frac{5}{2}}$	3134	1.58	1.61	1.44	—	—	26.47
$'^2D_{\frac{3}{2}}$	3454	12.47	12.88	13.94	—	—	157.71
$'^2P_{\frac{1}{2}}$	3360	6.93	6.49	6.65	—	—	86.37
$'^2D_{\frac{3}{2}}$–$'^2P_{\frac{3}{2}}$	3542	5.35	5.29	6.02	—	—	60.25
$'^2D_{\frac{3}{2}}$	3540	0.59	0.31	0.36	—	—	3.59
$'^2P_{\frac{3}{2}}$	3413	14.85	14.17	14.95	17.36	—	180.36
$'^2P_{\frac{1}{2}}$	3441	5.94	2.85	3.06	2.36	—	35.44
$'^2D_{\frac{1}{2}}$–$'^2P_{\frac{1}{2}}$	3538	2.97	3.32	3.76	4.96	—	75.94
$'^2P_{\frac{3}{2}}$	3411	2.97	2.39	2.52	1.84	—	61.00
$'^2P_{\frac{1}{2}}$	3439	5.94	5.60	6.00	4.48	—	139.48

the form chosen for S. Neglecting configuration interaction the wavefunctions are only eigenstates of the zeroth-order hamiltonian and thus to first order

$$S_\nu = (\nu_0/\nu)^2 \, S_r,$$

where ν is the frequency of the transition and ν_0 is related with the energy distance of the two configurations between which the transition takes place. The difference between the values for S_ν and S_r thus obtained gives an idea about the importance of higher-order effects and consequently about the accuracy obtained to first order. For comparison values for S_ν are also included in the tables. In table VIII the calculated lifetimes for the $2p^4 3p$ states are given.

TABLE VIII

Calculated lifetimes of the 3p-states, compared with some experimental results

Level		Lifetime (ns)	
		this work	Hesser (ref. 17)
$2s^2 2p^4 3p$	$^4D_{\frac{7}{2}}$	5.55	
	$^4D_{\frac{5}{2}}$	5.60	
	$^4D_{\frac{3}{2}}$	5.59	
	$^4D_{\frac{1}{2}}$	5.58	
	$^4P_{\frac{5}{2}}$	7.65	10.0 ± 1.0
	$^4P_{\frac{3}{2}}$	7.65	10.1 ± 1.0
	$^4P_{\frac{1}{2}}$	7.68	
	$^4S_{\frac{3}{2}}$	3.98	
	$^2D_{\frac{5}{2}}$	7.62	
	$^2D_{\frac{3}{2}}$	7.60	8.4 ± 0.8
	$^2P_{\frac{3}{2}}$	4.86	5.0 ± 0.5
	$^2P_{\frac{1}{2}}$	5.03	
	$^2S_{\frac{1}{2}}$	6.31	4.8 ± 0.5
	$'^2F_{\frac{7}{2}}$	7.02	$8.8 \pm 0.?$
	$'^2F_{\frac{5}{2}}$	7.20	
	$'^2D_{\frac{5}{2}}$	5.21	5.5 ± 0.6
	$'^2D_{\frac{3}{2}}$	5.29	
	$'^2P_{\frac{3}{2}}$	4.20	3.8 ± 0.4
	$'^2P_{\frac{1}{2}}$	4.16	

5. *Influence of configuration interactions on transition probabilities.* In the previous sections it has been clearly demonstrated that introducing configuration interactions may substantially improve the r.m.s. error in energy-level calculations. To what extent calculated transition probabilities may be influenced by configuration interactions is shown in table IX, where some transitions, particularly sensitive to small changes in the wavefunctions,

TABLE IX

Influence of configuration interactions on some transition probabilities

Transition	$S_r(J_l, J_u)$ in units $e^2a_0^2$				
		Conf. int. by means of the parameters			
$2p^43s$–$2p^43p$	without conf. int.	ϕ	ϕ α	ϕ α β	experiment ref. 6
$^2P_{\frac{1}{2}}$–$^2P_{\frac{1}{2}}$	8.87	11.50	11.65	11.69	11.89
$^2P_{\frac{3}{2}}$–$^2P_{\frac{1}{2}}$	0.25	0.82	1.06	1.10	0.98
$^4P_{\frac{1}{2}}$–$^4D_{\frac{1}{2}}$	4.42	4.23	4.55	4.58	4.59
$^2P_{\frac{1}{2}}$–$^2S_{\frac{1}{2}}$	6.21	6.11	5.86	5.82	5.69
$^2P_{\frac{3}{2}}$–$^2S_{\frac{1}{2}}$	0.33	0.57	0.79	0.83	1.02

have been selected. Values for $S_r(J_l, J_u)$ in different stages of configuration interaction are compared whith experimental data.

6. *Discussion.* Garstang[1]) obtained his results by making extensively use of perturbation theory, but, within the limitations set by his basic assumptions, his approximate numerical methods give reliable values. Only his results for 3s–3p transitions which $J_u = \frac{1}{2}$ deviate so strongly from those of other work that it seems reasonable to assume that an error of phase has been made[18]). Koozekanani and Trusty[5]) calculated their wavefunctions with the same method as used in this work, but some of their basic assumptions are different. In the first place they seem to neglect electrostatic interaction between $(^1S)^2P$ and (^1D) or $(^3P)^2P$ terms. Although the calculated energy of the $(^1S)^2P$ term cannot easily be fitted on the experimental value, the off-diagonal matrix elements connecting the $(^1S)^2P$ term with the (^1D) and $(^3P)^2P$ terms should not be neglected. Secondly they neglect, just as in ref. 1, configuration interactions. These approximations give an r.m.s. error in their level fit of 322 cm^{-1}, and consequently their wavefunctions and transition probabilities cannot be very accurate. Following Hodges *et al.*[6]) their experimental data are more reliable than those of Koopman[2]). By making use of theoretical transition probabilities[4]) they convert measured branching ratios into new values for transition probabilities, which of course are completely consistent with the measured branching ratios. In connecting to this method we should remark the following. The energies of the $^2F_{\frac{7}{2}}$, $^2F_{\frac{5}{2}}$, $^2D_{\frac{5}{2}}$, $^2D_{\frac{3}{2}}$ and $^2S_{\frac{1}{2}}$ states of the $2p^4(^1D)3d$ configuration given by Moore[19]) are wrong and have been given correctly in the revised analysis of Ne II by Persson and Minnhagen[10]). In their paper the levels formerly assigned to $^2F_{\frac{7}{2}}$ and $^2F_{\frac{5}{2}}$ are given as belonging to the $2p^4(^1D)4s$ configuration. Conse-

quently a least-squares fit of energy levels of the $2p^4 3d$ configuration based on the wrong energy values of Moore has no physical significance. We have tried to perform a level fit to these old energy values but did not succeed. Also Garstang[1]) did not and rejected the $2p^4(^1D)3d$ configuration. But Marantz[4]) seems to have used these old values in this parametrical calculations. Consequently his results for the wavefunctions and transition probabilities at least of the $2p^4(^1D)3d$ levels must be unreliable. This also holds for the $(^1D)3p$–$(^1D)3d$ transition probabilities of Hodges *et al.*[6]), who firstly, made use of the corresponding results of ref. 4 to evaluate them and, secondly, used some wrongly identified spectral lines, namely the ones originating from or ending on the $(^1D)^2D_{\frac{3}{2},\frac{5}{2}}$ and $(^1D)^2F_{\frac{5}{2}}$ levels. One should be aware of this when one compares our theoretical results for the 3p–3d transitions, based on the revised Ne II analysis, with existing experimental as well as theoretical work.

What concerns the accuracy of the theoretical results, it is already well known, that in contrast to lifetimes, transition probabilities and branching ratios may be very sensitive to small changes in the angular part of the wavefunctions. This sensitivety differs from transition to transition and makes it very difficult to give in general the accuracy of theoretical transition probabilities.

The difference in the calculated values for S_r and S_p to first order only gives an idea whether or not second-order effects on the transition probability may be important. However, second-order effects have not been investigate in this work.

Acknowledgements. The author is grateful to dr. R. H. Garstang, dr. P. E. Noorman and drs. J. Schrijver for valuable comments and suggestions and to dr. F. J. de Heer for his stimulating interest.

This work is part of the research program of the Stichting voor Fundamenteel Onderzoek der Materie (Foundation for Fundamental Research on Matter) and was made possibly by financial support from the Nederlandse Organisatie voor Zuiver Wetenschappelijk Onderzoek (Netherlands Organization for the Advancement of Pure Research).

REFERENCES

1) Garstang, R. H., Monthly Not. Roy. Astron. Soc. **110** (1950) 612; **114** (1954) 118.
2) Koopman, D. W., J. Opt. Soc. Amer. **54** (1964) 1354.
3) Wiese, W. L., Smith, M. H. and Glennon, D. M., Atomic Transition Probabilities, Nat. Bur. Stand. NSRDS-NBS4.
4) Maratz, H., thesis Cornell University (June 1968).
5) Koozekanani, S. H. and Trusty, G. L., J. Opt. Soc. Amer. **59** (1969) 1281.
6) Hodges, D., Marantz, H. and Tang, C. L., J. Opt. Soc. Amer. **60** (1970) 192.

7) Yamanouchi, T. and Amemiya, A., Proc. Phys. Soc. Japan **1** (1946) 18.
8) Racah, G., Physica **16** (1950) 651.
9) Trees, R. E., Cahill, W. F. and Rabinowitz, P., J. Res. Nat. Bur. Stand. **55** (1955) 335.
10) Persson, W. and Minnhagen, L., Ark. Fys. **37** (1968) 273.
11) Condon, E. U. and Shortly, G. H., Theory of Atomic Spectra, Cambridge University Press (London, 1951).
12) Rajnak, K. and Wybourne, B. G., Phys. Rev. **132** (1963) 280;
Racah, G. and Stein, J., Phys. Rev. **156** (1967) 58.
13) Feneuille, S., J. Phys. **28** (1967) 61, 497; **30** (1969) C1–31.
14) Feneuille, S., Klapisch, M., Koenig, E. and Liberman, S., Physica **48** (1970) 571.
15) Bengt Edlén, Handbuch der Physik, band XXVII, 102, Springer Verlag (Berlin, Göttingen, Heidelberg, 1964).
16) Bates, D. R. and Damgaard, A., Phil. Trans. Roy. Soc. London, Ser. A, **242** (1949) 101.
17) Hesser, J. E., Phys. Rev. **174** (1968) 68.
18) Garstang, R. H., private communication.
19) Moore, C. E., Atomic Energy levels, Vol. 1, circular of Nat. Bur. Stand. 467 (1949).

CHAPTER IV

TRANSITION PROBABILITIES AND RADIATIVE LIFETIMES FOR Ar II

B.F.J. Luyken

FOM-Instituut voor Atoom- en Molecuulfysica, Amsterdam, Nederland

Synopsis

Transition probabilities have been calculated for radiative transitions between states of the lower configurations of Ar II in intermediate coupling and using the multi-configuration model. The radial part of the wave functions has been evaluated by means of a parametrized central field potential and the angular part by a least squares adjustment of energy levels. Several examples of strong configuration interaction have been found, especially between members of the $3s^2 3p^4 nd$ series. The influence of these interactions on the transition probabilities, not included in earlier calculations, has been investigated. A comparison has been made with available experimental material. The agreement between theory and experiment has been improved for $3s^2 3p^4 4p \rightarrow 3s^2 3p^4 3d$ transitions as well as for $3s3p^6 \rightarrow 3s^2 3p^5$ transitions. On the contrary the $3s^2 3p^4 4p \rightarrow 3s^2 3p^4 4s$ transition probabilities turned out to be not very sensitive to the improvements in the wave functions. For all the excited states considered, lifetimes are given. A crude estimate of the obtained accuracy is made for all the results.

1. *Introduction.* So far calculations of transition probabilities and radiative lifetimes in Ar II [1]) have disregarded the influence of configuration interaction. As shown in several papers before [2,3]) these interactions may cause drastic changements in computed atomic properties, such as the distribution of the oscillator strength over the spectrum. In a previous paper [3]) the situation in Ne II was discussed and it was pointed out that in general the electrostatic configuration

interaction is weak. However, the cumulative effects of many interacting configurations are important and cannot be neglected in the calculation of transition probabilities. An extension of this study to the Ar II case seems quite a logic step in view of the overall scientific interest in this element of relatively high earth atmospheric abundance.

In order to be able to perform calculations on atomic properties one needs wave functions as accurate as possible. As in ref. 3 use has been made of the central field approximation, where one introduces a central potential V(r). This potential represents the mean effect of all atomic particles minus one electron on an electron, which moves at a distance r from the nucleus. The residual effects can be calculated by means of perturbation theory. The Hamilton operator (in atomic units) now takes the form [4]):

$$H = H_o + H_1 \tag{1}$$

where

$$H_o = \sum_{i=1}^{n} -\tfrac{1}{2}\nabla_i^2 + V(r_i)$$

and

$$H_1 = \sum_{i=1}^{n} -V(r_i) - \frac{Z}{r_i} + \xi(r_i)\,\vec{\ell}_i \cdot \vec{s}_i + \sum_{j<i} \frac{1}{r_{ij}} \tag{2}$$

When V(r) is known we may solve the eigenvalue problem in zero order without difficulty, resulting in zero-order energies and wave functions. The quality of the obtained results depends on the choice of V(r).

In this zero-order approximation the wave functions consist merely of one electron determinantal product functions. Matrix elements of H_1 between these zero-order wave functions are calculated in LS-coupling. The angular part of each matrix element can be exactly evaluated with standard techniques [4]), whereas the radial part is embodied in some direct as well as exchange-type Slater and spin-orbit integrals. So the matrix elements of H_1 consist of linear combinations of these radial integrals. The effect of H_1 to first order can now be calculated by diagonalizing its matrix, constructed on a single configuration basis.

In the absence of any configuration interaction this first order single configuration model may give fairly accurate energies. Interaction with configurations far removed in energy normally is weak and a second order treatment is sufficient in most cases. An effective

Hamiltonian is used [5,6], which operates within a first order basis. Correction terms arise in the matrix elements, which absorb in a parametric treatment (see further on) second order effects. In refs. 2 and 3 it has been demonstrated how spectacular the introduction of the effective corrections $\alpha L(L+1)$ and $\beta S(S+1)$ may be in relatively simple spectra as Ne I and Ne II, showing that the cumulative influences of many perturbing configurations, either of which is weak, may be very important.

When the configuration interaction is strong, which is often the case for configurations of nearly the same energy, a first as well as a second order perturbation treatment is inadequate and one is forced to consider the whole complex of interacting configurations at the same time. The original matrices are then connected by new matrix elements, which give rise to a number of additional parameters. Finally the whole complex of matrices is diagonalized.

Examples of these considerations will be met in our study of the Ar II spectrum.

The formalism, sketched above, is rather academical as long as no numerical data are available concerning the Slater- and spin-orbit integrals, because an analytic diagonalization is impossible. The only way to proceed is with numerical methods. In order to evaluate all quantities which have our interest, such as energy levels and transition probabilities, we used two different methods:

1.1 The classical parametric adjustment method (c.p.a.m.). All radial integrals appearing in the Hamilton matrix are treated as adjustable parameters. From a suitably chosen set of starting values for these parameters an iterative least squares adjustment minimizes the r.m.s. error (in the Racah sence) between observed and calculated energy levels of one or more configurations. With this method angular wave functions and integrals over radial wave functions are found, while no information is obtained about the radial wave functions themselves. The radial integrals automatically have incorporated an effective part arising from weak configuration interaction with many other configurations [5]. Another part of these interactions can be absorbed in this method by effective second order corrections on the calculated energy levels. By introducing such corrections the overall effect of many perturbing configurations on the energy levels will be embodied in a few additional parameters [6].

The introduction of effective second order corrections on the energy levels does not directly improve the obtained angular wave functions, because they still are zero-order ones. But nevertheless with their introduction other parameters, like for instance spin-orbit ones, fix much better with more realistic values. So the introduction of effective corrections indirectly has its influence on the quality of the obtained angular wave functions.

1.2 The parametrized potential method (p.p.m.). The method we followed here, is described and developed in ref. 7. It is based on the consideration that from a known central field potential V(r) a perturbation expansion can be carried on, in principle up till any order. In short it proceeds as follows: V(r) is expressed by an analytic formula, depending on a few parameters ($\alpha_1 \ldots \alpha_n$). In our case these parameters have been determined by minimizing the r.m.s. error between observed and calculated first order energies for a certain number of levels in the Ar II spectrum, and the best possible V(r) has been found. With this V(r) all radial wave functions of interest can be determined by solving the one-electron radial Schrödinger equation. With these wave functions we can evaluate all possible radial integrals, such as radial transition integrals, Slater- and spin-orbit integrals.

These two methods (, c.p.a.m. and p.p.m.,) supply us with all information we need to perform a calculation of transition probabilities and lifetimes. The c.p.a.m. gives angular wave functions, while the p.p.m. gives radial wave functions and from these radial transition integrals.

Besides, a comparison between the values of the Slater- and spin-orbit integrals, as calculated with the p.p.m. and those calculated with the c.p.a.m., is a useful test to check the consistency of these two completely independent methods.

The following configurations of Ar II have our prime interest: $1s^2 2s^2 2p^6 3s^2 3p^5$, $- 3s^2 3p^4 4p$, $- 3s^2 3p^4 4s$, $- 3s^2 3p^4 3d$, $- 3s^2 3p^4 4d$ and $- 3s 3p^6$.

To apply the c.p.a.m. to these configurations, matrices of H_1 have been constructed by making use of ref. 8 and formula 6 of ref. 3. The angular wave functions, which are calculated at the diagonalization of the matrices, have the following form:

$$\Psi_E(J,M) = \sum_i \alpha_i(E) \; |c_i L_i S_i \; JM > \qquad (3)$$

where a certain J,M-state of energy E is expanded on an LS-basis. The c_i's stand for the residual quantum numbers specifying the state, and the α_i's are the expansion coefficients. To be able to calculate transition probabilities and lifetimes we also need radial transition integrals of the form:

$$\int_0^\infty R_{n\ell}(r)\, R_{n'\ell'}(r)\, r\, dr \qquad (4)$$

where $R_{n\ell}(r)$ stands for the radial wave function of an $n\ell$-electron. These quantities have been calculated by the p.p.m.

2. *Results.*

2.1 Calculation of the radial wave function. Most of the configurations considered in this paper are of the type KL $3s^2 3p^4 n\ell$. The choice of the analytic form for the central field potential is determined by this type and consequently, following ref. 7, we get:

$$V(r) = -\frac{1}{r}\left[\sum_{n\ell} (4\ell+2)\, f_\ell(\alpha_{n\ell} r) + 4\, f_1(\alpha_{3p} r) + 2\right] \qquad (5)$$

The sum in (5) extends over all orbitals of the K and L shell and those of the 3s subshell,

$$f_\ell(\alpha_{n\ell} r) = e^{-\alpha_{n\ell} r} \sum_{j=0}^{2\ell+1} \frac{1}{j!} \left(1 - \frac{j}{2\ell+2}\right)(\alpha_{n\ell} r)^j \qquad (6)$$

and represents the contribution to the potential of a radial charge density

$$D_\ell(r) = -\frac{\alpha_{n\ell}^{2\ell+3}}{(2\ell+2)!} \left(r^{\ell+1} e^{-\alpha_{n\ell} r/2}\right)^2 \qquad (7)$$

This form of V(r), with optimal chosen parameters $\alpha_{n\ell}$, is expected to give as good as possible zero-order wave functions, in the sense that a rapid convergence of a perturbation expansion is ensured. However, this form of V(r) is certainly not the best possible choice for configurations of the type KL $3s3p^6$ and KL $3s^2 3p^5$ and consequently the obtained zero-order wave functions and energies for these configurations must be considered as less accurate.

A set of energy levels in Ar II and for comparison also in Ne II was chosen to minimize in first order the r.m.s. deviation between calculated and observed values by varying the parameters $\alpha_{n\ell}$. The so obtained

parameters, potentials and r.m.s. values (Δ) for Ne II and Ar II are given in table I and figure 1.

TABLE I

Parameters and r.m.s. deviations for Ne II and Ar II central field potentials

	Ne II	Ar II
number of levels	27	31
number of configurations	7	14
α_{1s} (a.u.)	13.269	24.629
α_{2s} "	6.820	
α_{2p} "	3.683	
α_{2} "		5.517
α_{3s} "		3.342
α_{3p} "		2.330
Δ (cm^{-1})	459	1379

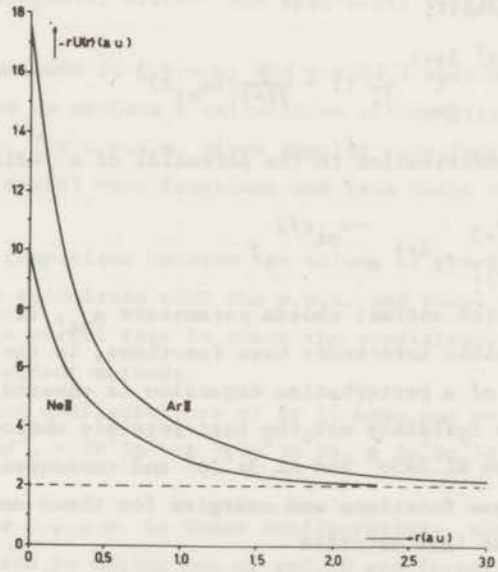

Fig. 1 - Central field potentials for Ne II and Ar II as obtained with the p.p.m.

The r.m.s. value in case of Ne II (459 cm^{-1}) is a reasonable result in view of the large energy interval covered by the configurations considered (310000 cm^{-1}). In Ar II the r.m.s. error is much larger (1379 cm^{-1}), due to important configuration interaction. In particular the $3p^4 4s$ and $3p^4 3d$ energies are pushed away from each other by about 2000 cm^{-1} as a consequence of a mutual configuration interaction.

2.2 Calculation of angular wave functions. Angular wave functions have been obtained by the c.p.a.m. Because of a rather strong configuration interaction, the three terms of the $3p^4$-core, ^1S, ^1D and ^3P, are perturbed and their energy separation does not fit in with the Slater theory. This phenomenon however, is not important for this study and therefore not worthwhile to consider. Consequently we rejected the doublets based on the ^1S core term from the calculations.

2.2.a. configurations of odd parity

$3p^4 4p$ configuration. To start with, a first order calculation has been performed in the single configuration approximation. The parameters and their values are listed in the first and second column of table II. The success of the fit is expressed by the value of the r.m.s. deviation (Δ). Next a second order approximation has been done by introducing the effective corrections $\alpha L(L+1)$ and $\beta S(S+1)$ to the final states. This gives a manifest improvement (see column 3 and 4 of table II) and the fact that such an adequate description is reached already at a second order approximation, demonstrates that this configuration is only weakly perturbed. Any interaction with the $3p^5$ ground state - present in Ne II - could not be observed. In the last column the parameter values, as obtained with the p.p.m. are given for comparison with those obtained with the c.p.a.m. The tendency of some radial integrals, evaluated with the former method, to be larger than those obtained with the latter, is a known fact. In the c.p.a.m. the parameters automatically have incorporated an effective part, originating from far configuration interaction, which reduces their values. Especially the $G_o(3p,4p)$ almost differs by a factor of two. In view of the conclusions, drawn in ref. 9 in the case of Ne I, this discrepancy can be partly accounted for by weak interaction with $3p^4 np$ ($n>4$) configurations. Also continuum states may be responsible.

TABLE II

Parameters and r.m.s. deviations for the $3p^4 4p$ configuration

Parameter	Least squares adjustment (c.p.a.m.)			parametrized potential (p.p.m.)
	cm^{-1}			
E	193324 ± 162	192869 ± 156	193275 ± 137	
$F_2(3p,3p)$	2218 ± 7.8	2193 ± 8.1	2221 ± 8.9	2578
$F_2(3p,4p)$	369 ± 5.0	375 ± 3.6	379 ± 2.6	450
$G_o(3p,4p)$	1810 ± 27	1877 ± 24	1897 ± 16.5	3080
$G_2(3p,4p)$	94.9 ± 5.6	89.3 ± 4.0	108 ± 5.5	145
ζ_{3p}	1064 ± 69	1042 ± 46	1049 ± 30	1078
ζ_{4p}	110 ± 60	110 ± 40	97.7 ± 27	124
α	-	26.6 ± 6.6	17.1 ± 5.0	
β	-	-	69.5 ± 18	
Δ	79.6	52.9	33.2	

In view of the above arguments the agreement in the results of both methods is good. We have adopted the second order treatment in the c.p.a.m. as an adequate description and decided to refrain from a near configuration interaction study for the odd-parity configurations. In table III the obtained energies, Lande-g factors and percentage composition of the eigenvectors are given.

$3p^5$ ground-state configuration. In the c.p.a.m. this configuration has been treated together with the $3p^4 4p$ one and we have tried to find values for the interaction integrals $R^{(o)}(3p,3p;\ 3p,4p)$ and $R^2(3p,3p;\ 3p,4p)$. However, their values oscillated in course of the iteration procedure and could not be fixed. The best possible fit was obtained by keeping their values fixed to zero. Consequently the $3p^5\ ^2P$ wave function is pure.

2.2.b. configurations of even parity

A first order treatment with the c.p.a.m. turns out to give poor results for the $3p^4 3d$ configuration (see 2nd column of table IV). Introducing the α and β second order corrections has no influence at all.

TABLE III

Eigenvalues, Landé-g values and composition of states in the $3s^2 3p^4 4p$ configuration. Values between brackets were excluded.

Level	E_{theor} cm^{-1}	E_{exp} cm^{-1}	$E_{theor}-E_{exp}$ cm^{-1}	g_{theor}	g_{exp}	Percentage	Composition
$(^1D)^2F_{7/2}$	170549.5	170530.3	19.2	1.144	1.140	99.7%	$(^1D)^2F_{7/2}$
$(^3P)^4D_{7/2}$	157214.7	157233.9	-19.2	1.428	1.427	99.7%	$(^3P)^4D_{7/2}$
$(^1D)^2D_{5/2}$	173362.6	173393.4	-30.8	1.200	1.202	99.5%	$(^1D)^2D_{5/2}$
$(^1D)^2F_{5/2}$	170436.2	170400.9	35.3	.859	.857	99.6%	$(^1D)^2F_{5/2}$
$(^3P)^2D_{5/2}$	158754.2	158730.2	24.0	1.233	1.241	81.2%	$(^3P)^2D_{5/2}$
$(^3P)^4D_{5/2}$	157671.1	157673.3	- 2.2	1.342	1.334	80.1%	$(^3P)^4D_{5/2}$
$(^3P)^4P_{5/2}$	155048.1	155043.1	5.0	1.593	1.599	97.3%	$(^3P)^4P_{5/2}$
$(^1S)^2P_{3/2}$	(191676)	191974.5	-	1.333	1.332	99%	$(^1S)^2P_{3/2}$
$(^1D)^2D_{3/2}$	173316.8	173347.8	-31.0	.811	.804	98%	$(^1D)^2D_{3/2}$
$(^1D)^2P_{3/2}$	172233.3	172213.8	19.5	1.325	1.332	85.9%	$(^1D)^2P_{3/2}$
$(^3P)^4S_{3/2}$	161079.1	161048.7	30.4	1.992	1.987	98%	$(^3P)^4S_{3/2}$
$(^3P)^2P_{3/2}$	160185.6	160239.4	46.2	1.222	1.244	67.6%	$(^3P)^2P_{3/2}$ +
						21.7%	$(^3P)^2D_{3/2}$ +
						9.2%	$(^1D)^2P_{3/2}$
$(^3P)^2D_{3/2}$	159405.1	159393.3	11.8	.938	.918	72.6%	$(^3P)^2D_{3/2}$ +
						18.5%	$(^3P)^2P_{3/2}$
$(^3P)^4D_{3/2}$	158152.0	158167.7	-15.7	1.190	1.199	91%	$(^3P)^4D_{3/2}$
$(^3P)^4P_{3/2}$	155363.9	155351.0	12.9	1.722	1.720	96%	$(^3P)^4P_{3/2}$
$(^1S)^2P_{1/2}$	(191602.8)	192333.4	-	.667	.760	99%	$(^1S)^2P_{1/2}$
$(^1D)^2P_{1/2}$	172818.2	172816.2	2.0	.668	.667	84%	$(^1D)^2P_{1/2}$
$(^3P)^2S_{1/2}$	161132.2	161089.3	42.9	1.727	1.695	79%	$(^3P)^2S_{1/2}$
$(^3P)^2P_{1/2}$	159683.1	159706.5	-23.5	.943	.983	65.1%	$(^3P)^2P_{1/2}$ +
						20.0%	$(^3P)^2S_{1/2}$ +
						12.4%	$(^1D)^2P_{1/2}$
$(^3P)^4P_{1/2}$	155718.5	155708.2	10.3	2.635	2.638	98.3%	$(^3P)^4P_{1/2}$

TABLE IV

Parameters and r.m.s. deviations for $3s^2 3p^4 3d + 3s^2 3p^4 4d + 3s^2 3p^4 4s + 3s3p^6$

Parameter	Least squares adjustment (c.p.a.m.)		Parametrized potential (p.p.m.)
$E(3s^2 3p^4 3d)$	189512 ± 1099	191133 ± 517	
$E(3s^2 3p^4 4d)$	220438 ± 1000	220597 ± 423	
$E(3s^2 3p^4 4s)$	170158 ± 1556	172881 ± 626	
$E(3s\ 3p^6\ )$	108721	141892 ± 408	
$F_2(3p,3p;3d)$	2158 ± 144	2252 ± 35.5	
$F_2(3p,3p;4d)$	2011 ± 76	2233 ± 26.0	} 2578
$F_2(3p,3p;4s)$	2105 ± 108	2283 ± 42.5	
$F_2(3p,3d)$	1023 ± 36	879 ± 17.4	1195
$F_2(3p,4d)$	193 ± 33	369 ± 17.1	222
$G_1(3p,3d)$	1769 ± 32	1837 ± 23.4	3411
$G_1(3p,4d)$	482 ± 51	490 ± 34.4	494
$G_1(3p,4s)$	1261 ± 238	1261 ± 52.2	1719
$G_3(3p,3d)$	100 ± 8.7	74 ± 4.1	123
$G_3(3p,4d)$	31.6 ± 5.7	42.3 ± 3.0	19.0
ζ (3p,3p;3d)	1799 ± 436	1003 ± 117	
ζ (3p,3p;4d)	523 ± 531	1148 ± 146	} 1078
ζ (3p,3p;4s)	1034 ± 676	1048 ± 148	
ζ (3d,3d)	204 ± 226	6.1 ± 54.6	18.6
ζ (4d,4d)	20.3 ± 227	8.3 ± 51.8	4.2
$R_2(3p,3d;3p,4d)$	-	15750 ± 777	13801
$R_1(3p,3d;4d,3p)$	-	16470 ± 267	19112
$R_3(3p,3d;4d,3p)$	-	21633 ± 1372	11547
$R_2(3p,4s;3p,3d)$	-	- 2975 ± 279	- 5332
$R_1(3p,4s;3d,3p)$	-	(988)	318
$R_1(3p,3p;3s,3d)$	-	42858 ± 611	65462
$R_1(3p,3p;3s,4d)$	-	29548 ± 774	25446
α (3d)	-	54.7 ± 12.7	
α (4d)	-	28.0 ± 15.1	
β (3d)	-	486 ± 76.4	
Δ	767	167	

Here we have to deal with a case of strong configuration interaction where a second order treatment is insufficient.

In this stage of the calculation the results of the p.p.m. are very useful. A large number of configuration interaction integrals has been computed with this method and this gives insight in the question which configurations indeed do interact strongly with each other. In this way a selection of interacting configurations has been made in order to be studied with the c.p.a.m. These are interactions of $3s^2 3p^4 3d$ with $3s^2 3p^4 nd$ ($n > 3$), and with $3s3p^6$. This latter interaction is remarkably strong, as was already pointed out by Minnhagen [10]) and thereafter quantitatively investigated by Kjöllerstrom et al.[11]). Also the $3s^2 3p^4 4s$ configuration must be included in this complex. With these indications the following complex of interacting configurations has been investigated with the c.p.a.m.: $3s^2 3p^4 3d + 3s^2 3p^4 4d + 3s^2 3p^4 4s + 3s3p^6$. In order to confine the number of free parameters the weaker configuration interaction, $3p^4 4s - 3p^4 4d$ has been neglected. Only electrostatic configuration interaction has been included, because magnetic interaction via the spin-orbit operator $\zeta(3d,4d)$ is found to be neglectable small, using the p.p.m..

With the exception of $R^{(1)}(3p,4s;3d,3p)$ all parameters could be adjusted. This $R^{(1)}$ was fixed to 988 cm^{-1}, which value turned out to be the best one in several trials.

Finally, residual effects of weak interactions with other configurations, not included in our matrices have been partly removed by introducing the effective second order corrections $\alpha(3d)$, $\alpha(4d)$ and $\beta(3d)$ ($\beta(4d)$ turned out to be irrelevant). Three anomalously lying levels of the $3p^4 4d$ configuration, $(^1D)^2D_{5/2}$, $(^1D)^2D_{3/2}$ and $(^1D)^2P_{3/2}$ were excluded. They probably interact rather strongly with corresponding levels in the $3p^4 5d$ configuration, which are partly missing in the Ar II analysis [10]). The finally obtained result is given in the third column of table IV.

At first sight the obtained r.m.s. value of 167 cm^{-1} is a reasonable result in view of the large energy interval covered by the complex of considered configurations. The main contribution to this error comes from the $3p^4 4d$ configuration, while the other configurations fit in much better with their experimental energies. But for several reasons the quality of this result could be overestimated. Like the p.p.m. calculation shows, a considerable configuration interaction is present

between the $3p^4 3d$ and the higher members of the same series, in particular caused by the large exchange contributions, incorporated in the integrals $R^{(1)}(3p,3d;nd,3p)$ and $R^{(3)}(3p,3d;nd,3p)$. On the contrary the $3p^4 np$ series does not have these large exchange integrals, for which reason the $3p^4 4p$ could be described with sufficient accuracy in second order. Grafically this distinction between the $3p^4 np$ and $3p^4 nd$ series is plotted in terms of the relevant $R^{(k)}$ integrals in figs. 2a and b. Besides the whole $3p^4 nd$ series exhibits a rather large series perturbation. Also here the main contribution comes from the exchange.

In a c.p.a. calculation, where the matrix is restricted to n=4 in the $3p^4 nd$ series, this will have little influence on the calculated energies, because the influence of configurations $3p^4 nd$ ($n > 4$) on the energies of the $3p^4 3d$ configuration will be absorbed by the interaction integrals between $3p^4 3d$ and $3p^4 4d$, having the same angular dependence as those between $3p^4 3d$ and $3p^4 nd$ ($n > 4$), irrespective of the quantum number n. These over-impregnated $R^{(k)}(3p,3d;3p,4d)$ integrals have in turn their influence on the calculated energies of the $3p^4 4d$ configuration, but this will be partly remedied by the relevant $F^{(k)}$ and $G^{(k)}$ integrals within the $3p^4 4d$ configuration.

So there seems to be a good fit of energy levels, but several parameters may have got wrong values. Correspondingly, the wave functions obtained with this in fact incorrect restriction of the matrix size could be seriously affected and this may have a disastrous influence on other atomic properties to calculate. So in principle we should be suspicious of calculated transition probabilities for transition to and from the $3p^4 3d$ and $3p^4 4d$ configurations. This will be further discussed in sec. 3.2. Fortunately the wave functions of other even parity configurations are only weakly affected by this and can be used without objection as will be shown later on.

To avoid the above difficulty, it would be necessary to construct matrices which include a very large number of $3p^4 nd$ configurations. An extension of our matrix to n=5 and n=6 is not worthwhile, because firstly even then it means a severe restriction, secondly in the analysis of $3p^4 5d$ and $3p^4 6d$ several important terms are missing, leading to difficulties in a c.p.a. calculation and thirdly the number of free parameters in a c.p.a. calculation becomes too large. Conclusively, it seems not worthwhile to spend more time to improve the wave functions of the $3p^4 nd$ configurations with our method. The final

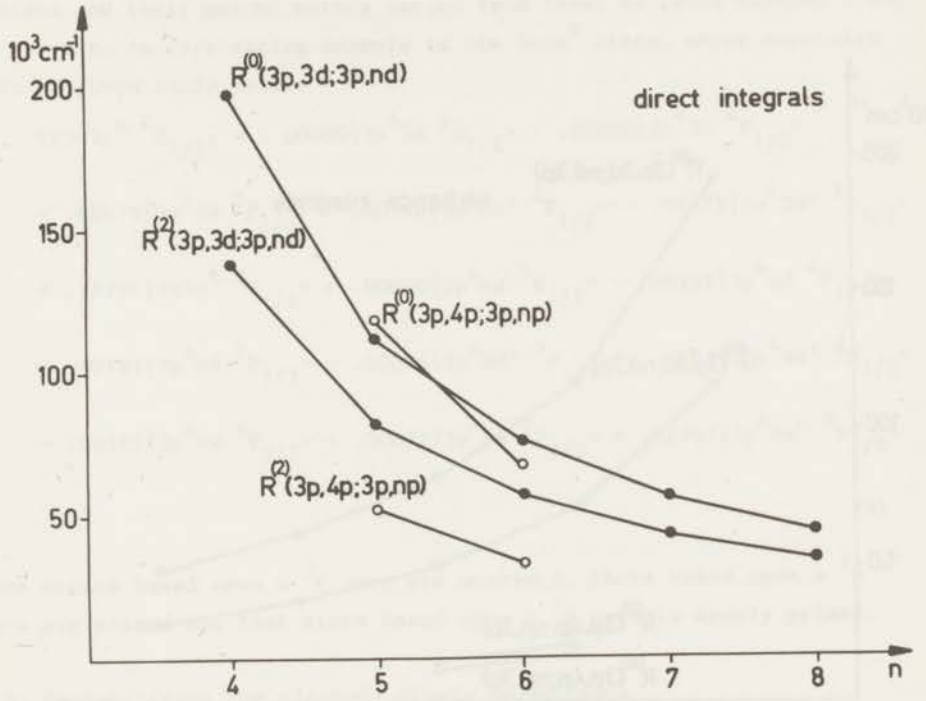

Fig. 2a - Comparison between the direct configuration interaction integrals $R^{(k)}(3p,4p;3p,np)$ and $R^{(k)}(3p,3d;3p,nd)$, which describe the direct intrachannel interaction within the $3s^2 3p^4 np$ channel and the $3s^2 3p^4 nd$ channel respectively.

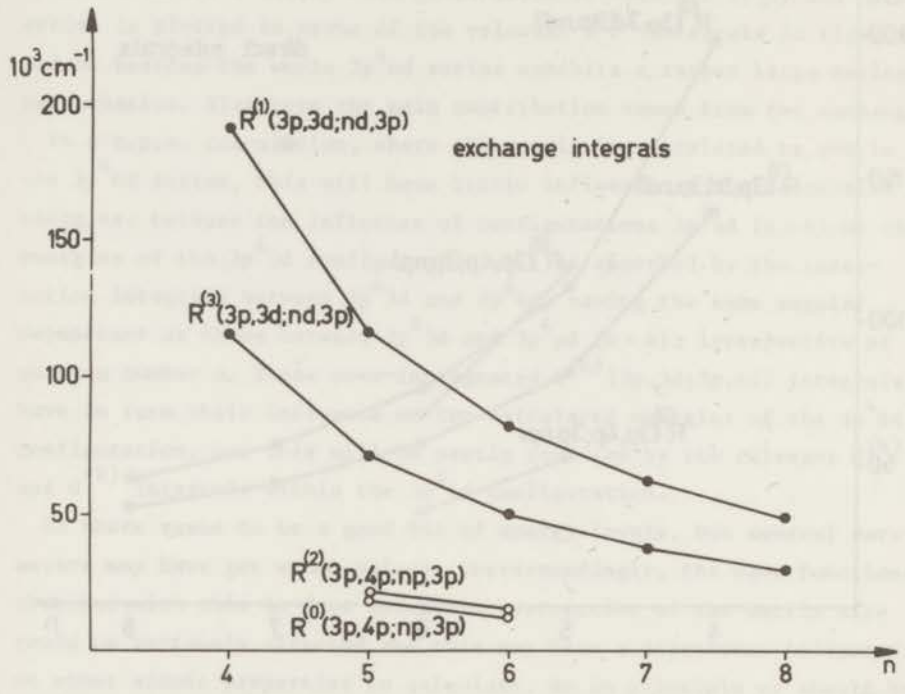

Fig. 2b - Comparison between the exchange configuration interaction integrals $R^{(k)}(3p,4p;np,3p)$ and $R^{(k)}(3p,3d;nd,3p)$, which describe the exchange intrachannel interaction within the $3s^2 3p^4 np$ channel and the $3s^2 3p^4 nd$ channel.

results of our calculation are contained in table IV, third column, where for comparison also values of integrals computed with the p.p.m. are given in the fourth column.

The coupling scheme of the $3p^4 3d$ and $3p^4 4d$ configurations is intermediate and their mutual mixing varies from level to level between 2 and 20 percent. An interesting example is the $3s3p^6$ state, whose expansion will be given fully below:

$$\begin{aligned}\Psi(3s3p^6\ {}^2S_{1/2}) = {} & .00000|3p^4 3d\ {}^4D_{1/2}> - .00860|3p^4 3d\ {}^4P_{1/2}> \\ & + .00479|3p^4 3d\ {}^2P_{1/2}> - .00148|3p^4 3d'\ {}^2P_{1/2}> - .55573|3p^4 3d'\ {}^2S_{1/2}> \\ & + .78764|3s3p^6\ {}^2S_{1/2}> + .00000|3p^4 4d\ {}^4D_{1/2}> - .00335|3p^4 4d\ {}^4P_{1/2}> \\ & + .00181|3p^4 4d\ {}^2P_{1/2}> - .00056|3p^4 4d'\ {}^2P_{1/2}> - .26416|3p^4 4d'\ {}^2S_{1/2}> \\ & - .00107|3p^4 4s\ {}^4P_{1/2}> + .00077|3p^4 4s\ {}^2P_{1/2}> + .02991|3p^4 4s''\ {}^2S_{1/2}>\end{aligned} \tag{8}$$

Here states based upon a ^3P core are unprimed, those based upon a ^1D core are primed and that state based upon a ^1S core is doubly primed.

3. *Probabilities for electric dipole transitions.*

3.1. Theoretical formulation. The calculations described in the foregoing section give wave functions of the form (3). The transition probabilities for electric dipole radiation between an initial state

$$\Psi = \sum_i \alpha_i\ |c_i L_i S_i\ JM>$$

and a final state

$$\Psi' = \sum_j \beta_j\ |c_j L'_j S'_j\ J'M'>\ ,$$

summed over final sublevels M' and averaged over initial sublevels M, are in the length formulation given by [12])

$$A(J,J') = \frac{2.026\ 10^{18}}{(2J+1)\lambda^3}\ \Big|\sum_{ij} \alpha_i^* \beta_j < c_i L_i S_i J \Big\| \sum_k r_k\ \vec{C}^{(1)}(k) \Big\| c_j L'_j S'_j J'>\Big|^2 \tag{9}$$

where λ is the wavelength in $\mathring{A}$, $r_k\ \vec{C}^{(1)}(k)$ the position operator of the k^{th} electron with $\vec{C}^{(1)}$ the spherical Racah tensor of rank 1.

The matrix element is expressed in atomic units and the sum over k extends over all atomic electrons.

In the summation over i and j different configurations participate. We shall write out in detail the expressions which result for the different combinations of configurations between which the transition takes place. For a $3s^2 3p^4 n\ell - 3s^2 3p^4 n'\ell'$ transition we derive with standard techniques [4])

$$\langle 3p^4(\bar{L}\,\bar{S})\, n\ell\; L\; S\; J \| \sum_k r_k\, \overset{+}{C}^{(1)}(k) \| 3p^4(\bar{L}'\bar{S}')n'\ell'\; L'S'J' \rangle =$$

$$\delta_{SS'}\delta_{\bar{S}\bar{S}'}\delta_{\bar{L}\bar{L}'}\, [J,J',L,L',\ell,\ell']^{\frac{1}{2}}\, (-1)^{J'+S+\ell'+\ell+\bar{L}} \times$$

$$\begin{Bmatrix} S & L & J \\ 1 & J' & L' \end{Bmatrix} \begin{Bmatrix} \bar{L} & \ell & L \\ 1 & L' & \ell' \end{Bmatrix} \begin{pmatrix} \ell & 1 & \ell' \\ 0 & 0 & 0 \end{pmatrix} \int_0^\infty R_{n\ell}(r)\, R_{n'\ell'}(r)\, r\, dr \qquad (10)$$

where $[a,b,\ldots] \equiv (2a+1)\,(2b+1)\,\ldots$ (11)

and the barred quantum numbers refer to the core.

For a $3s^2 3p^5 - 3s^2 3p^4 n\ell$ transition we get:

$$\langle p^5\; LSJ \| \sum_k r_k\, \overset{+}{C}^{(1)}(k) \| p^4(\bar{L}'\bar{S}')\ell' L'S'\bar{J}' \rangle =$$

$$(5)^{\frac{1}{2}} \sum_{\bar{L}\bar{S}} (p^5\; LS\; \{|p^4(\bar{L}\bar{S})p\; LS)\; \delta_{SS'}\delta_{\bar{S}\bar{S}'}\delta_{\bar{L}\bar{L}'} \times$$

$$[J,J',L,L',1,\ell']^{\frac{1}{2}}\, (-1)^{J'+S+\ell'+1+\bar{L}}$$

$$\begin{Bmatrix} S & L & J \\ 1 & J' & L' \end{Bmatrix} \begin{Bmatrix} \bar{L} & 1 & L \\ 1 & L' & \ell' \end{Bmatrix} \begin{pmatrix} \ell' & 1 & 1 \\ 0 & 0 & 0 \end{pmatrix} \int_0^\infty R_{3p}(r)\, R_{n'\ell'}(r)\, r\, dr \qquad (12)$$

where $(p^5\; LS\; \{|p^4(\bar{L}\bar{S})p\; LS)$ is the usual coefficient of fractional parentage.

Finally for a $3s^2 3p^5 - 3s3p^6$ transition we derive in a few steps

$$\langle s^2 p^5\; LSJ \| \sum_k r_k\, \overset{+}{C}^{(1)}(k) \| sp^6\; L'S'J' \rangle =$$

$$(2)^{\frac{1}{2}}\, [J]^{\frac{1}{2}} \begin{Bmatrix} \frac{1}{2} & 1 & J \\ 1 & \frac{1}{2} & 0 \end{Bmatrix} \int_0^\infty R_{3p}(r)\, R_{3s}(r)\, r\, dr \qquad (13)$$

In our multi-configurational treatment, evaluation of (9) results in a sum over expressions (10), (12) and (13). The angular and radial parts cannot be separated anymore as in a one-configuration treatment.

Besides a length formulation also the velocity formulation of the matrix element in (9) is possible. By making use of the commutation relation between $\vec{r}_i$ and H_o we derive for our many-configuration case an expression for the transition probability in the velocity formulation:

$$A^{\rightarrow}_{\nabla} = \frac{2.026\ 10^{18}}{(2J+1)\lambda^3} \left| \sum_{i,j} \alpha_i^* \beta_j \frac{\nu_{ij}^{(o)}}{\nu} \langle c_i L_i S_i J \| \sum_k r_k \vec{C}^{(1)}(k) \| c_j L_j' S_j' J' \rangle \right|^2 \tag{14}$$

$A^{\rightarrow}_{\nabla}$ is obtained in our method simply by weighting the different factors occurring in (9) by $\nu_{ij}^{(o)}/\nu$, where ν is the frequency of the transition and $\nu_{ij}^{(o)} = \frac{1}{2\pi}(\epsilon_i - \epsilon_j)$. ϵ_i and ϵ_j are the mono-electron energies of the orbitals $n_i\ell_i$ and $n_j\ell_j$, as obtained with the p.p.m.

If one uses exact wave functions, length and velocity formulation are equivalent. If one uses approximate wave functions, both formulations give different results. Usually it is assumed that this difference may be an indication about the quality of the wave functions, but it is not obvious if this is true in our method.

With the results of section 2 we are able to calculate probabilities for transitions between levels of the following complexes of configurations: $3s^2 3p^4 4p + 3s^2 3p^5$ of odd parity and $3s^2 3p^4 3d + 3s^2 3p^4 4d + 3s^2 3p^4 4s + 3s 3p^6$ of even parity. Use has been made of formulae (9) and (14). The coefficients α_i and β_j are known from section 2.2, the radial transition integrals, occurring in (10), (12) and (13) have been calculated with the p.p.m. Those radial transition integrals which are of interest, are listed in table V.

3.2. Results. First of all in table VI the obtained probabilities for transitions of $3s^2 3p^4(^3P)4p$ levels to $3s^2 3p^4(^3P)4s$ and $3s^2 3p^4(^3P)3d$ levels are given and compared with earlier calculations [13,14]) and experimental results [15]). Only those transitions are listed which have a calculated transition probability in the length formulation larger than 1×10^6 (s^{-1}). In the last column our results in the velocity formulation are given for comparison. However, following reference 16 in our approximate multi-configurational treatment the length formulation is the correct one and should be used.

Our results for the 4p → 4s transitions (see table VI) are not very sensitive to the configuration interaction. Compared with earlier calculations there are differences from transition to transition, but the

TABLE V

Radial transition integrals

nℓ	n'ℓ'	$\int_0^\infty R_{n\ell}(r)\, R_{n'\ell'}(r)\, r\, dr$ in a.u.
4p	4s	- 4.1855
4p	3d	2.3949
4s	3p	.6753
3d	3p	- 1.5882
3p	3s	- 1.4426
4d	3p	- .3444
4d	4p	- 4.2705
5d	4p	- 1.1500
6d	4p	- .5917
7d	4p	- .3813
8d	4p	- .2749

overall agreement with experimental values is about the same. The transitions originating from the ^4P term deviate mostly about 5% from experiment. Apart from a few weak lines the other transitions deviate in the order of 10-25% from experimental values, with a mean deviation of 12%.

In earlier theoretical work difficulties have been encountered at the 4p → 3d transitions, where large deviations from experimental values have been found. In most cases theoretical values were much higher (30-100%). The origin of this is now understood in terms of the large mixing between the $3p^4nd$ configurations. The radial transition integral 4p-3d (see fig. 3), is positive, while the 4p-nd (n > 3) ones are all negative. Because of the equal phase signs of the eigenvector components of corresponding 3d and 4d states, this means that the 4p-3d oscillator-strength in fact is partly cancelled and transferred to higher nd configurations and probably even to continuum ϵd states. A simple first-order calculation ignores all these effects and gives too high 4p → 3d transition probabilities.

In our case, where the nd configuration interaction is cut off at n=4, a too large cancellation takes place and calculated probabilities are too low. This is because firstly in the wave functions of the 3d states the 4d components are too large (see sec. 2.2.b) and secondly the

TABLE VI

transition	λ(Å)	$3s^2 3p^4 n\ell$ - $3s^2 3p^4 4p$ transitions A(J,J') (s^{-1}) Statz (theor.)	Rudko (theor.)	Shumaker (exp.)	this work (theor.)	$A_{\nu}^{\pm}$(J,J') (s^{-1})
$4s\,^4P_{5/2}$-$4p\,^4D_{7/2}$	4348	139 10^6	135 10^6	137 10^6	143 10^6	143 10^6
$3d\,^4F_{9/2}$	6644	-	-	-	18.3	13.9
$3d\,^4F_{7/2}$	6887	-	-	-	1.70	1.38
$3d\,^4D_{7/2}$	4014	-	17.0	11.9	14.8	4.09
$3d\,^4D_{5/2}$	4039	-	2.81	1.41	1.86	0.43
$4s\,^4P_{5/2}$-$4p\,^4D_{5/2}$	4267	19.2	21.0	17.3	21.6	17.4
$4s\,^4P_{3/2}$	4426	104	94.6	92.0	101	86.7
$4s\,^2P_{3/2}$	5145	7.07	9.17	10.8	8.7	10.0
$3d\,^4F_{7/2}$	6684	-	-	-	14.06	10.8
$3d\,^4F_{5/2}$	6864	-	-	-	2.53	2.04
$3d\,^4D_{7/2}$	3944	-	6.29	4.47	5.72	1.53
$3d\,^4D_{5/2}$	3968	-	6.6	5.2	6.23	1.75
$3d\,^4D_{3/2}$	3992	-	3.06	1.69	2.27	0.55
$4s\,^4P_{5/2}$-$4p\,^4D_{3/2}$	4178	1.23	1.52	1.4	1.56	1.24
$4s\,^4P_{3/2}$	4331	64.2	62.7	63	65.9	54.2
$4s\,^4P_{1/2}$	4430	67.8	62.2	59	67.2	57.5
$4s\,^2P_{1/2}$	5287	1.40	1.96	1.7	1.42	1.74
$3d\,^4D_{5/2}$	3892	-	10.5	8.1	9.51	2.49
$3d\,^4D_{3/2}$	3915	-	4.03	3.6	4.06	1.13
$3d\,^4D_{1/2}$	3931	-	3.28	2.2	2.74	0.69
$3d\,^4F_{5/2}$	6638	-	-	14.3	15.7	11.9
$3d\,^4F_{3/2}$	6757	-	-	~1.0	3.52	2.76
$4s\,^4P_{3/2}$-$4p\,^4D_{1/2}$	4283	14.9	15.1	13.3	15.8	12.8
$4s\,^4P_{1/2}$	4380	122	117	115	122	103
$3d\,^4D_{3/2}$	3875	-	15.1	8	10.9	2.86
$3d\,^4D_{1/2}$	3891	-	6.15	4.3	6.03	1.63
$3d\,^4F_{3/2}$	6640	-	-	20.1	20.6	15.6
$4s\,^4P_{5/2}$-$4p\,^4P_{5/2}$	4806	87.4	82.8	87.2	90.8	90.2
$4s\,^4P_{3/2}$	5009	13.7	15.0	16.3	16.8	18.0
$3d\,^4D_{7/2}$	4401	-	51.8	35.7	45.3	15.0
$3d\,^4D_{5/2}$	4431	-	16.5	12.2	15.6	5.54
$3d\,^4D_{3/2}$	4461	-	2.28	1.73	2.15	0.77

TABLE VI (continued)

transition	λ(Å)	A(J,J')(s^{-1})				$A_{\nabla}^{\pm}$(J,J') (s^{-1})
		Statz (theor.)	Rudko (theor.)	Shumaker (exp.)	this work (theor.)	this work (theor.)
$4s\,^4P_{5/2}$-$4p\,^4P_{3/2}$	4736	63.8	61.1	65.0	68.2	65.2
$4s\,^4P_{3/2}$	4933	16.1	14.8	15.8	16.3	17.0
$4s\,^4P_{1/2}$	5062	20.8	21.6	24.5	24.9	27.0
$3d\,^4D_{5/2}$	4371	-	39.0	25.8	32.6	10.3
$3d\,^4D_{3/2}$	4400	-	25.7	18.2	22.9	7.72
$3d\,^4D_{1/2}$	4421	-	4.62	3.6	4.18	1.43
$4s\,^4P_{3/2}$-$4p\,^4P_{1/2}$	4848	89.7	86.5	94.0	97.5	97.4
$4s\,^4P_{1/2}$	4972	9.45	9.68	10.7	11.5	12.0
$3d\,^4D_{3/2}$	4332	-	32.2	23	27.0	8.45
$3d\,^4D_{1/2}$	4352	-	38.1	25.3	33.0	10.6
$4s\,^4P_{5/2}$-$4p\,^4S_{3/2}$	3729	87	85.0	66	79.4	50.2
$4s\,^4P_{3/2}$	3851	73	69.4	53	66.6	44.6
$4s\,^4P_{1/2}$	3929	45.1	43	33	40.9	28.4
$4s\,^2P_{3/2}$	4384	0.16	0.94	1.2	1.83	1.54
$3d\,^4P_{3/2}$	7380	-	-	-	6.27	6.47
$3d\,^4P_{5/2}$	7589	-	-	-	10.3	10.9
$3d\,^2P_{1/2}$	7234	-	-	-	3.23	3.27
$4s\,^4P_{5/2}$-$4p\,^2D_{5/2}$	4082	3.57	3.78	3.0	3.42	2.52
$4s\,^4P_{3/2}$	4228	9.88	13.1	14.4	12.6	9.81
$4s\,^2P_{3/2}$	4880	89.6	84.5	87.0	90.2	93.7
$3d\,^4F_{7/2}$	6243	-	-	-	2.99	2.00
$3d\,^4D_{7/2}$	3786	-	2.26	1.3	1.87	0.46
$4s\,^4P_{3/2}$-$4p\,^2D_{3/2}$	4113	1.07	2.73	0.91	1.07	0.80
$4s\,^4P_{1/2}$	4202	1.12	3.49	1.8	2.79	2.15
$4s\,^2P_{3/2}$	4727	72.7	45.6	56	64.7	62.3
$4s\,^2P_{1/2}$	4965	26.3	46.1	38.5	34.5	37.5
$3d\,^4F_{5/2}$	6139	-	-	-	1.10	0.70
$3d\,^2P_{1/2}$	6809	-	-	-	1.14	1.33
$4s\,^4P_{5/2}$-$4p\,^2P_{3/2}$	3845	0.2	0.91	~ 2	1.34	0.88
$4s\,^4P_{3/2}$	3975	0.81	0.68	~ 2	1.62	1.11
$4s\,^2P_{3/2}$	4545	27.7	51.9	45.8	40.9	35.6
$4s\,^2P_{1/2}$	4765	71.5	44.7	63.7	64.6	63.0
$3d\,^2P_{3/2}$	6861	-	-	2.7	2.65	1.78

TABLE VI (continued)

transition	λ(Å)	A(J,J') (s^{-1}) Statz (theor.)	Rudko (theor.)	Shumaker (exp.)	this work (theor.)	A_{∇}^{Δ}(J,J') (s^{-1}) this work (theor.)
$4s^2P_{3/2}$-$4p^2P_{1/2}$	4658	75.5	85.5	89	86.5	81.3
$4s^2P_{1/2}$	4889	19.8	12.5	17.6	20.1	19.4
$3d^2P_{1/2}$	6666	-	-	8	6.06	4.05
$4s^2P_{3/2}$-$4p^2S_{1/2}$	4376	37.1	23	22.2	26.8	23.7
$4s^2P_{1/2}$	4579	84.2	89.9	90.4	87.5	80.7
$3d^2P_{1/2}$	6104	-	-	1.3	2.77	2.67
$3d^2P_{3/2}$	6483	-	-	11	11.2	8.70

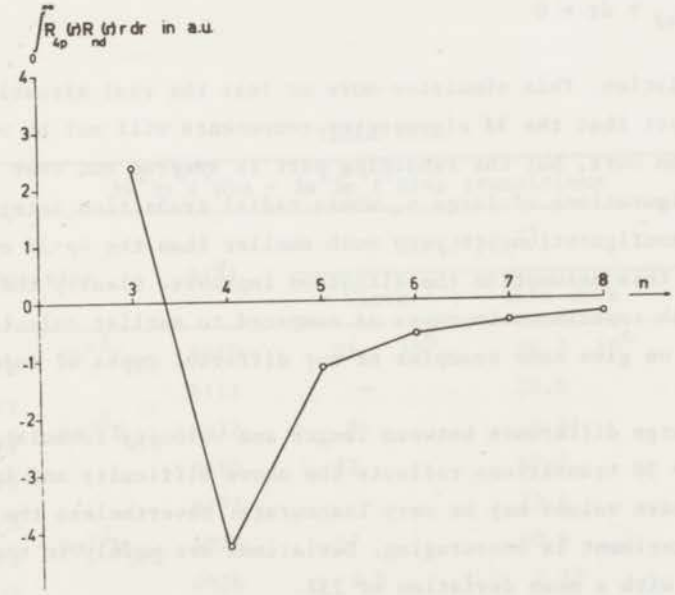

Fig. 3 - Radial transition integrals $\int_0^\infty R_{4p}(r)R_{nd}(r)\, r\, dr$.

4d → 4p transition integral is almost twice as large as the 4p-3d one, but negative. In a fictitious case, where many nd configurations would be considered, the contribution of many high nd configurations together would be preponderate over that of the 4d one alone; this "smearing out" effect to high nd configurations would reduce the cancellation, because the radial transition integrals 4p-nd (n > 4) become smaller and smaller (see fig. 3). A way to improve the now obtained transition probabilities would be the application of the effective operator formalism for the dipole operator [2]. Second order effects of perturbations from the higher nd configurations on the calculated transition probabilities could then be taken into account. But it is very improbable that a second order treatment of these strong perturbations is sufficient and therefore we refrained from this idea.

The too large cancellation, as found in our approximation, has been overcome now by putting

$$\int_0^\infty R_{4p}\, R_{4d}\, r\, dr = 0$$

in our calculation. This simulates more or less the real situation, where we expect that the 3d eigenvector components will not be very different from ours, but the remaining part is smeared out over many nd configurations of large n, whose radial transition integrals with the 4p configuration are very much smaller than the 4p-3d one. Indeed, with this assumption the situation improves. Clearly the agreement with experiment improves as compared to earlier calculations. In table VII we give some examples of our different types of calculations.

The very large difference between length and velocity formulation for some 4p → 3d transitions reflects the above difficulty and indicates that these values may be very inaccurate. Nevertheless the agreement with experiment is encouraging. Deviations are mainly in the range 15-30% with a mean deviation of 23%.

In table VIII we present 4p' → 4s' and 4p' → 3d' transition probabilities with a $p^4(^1D)$ core state, as usually indicated by means of a prime, and we compare with values given by Wiese [17]. His marked numbers have been obtained from calculations [14]) and most of those deviate seriously from our values. This is caused by the mixing between the 4s' ^2D term with 3d ^2D which has not been explicitly taken into account in ref. 14.

TABLE VII

Some 4p → 3d transition probabilities, calculated in different ways and compared with the experimental values of ref. 15

transition	A(J,J') (s^{-1}) without C.I.	with C.I.	with C.I. but $\int R_{4p} R_{3d} r\, dr = 0$	exp. ref. 15
$3d\,^4D_{7/2} - 4p\,^4D_{7/2}$	$17.5\ 10^6$	$2.54\ 10^6$	$14.79\ 10^6$	$11.9\ 10^6$
$3d\,^4D_{5/2} - 4p\,^4D_{5/2}$	7.19	1.18	6.23	5.2
$3d\,^4F_{5/2} - 4p\,^4D_{3/2}$	17.22	3.92	15.76	14.3
$3d\,^4D_{5/2} - 4p\,^4P_{3/2}$	37.33	5.18	32.63	25.8

TABLE VIII

$3s^2 3p^4(^1D)n - 3s^2 3p^4(^1D)4p$ transitions

transition	λ(Å)	A(J,J') (s^{-1}) Wiese [17]	this work	$A_{\frac{\nabla}{\Delta}}$(J,J') ($s^{-1}$) this work
$4s'\,^2D_{5/2} - 4p'\,^2F_{7/2}$	4610	$91\ 10^6$	$74.7\ 10^6$	$65.2\ 10^6$
$3d'\,^2G_{9/2}$	6115	-	24.0	15.4
$4s'\,^2D_{5/2} - 4p'\,^2F_{5/2}$	4637	9	6.41	5.55
$4s'\,^2D_{3/2}$	4590	82	47.2	39.7
$3d'\,^2F_{5/2}$	6172	-	23.6	15.4
$4s'\,^2D_{5/2} - 4p'\,^2D_{5/2}$	4072	57	40.6	39.7
$4s'\,^2D_{3/2}$	4036	4.5	2.22	2.19
$4s'\,^2D_{5/2}$ $4p'\,^2D_{3/2}$	4080	26*	8.76	8.11
$4s'\,^2D_{3/2}$	4043	140*	13.1	16.8
$4s'\,^2D_{5/2}$ $4p'\,^2P_{3/2}$	4278	100*	78.1	55.2
$4s'\,^2D_{3/2}$	4237	21*	7.21	5.88
$4s'\,^2D_{3/2}$ $4p'\,^2P_{1/2}$	4132	140*	70.6	45.8

$4p' \rightarrow 3d$ and $4p' \rightarrow 4s$ transition probabilities are presented in table IX and compared with the renormalized values of Wiese [17]. His values were all about a factor of two lower than our theoretical values. The origine of this discrepancy is unknown.

In the vacuum-ultra violet wavelength region the emission originates from transitions to the $3s^2 3p^5$ ground state. Results for $3p^5$-$3p^4 4s$ and $3p^5$-$3p^4 3d$ transitions are listed in table X. No experimental results are available for these transitions.

Special attention has to be paid to the $sp^6\ ^2S_{\frac{1}{2}} - s^2p^5\ ^2P$ transitions for which earlier calculations [18,19] differ by factor 48 and 24 as compared to the accurate measurement of Lawrence [20].

Without inclusion of configuration interaction we calculated values which were too high by a factor of 20. However, with configuration interaction there is a large amount of cancellation between the contributions of the eigenvector components $3s^2 3p^4(^1D)3d\ ^2S_{1/2}$ and $3s^2 3p^4(^1D)4d\ ^2S_{1/2}$ at one hand and the $3s3p^6\ ^2S_{1/2}$ at the other hand, leading to a deviation of only 25% from the experimental value (see table XI). Presumably the inclusion of more p^4d configurations and perhaps some of the type $3s3p^5\ n\ell n'\ell'$ could bring theory still closer to experiment.

Finally in table XII some transitions are listed which in a one-configuration approximation would have a dipole strength equal to zero, because then two electrons have to change simultaneously their quantum numbers.

3.3. Lifetimes. The states which have been considered in this work can only decay via radiative transitions. Consequently it is an easy matter to obtain the lifetime of each excited state. The lifetime (τ_i) of a certain state i is calculated as follows:

$$\tau_i = \left(\sum_j A_{ij}\right)^{-1} \qquad (15)$$

The sum in (15) extends over all states j, which can be reached from i by radiative decay. A_{ij} stands here for the transition probability for the state i to a state j. Using the results of sec. 3.2 and applying (15) we have obtained lifetimes for all excited states, considered in this paper.

Lifetimes for $3p^4 4p$, $3p^4 3d$, $3p^4 4s$ and $3s3p^6$ states are given respectively in the tables XIII, XIV, XV and XVI. Reliable experimental

TABLE IX

$3s^2 3p^4 (^3P) n\ell - 3s^2 3p^4 (^1D) 4p$ transitions

transition	λ(Å)	A(J,J') (s^{-1})		$A_{\nabla}^{\rightarrow}$(J,J') (s^{-1})
		Wiese [17]	this work	this work
$3d\,^2D_{5/2}$-$4p'\,^2F_{7/2}$	5142	$9.5\ 10^6$	$26.9\ 10^6$	$34.1\ 10^6$
$3d\,^2F_{5/2}$	4905	4.5	8.07	8.24
$3d\,^2D_{5/2}$-$4p'\,^2F_{5/2}$	5176	-	3.23	3.56
$3d\,^2D_{3/2}$	5017	23.1	50.3	57.9
$3d\,^2F_{7/2}$-$4p'\,^2D_{5/2}$	4129	-	2.52	0.74
$3d\,^2F_{5/2}$	4301	6.1	10.4	8.31
$3d\,^2D_{5/2}$	4482	49.4	94.5	65.8
$3d\,^2D_{3/2}$	4362	5.7	10.9	8.1
$3d\,^2P_{3/2}$	3606	-	6.96	1.51
$3d\,^2D_{5/2}$-$4p'\,^2D_{3/2}$	4491	-	11.2	9.10
$3d\,^2D_{3/2}$	4371	65	118	85.2
$3d\,^2F_{5/2}$	4309	-	9.14	4.71
$3d\,^2P_{1/2}$	3491	-	7.16	1.56
$3d\,^2D_{5/2}$-$4p'\,^2P_{3/2}$	4732	-	19.6	22.9
$3d\,^2D_{3/2}$	4599	-	13.5	12.3
$3d\,^2F_{5/2}$	4531	-	4.95	4.98
$3d\,^2P_{3/2}$	3766	-	15.5	4.35
$3d\,^2P_{1/2}$	3635	-	2.21	0.60
$4s\,^2P_{1/2}$	3034	-	8.07	3.41
$4s\,^2P_{3/2}$-$4p'\,^2P_{1/2}$	2892	-	15.5	5.97
$4s\,^2P_{1/2}$	2979	-	35.1	14.4
$3d\,^2P_{3/2}$	3683	-	3.95	.88
$3d\,^2P_{1/2}$	3557	-	11.7	3.01
$3d\,^2D_{3/2}$	4475	-	62.2	58.6

TABLE X

$3s^2 3p^5 - 3s^2 3p^4 n\ell$ transitions

transition	λ(Å)	A(J,J') (s^{-1})		$A_{\pm}$(J,J') (s^{-1})
		Statz [13]	this work	this work
$3p^5\ ^2P_{3/2}$ - $4s\ ^4P_{5/2}$	744.9	-	0.015 10^8	0.017 10^8
$4s\ ^4P_{3/2}$	740.3	0.31 10^8	0.32	0.37
$4s\ ^2P_{1/2}$	718.1	9.5	8.25	8.94
$4s\ ^2P_{3/2}$	723.4	23	19.3	21.3
$4s'\ ^2D_{5/2}$	671.9	-	0.36	0.28
$4s'\ ^2D_{3/2}$	672.9	-	0.19	0.21
$3p^5\ ^2P_{1/2}$ - $4s\ ^4P_{3/2}$	748.2	0.059	0.030	0.036
$4s\ ^4P_{1/2}$	745.3	0.073	0.079	0.091
$4s\ ^2P_{3/2}$	730.9	4.5	3.15	3.54
$4s\ ^2P_{1/2}$	725.6	19	14.6	16.2
$3p^5\ ^2P_{3/2}$ - $3d\ ^4P_{5/2}$	676.3	-	0.045	0.047
$3d\ ^4F_{5/2}$	698.8	-	0.014	0.016
$3d\ ^2F_{5/2}$	666.0	-	1.41	1.35
$3d\ ^2D_{5/2}$	661.9	-	16.7	16.0
$3d\ ^2P_{3/2}$	686.5	-	0.25	0.28
$3d\ ^4P_{3/2}$	677.9	-	0.037	0.039
$3d\ ^2D_{3/2}$	664.6	-	2.62	2.53
$3d\ ^2P_{1/2}$	691.0	-	0.096	0.117
$3d\ ^4P_{1/2}$	679.2	-	0.045	0.034
$3d'\ ^2F_{5/2}$	612.4	-	0.20	0.17
$3d'\ ^2D_{5/2}$	580.3	-	159	118
$3d'\ ^2D_{3/2}$	578.6	-	44.3	32.8
$3d'\ ^2P_{3/2}$	573.4	-	162	121
$3d'\ ^2P_{1/2}$	572.0	-	76.6	56.3
$3d'\ ^2S_{1/2}$	543.2	-	157	82.6
$3p^5\ ^2P_{1/2}$ - $3d\ ^4F_{3/2}$	704.5	-	0.020	0.023
$3d\ ^2P_{1/2}$	693.3	-	0.098	0.114
$3d\ ^2D_{3/2}$	670.9	-	14.6	14.3
$3d\ ^2P_{1/2}$	697.9	-	0.29	0.32
$3d'\ ^2D_{3/2}$	583.4	-	104	77.9
$3d'\ ^2P_{3/2}$	578.1	-	48.8	36.8
$3d'\ ^2P_{1/2}$	576.7	-	132	100
$3d'\ ^2S_{1/2}$	547.5	-	87.6	47.6

results are only available for $3p^4 4p$ states [21], which have been obtained under such conditions, that the possibility of cascade has been completely ruled out. Consequently these results are believed to be fairly accurate, and for this reason they have been used as a common basis for the renormalization of many experimental as well as theoretical data, gathered and listed by Wiese et al. [17].

As table XIII shows, our values are systematically lower than those of ref. 21, by about 15%. This may be caused partly by systematic errors in our computed theoretical radial transition integrals and partly by our systematically too high 4p → 3d transition probabilities, in comparison to those of ref. 15.

No experimental data are available for lifetimes of the even parity states, with the exception of the $3s3p^6$ state [20] (see table XVI). Several among the even parity states are relatively long living, but some $3p^4(^1D)3d$ states (see table XIV) have small radiative lifetimes. This is caused by the large $3p^4(^1D)3d \rightarrow 3p^5$ transition probabilities (see table X). By the large mixing between some $3p^4(^1D)3d$ and $3p^4(^3P)3d$ states a transfer of oscillator strength takes place from the latter to the former states.

TABLE XI

$3s^2 3p^5 - 3s3p^6$ transitions

transition	λ(Å)	A(J,J') (s^{-1})		
		Lawrence [20] (exp)	this work	
			without C.I.	with C.I.
$^2P_{3/2} - {}^2S_{1/2}$	919.78	1.41 10^8	36.1 10^8	1.83 10^8
$^2P_{1/2}$	932.05	0.67	17.4	0.93

TABLE XII

$3s3p^6$ - $3s^2 3p^4 4p$ transitions

transition	λ(Å)	A(J,J')(s^{-1})	A_{∇}^{+}(J,J')(s^{-1})
$^2S_{1/2}$ - $4p'\,^2P_{3/2}$	1575	107 10^6	4.57 10^6
$4p'\,^2P_{1/2}$	1560	108	4.50
$4p\ ^2P_{3/2}$	1941	5.94	0.38
$4p\ ^2P_{1/2}$	1961	8.72	0.58
$4p'\,^2D_{3/2}$	1547	1.53	0.063
$4p\ ^2D_{3/2}$	1973	1.32	0.092
$4p\ ^2S_{1/2}$	1909	1.61	0.11

TABLE XIII

Lifetimes of $3s^2 3p^4 4p$-states

level	lifetime (ns)	
	this work	exp. [21]
$^4P_{5/2}$	5.833	
$^4P_{3/2}$	5.882	
$^4P_{1/2}$	5.888	
$^4D_{7/2}$	5.574	
$^4D_{5/2}$	6.107	7.5 ± .5
$^4D_{3/2}$	5.778	7.4 ± .2
$^4D_{1/2}$	5.654	
$^4S_{3/2}$	4.737	
$^2D_{5/2}$	8.448	9.1 ± .6
$^2D_{3/2}$	8.724	9.8 ± .2
$^2P_{3/2}$	8.036	9.4 ± .5
$^2P_{1/2}$	7.802	8.7 ± .3
$^2S_{1/2}$	7.498	8.8 ± .3
$'\,^2F_{7/2}$	7.359	
$'\,^2F_{5/2}$	7.569	
$'\,^2P_{3/2}$	3.325	
$'\,^2P_{1/2}$	3.258	
$'\,^2D_{5/2}$	5.803	
$'\,^2D_{3/2}$	5.704	

TABLE XIV

Lifetimes of $3s^2 3p^4 3d$-states

level	lifetime (ns)
$^4F_{9/2}$	metastable
$^4F_{7/2}$	metastable
$^4F_{5/2}$	$7.16\ 10^2$
$^4F_{3/2}$	$4.11\ 10^2$
$^4D_{7/2}$	metastable
$^4D_{5/2}$	$5.87\ 10^3$
$^4D_{3/2}$	$1.31\ 10^4$
$^4D_{1/2}$	$6.85\ 10^4$
$^4P_{5/2}$	$2.21\ 10^2$
$^4P_{3/2}$	$2.50\ 10^2$
$^4P_{1/2}$	$2.17\ 10^2$
$^2F_{7/2}$	metastable
$^2F_{5/2}$	7.07
$^2D_{5/2}$	$5.99\ 10^{-1}$
$^2D_{3/2}$	$5.79\ 10^{-1}$
$^2P_{3/2}$	$2.88\ 10^1$
$^2P_{1/2}$	$2.56\ 10^1$
$'^2G_{9/2}$	metastable
$'^2G_{7/2}$	metastable
$'^2F_{7/2}$	$2.82\ 10^4$
$'^2F_{5/2}$	$4.91\ 10^1$
$'^2D_{5/2}$	$6.28\ 10^{-2}$
$'^2D_{3/2}$	$6.75\ 10^{-2}$
$'^2P_{3/2}$	$4.75\ 10^{-2}$
$'^2P_{1/2}$	$4.80\ 10^{-2}$
$'^2S_{1/2}$	$4.10\ 10^{-2}$

TABLE XV

Lifetimes of $3s^2 3p^4 4s$-states	
level	lifetime (ns)
$^4P_{5/2}$	$6.71\ 10^1$
$^4P_{3/2}$	$2.87\ 10^1$
$^4P_{1/2}$	$1.19\ 10^2$
$'^2D_{5/2}$	$2.76\ 10^1$
$'^2D_{3/2}$	$5.30\ 10^1$

TABLE XVI

Lifetime of the $3s3p^6$-state in ns	
this work	Lawrence [20])
3.62	4.80 ± 0.1

4. *Discussion and conclusions.* This study of the lower configurations of Ar II by means of the multi-configuration model has brought forward several interesting aspects:

1) It has been demonstrated that the states of the $3s^2 3p^4 3d$ configuration mix strongly with states of higher $3s^2 3p^4 nd$ configurations (intrachannel interaction). This interaction induces a transfer of oscillator strength from the $3s^2 3p^4 3d$ to higher members of the same channel, which effect cannot be neglected in a calculation of transition probabilities, where this configuration is involved. In this paper we have not been able to give accurate $3s^2 3p^4 4p \rightarrow 3s^2 3p^4 3d$ transition probabilities, due to the fact that we cut off the mixing between the members of the $3s^2 3p^4 nd$ channel at n=4. More refined calculations, where one will be forced to include many $3s^2 3p^4 nd$ configurations - probably even continuum states - will be very elaborate and consume a lot of computer time.

By some artificial means we have tried to simulate the real situation for the $4p \rightarrow 3d$ transitions, and succeeded in getting results, which are closer to the experimental values than any other theoretical approach has got before.

2) An intrachannel interaction, contrary to the behaviour of the $3s^2 3p^4 nd$ channel in sub (1), is not so strongly present in the $3s^2 3p^4 np$ channel. Like the calculations with the p.p.m. have demonstrated, this difference comes from the exchange integrals in the matrix elements, which connect the configurations with each other in the Hamilton matrix. These exchange integrals are much larger within the $3s^2 3p^4 nd$ channel, than in the $3s^2 3p^4 np$ one.

3) The large discrepancy between the measured and earlier calculated (in the single-configuration treatment) lifetime of the $3s3p^6\ ^2S_{1/2}$ state has been overcome now in our multi-configuration treatment. The mixing with the $3s^2 3p^4 (^1D) nd\ ^2S_{1/2}$ states appeared to be mainly responsible.

4) The $3s^2 3p^4 4s$ configuration is only weakly perturbed by the $3s^2 3p^4 3d$ configuration (interchannel interaction). Consequently the calculated probabilities for the $3s^2 3p^4 4p \rightarrow 3s^2 3p^4 4s$ transitions did not undergo drastic changes compared with earlier calculations. So any improvement for these transitions has not been reached in this work.

5) When we put the question which configuration interaction in Ar II is strong and which one is not, we are led to the conclusion that in particular those interactions predominate, which involve a double electron transition and which, besides a swapping of excitation, also exchange one unit of angular momentum. For instance $R^{(1)}$ (3p,3p;3s,3d), $R^{(1)}$ (3p,3d;4d,3p) and $R^{(3)}$ (3p,3d;4d,3p) are the largest configuration interaction integrals, which have been met in this work. In each of these cases one electron requires $\Delta\ell = +1$ and the other $\Delta\ell = -1$. In the contrary $R^{(1)}$ (3p,4s;3d,3p) is small, because both electrons, the 3p as well as the 4s, require $\Delta\ell = +1$ at the transition. The general validity of this rule has yet to be investigated.

The accuracy of our results cannot be derived in a straightforward manner. The discrepancy between the values of length- and velocity formulation, in our method, is no absolute measure for the obtained accuracy. This follows for instance if we look at the results for some $3s^2 3p^4 4p \rightarrow 3s^2 3p^4 3d$ transition probabilities, which differ sometimes a factor of four in length- and velocity formulation. The deviation between length formulation (which should be used for a comparison with experimental values [16]) and experiment however, is in no case larger than 50%, whereas the accuracy of the experimental values is estimated on 25% [17]. The only indication, when the discrepancy between length- and velocity formulation is small, is, that the obtained accuracy will be larger than when this discrepancy is large. In this work, for instance, the $3s^2 3p^4 4p \rightarrow 3s^2 3p^4 4s$ transition probabilities have been obtained with greater accuracy than those for $3s^2 3p^4 4p \rightarrow 3s^2 3p^4 3d$. Also the $3s^2 3p^4 4p \rightarrow 3s 3p^6$ transition probability could be inaccurate because length- and velocity formulation differ by a factor of about twenty. The only way to get an insight concerning the accuracy of the theoretical results is to compare the available theoretical and experimental data.

Another qualitative criterion is the so called cancellation factor for a theoretically calculated transition probability, defined as:

$$C = \frac{|\sum_i M_i|^2}{[\sum_i |M_i|]^2} \qquad (16)$$

where M_i is the i^{th} matrix element in the sum (9). When the cancellation between the various matrix elements in (9) is large, C becomes

small. When no cancellation occurs C equals one. In the case of a small C-value, the obtained transition probability could be very inaccurate. In this work we have found for the majority of transitions $0.1 \leq C \leq 1$, but for some $3s^2 3p^4 3d \rightarrow 3s^2 3p^5$ transitions C equals 0.001.

Finally, we have made a crude accuracy estimate for each group of transitions, as indicated in table XVII. We used the following criteria:

1) the agreement between existing theoretical and experimental data, in cases where the latter ones are available;

2) a comparison of length- and velocity formulation. Large discrepancies, which systematically occur in one group of transitions, reduce the claimed accuracy of the transitions belonging to that group.

3) the cancellation factors. Within each group of transitions these factors are generally of the same order of magnitude. The highest cancellation factors have been met at the $3s^2 3p^4 3d \rightarrow 3s^2 3p^5$ transition probabilities.

When no experimental data are available for a group of transitions, the accuracy has been obtained from the criteria (2) and (3) by comparison with transitions for which experimental data do exist and where the connection between criteria (2) and (3) on one side and criterium (1) on the other side, has been empirically established.

Within each group there may occur differences in accuracy from transition to transition, especially the smaller transition probabilities could be expected to be more uncertain than the larger ones within each group.

To be safe at our estimate, the values of Table XVII might be overestimated and should be considered as upper limits of the uncertainty.

It is doubtful whether the inclusion of more and more configurations will improve the calculations, because this means in many cases a higher cancellation and consequently a reduced accuracy. It seems therefore that the calculation of transition probabilities in complex spectra by using the multi-configuration model has qua precision un upper bound.

TABLE XVII

Uncertainties for groups of transitions, considered in the tables VI until XIII.

transition	estimated uncertainty in A(J,J')
$3s^2 3p^4 4s - 3s^2 3p^4 4p$	25%
$3s^2 3p^4 3d - 3s^2 3p^4 4p$	40%
$3s^2 3p^5 - 3s^2 3p^4 4s$	30%
$3s^2 3p^5 - 3s^2 3p^4 3d$	50%
$3s^2 3p^5 - 3s 3p^6$	50%
$3s 3p^6 - 3s^2 3p^4 4p$	50%

Acknowledgements. The author is grateful to Dr. P.E. Noorman, Dr. S. Feneuille and Drs. J. Schrijver for their valuable comments and discussions.

This work is part of the research program of the Stichting voor Fundamenteel Onderzoek der Materie (Foundation for Fundamental Research on Matter) and was made possible by financial support from the Nederlandse Organisatie voor Zuiver-Wetenschappelijk Onderzoek (Netherlands Organization for the Advancement of Pure Research).

REFERENCES

1) B.M. Glennon and W.L. Wiese, "Bibliography on Atomic Transition Probabilities", National Bureau of Standards. Miscellaneous Publication 278, April (1966). Suppl. December (1967) (U.S. Government Printing Office, Washington, D.C.).

2) S. Feneuille, M. Klapisch, E. Koenig and S. Liberman, Physica 48, 571 (1970).

3) B.F.J. Luyken, Physica 51, 445 (1971).

4) B.R. Judd, "Operator Techniques in Atomic Spectroscopy", McGraw-Hill Book Comp., Inc.

5) K. Rajnak and B.G. Wybourne, Phys.Rev. 132, 280 (1963).
G. Racah and J. Stein, Phys.Rev. 156, 58 (1967).

6) S. Feneuille, J.Phys. 28, 61, 497 (1967); 30, C1-31 (1969).

7) M. Klapisch, Thesis, Paris (1969).

8) T. Yamanouchi and A. Amemiya, Proc.Phys.Soc.Jap. 1, 18 (1946); B.G. Wybourne, J.Math.Phys. 4, 3, 354 (1963).

9) E. Koenig, thesis 3^{e} cycle, Paris (1970).

10) L. Minnhagen, Arkiv Fysik 25, 203 (1963).

11) B. Kjöllerström, N.H. Möller and H. Svensson, Arkiv Fysik 29, 12, 167 (1965).

12) Principles of Atomic Spectra, B.W. Shore and D.H. Menzel, John Wiley and Sons, Inc., New York, London, Sydney (1968).

13) H. Statz, F.A. Horrigan, S.H. Koozekanani, C.L. Tang and G.F. Koster, J.Appl.Phys. 36, 2278 (1965); G.F. Koster, H. Statz and C.L. Tang, J.Appl.Phys. 39, 4045 (1968).

14) R.I. Rudko and C.L. Tang, J.Appl.Phys. 38, 4731 (1967); 39, 4046 (1968); H. Marantz, Thesis, Cornell University (1968).

15) J.B. Shumaker Jr. and C.H. Popenoe, J.Opt.Soc.Am. 59, 8, 980 (1969).

16) A.F. Starace, Phys.Rev. 3, 4, 1242 (1971).

17) W.L. Wiese, M.W. Smith and B.M. Miles, "Atomic Transition Probabilities", Vol.II, NSRDS-NBS 22, oct. (1969).

18) C.M. Varsavsky, Astrophys.J. Suppl.Ser. 6, 75 (1961).

19) P.S. Bagus, U.S. Atomic Energy Commission Report No. ANL-6959, 1964 (unpublished).

20) G.M. Lawrence, Phys.Rev. 179, 1, 134 (1969).

21) W.R. Bennet Jr., P.J. Kindlmann, G.N. Mercer and J. Sunderland, Appl.Phys. Letters 5, 8 (1964).

CHAPTER V

BRANCHING RATIOS FOR TRANSITIONS IN Ne II AND Ar II

B.F.J. Luyken, F.J. de Heer, R.Ch. Baas and H. Tawara*

FOM-Instituut voor Atoom- en Molecuulfysica, Amsterdam, Nederland

Synopsis

Branching ratios have been measured for Ne II and Ar II transitions by observing the emission of photons produced by a beam of electrons incident on Ne and Ar at pressures between 10^{-3} and 10^{-2} Torr. In this way many difficulties encountered previously by using more conventional light sources to obtain absolute transition probabilities, are avoided. Our results are compared with branching ratios from recent theoretical calculations and previous experimental work. The theoretical results for Ne II appear to be quite reliable, while those for Ar II are not yet satisfactory.

1. *Introduction.* The present experiments were started in order to check the calculations on transition probabilities in Ne II and Ar II as described in chapters III and IV. A critical judgement of these calculations by comparison with previous experimental data [1,2,3] appeared to be difficult, because sometimes large discrepancies exist between the results of different experiments. Most experimental transition probabilities have been obtained by means of emission from arc- and flame sources and shock tubes. In these experiments the following critical assumptions and factors have to be considered in order to obtain reliable absolute transition probabilities (see also Wiese [4]):

* On leave of absence from "Nuclear Engineering Department, Kyushu University, Fukuoka, Japan."
Research fellow in the cultural agreement between Japan and the Netherlands.

a) existance of local thermodynamic equilibrium;
b) self absorption;
c) demixing effects in arcs;
d) effects of boundary layers in shock tubes and inhomogeneous zones;
e) high density corrections in plasma sources;
f) intensity contributions in the line wings and the background below the lines;
g) contaminations of sputtered electrode material in arcs and shock tubes.

In our experiment we have tried to avoid the many complications, given above by confining ourselves to the determination of branching ratios and by carrying out measurements on the emission of photons produced by an electron beam shot into a gas of relatively low pressure between 10^{-3} and 10^{-2} Torr.

A branching ratio is defined as:

$$A_{ij}A_{ik}^{-1} \qquad j \neq k \tag{1}$$

where A_{ij} represents the transition probability for a transition from a level i to a level j. In doing so one avoids the difficult determination of absolute transition probabilities.

Experimental branching ratios are very useful to judge the quality of theoretical results. In chapter III and IV we showed that the calculated branching ratios appeared to be extremely sensitive to small changes in the angular wave functions. Therefore a comparison between theoretical and experimental branching ratios gives us an insight into the quality of the intermediate coupling composition of the angular wave functions, provided one uses a single-configuration model. This can be seen as follows:

Considering eqs. (2) and (5) of chapter III it is clear that in a single-configuration model the angular and radial parts of the transition matrix element can be separated. For all transitions between levels of two configurations the radial transition matrix element has the same value and consequently a branching ratio is only dependent on the angular matrix elements.

When the agreement between theoretical and experimental branching ratios is good, this does not mean that there is also a good agreement between the transition probabilities themselves, because they depend

also on the radial transition matrix elements. In order to see if the radial matrix element has the correct value one could compare theoretically and experimentally determined lifetimes, because lifetimes are sensitive to radial factors more than to angular factors. A demonstration of this statement could be found in ref. 5.

In the case of a multi-configuration model, as our Ar II calculations in chapter IV, angular and radial transition matrix elements cannot be separated and consequently branching ratios in this case are dependent on both.

In this work we have measured the $ns^2np^4ml - ns^2np^4(n+1)p$ transitions in Ne II between about 3000 and 4000 Å and in Ar II between about 3500 and 6000 Å.

2. *Experimental procedure.* The apparatus used for the production of Ne II and Ar II lines has been described in chapter II before and is generally used for the determination of cross sections for electrons fired into different target gases. In chapter II the emission of photons was studied in the vacuum ultra violet, but here we shall confine ourselves to the wavelength region of 3000 to 6000 Å. The monochromator used in this case is a half-meter Ebert type of Yarrel-Ash provided with curved slits to obtain a resolution of about 0.2 Å. The grating used in the monochromator has 1200 lines per mm and is blazed at 5000 Å. The inverse dispersion is 8.3 Å/mm at 5000 Å and the effective f value of the instrument is 8.6. In order to use the full opening angle of the monochromator with respect to the light emitted along the electron beam, an optical lense system was used. The detection of the light occurs in a DC mode by means of an E.M.I. 6256 S photomultiplier. To have an immediate check on the photon yield of the photomultiplier, a small light source is mounted in the monochromator which can be moved in front of the photocathode. This light source consists of a luminescent material (ZnS) activated by a radioactive substance ($Ra\ Cl_3$).

For the determination of a branching ratio we have to measure the fluxes of two spectral lines with the same upper level i, and with lower levels j and k. The spectral lines are produced by electrons incident on Ne or Ar. The energy, E_{el}, of these electrons is chosen in such a way, that the cross section of the level i is close to its maximum, in order to get as many photons as possible. Consequently E_{el} was taken equal to about 200 eV for Ne II and to about 90 eV for Ar II.

Electron beam currents up till 1 mA were used. The pressure of the target gas was taken between 10^{-3} and 10^{-2} Torr.

When we measure the signals S_{ij} and S_{ik} from the photomultiplier we keep the conditions for excitation of level i and for observation of the photon fluxes the same, that will say we keep the electron energy, electron current, gas pressure and monochromator slit widths constant. We only vary the wavelength by switching from the transition $i \rightarrow j$ to $i \rightarrow k$. The slit widths are the same at the entrance and at the exit of the monochromator and are chosen as wide as possible dependent on the neighbourhood of other spectral lines. The resolution used varied between 0.5 and 1.6 Å. The photon fluxes are obtained by scanning four times slowly through the profile of one spectral line, immediately followed by the same procedure for the other line. Both lines are recorded with an X-Y recorder. This procedure is repeated at least one time, dependent on the reproducibility of the results. Final results are obtained by taking the peak height of the line profile, corrected for background at the basis and averaging over all scannings. From these measurements the branching ratio can be calculated according to the next equation:

$$A_{ij}/A_{ik} = (S_{ij}/S_{ik})k(\lambda_{ik})/k(\lambda_{ij}) \qquad (2)$$

where S_{ij} and S_{ik} are the signals of the photomultiplier for the two spectral lines under consideration and $k(\lambda_{ij})$ and $k(\lambda_{ik})$ the corresponding quantum yields of the whole optical equipment, defined as the output signal per incoming photon of wavelengths λ_{ij} and λ_{ik}.

The quantum yield of the optical equipment has been determined by means of a standard tungsten bandlamp, as described in refs. 6 and 7. Because of its relatively low intensity at wavelengths shorter than 3600 Å, difficulties arise in that wavelength region due to stray light. Therefore we also carried out relative quantum yield measurements with the tungsten standard introduced by Stair et al. [8], which is better suited for the shorter wavelengths because it can be operated at higher temperatures and has relatively more intensity at shorter wavelengths. In the overlapping wavelength region the relative quantum yield obtained with the two standards agreed within about 1%. It is clear from equation (2) that only the relative quantum yield is needed for the determination of branching ratios.

Because of the anisotropy of the excitation mechanism in the beam experiment a selective occupation of the magnetic sublevels may occur, which will result in a certain amount of polarization of the emitted radiation. The polarization is connected with an anisotropy in emission of radiation; in this experiment we observe at 90^{o} with respect to the electron beam. In order to correct for possible polarization effects, the polarization function of our optical equipment was determined by means of the before mentioned light sources and a Glan Thompson prism. Further it was checked whether the relevant spectral lines were polarized. The procedure is more extensively described in ref. 7. For Ne II no polarization was found; for Ar II measurements on the polarization, which could only be carried out for the relatively strongest lines, are in progress. So far some lines appear to be polarized but the effect on our branching ratios is not larger than 5%.

3. *Results*. Branching ratios for $2s^2 2p^4 3s - 2s^2 2p^4 3p$ transitions in Ne II are given in Table 1. They are compared with the experimental results of Koopman [1]) and Hodges et al. [2]) and with the theoretical branching ratios, derived from the results of chapter III. It is clear from this table that most of our new experimental branching ratios for Ne II are in good agreement with theory, which is not always the case with the earlier experimental data of Koopman and Hodges et al..

Unfortunately we were not able to measure accurately $3d \rightarrow 3p$ transitions which also are present in the wavelength region studied here. The reason is that the excitation cross sections of the $2s^2 2p^4 3d$ levels for electron impact appeared to be an order of magnitude smaller than those of the $2s^2 2p^4 3p$ levels, resulting in too weak spectral lines.

In Table II the experimental determined branching ratios for $3s^2 3p^4 4s - 3s^2 3p^4 4p$ and $3s^2 3p^4 3d - 3s^2 3p^4 4p$ transitions in Ar II have been presented and compared with experimental results of ref. 3 and with theoretical results derived from chapter IV. Most of our measured branching ratios are in agreement with those of Shumaker [3]) but in some cases there is a rather large discrepancy with theory.

Just as in the case of Ne II, for Ar II several spectral lines could not be measured because of their weakness or because we were unable to separate them from neighbouring lines due to the finite spectral resolution of our monochromator.

TABLE I

$2s^2 2p^4 3s - 2s^2 2p^4 3p$ transitions in Ne II

lower level	upper level	λ in Å	branching ratio			
			experiment			theory
			Koopman [1]	Hodges [2]	this work	(chap. III)
$^4P_{3/2}$	$^4D_{5/2}$	3355	2.94	3.33	2.99 ± 0.15	3.12
$^4P_{5/2}$	$^4D_{5/2}$	3297				
$^4P_{3/2}$	$^4D_{3/2}$	3327	8.43	24.6	≲ 22	15.81
$^4P_{5/2}$	$^4D_{3/2}$	3270				
$^4P_{3/2}$	$^4D_{3/2}$	3327	1.27	1.39	1.06 ± 0.04	1.11
$^4P_{1/2}$	$^4D_{3/2}$	3360				
$^4P_{5/2}$	$^4P_{5/2}$	3694	3.7	2.11	3.42 ± 0.17	3.48
$^4P_{3/2}$	$^4P_{5/2}$	3766				
$^4P_{5/2}$	$^4P_{3/2}$	3664	3.09	2.26	3.69 ± 0.15	3.76
$^4P_{3/2}$	$^4P_{3/2}$	3734				
$^4P_{5/2}$	$^4P_{3/2}$	3664	1.92	1.09	1.64 ± 0.10	1.69
$^4P_{1/2}$	$^4P_{3/2}$	3777				
$^4P_{3/2}$	$^4P_{1/2}$	3709	6.51	6.71	6.41 ± 0.26	6.38
$^4P_{1/2}$	$^4P_{1/2}$	3751				
$^2P_{1/2}$	$^2D_{3/2}$	3727	4.55	3.28	3.10 ± 0.06	3.03
$^2P_{3/2}$	$^2D_{3/2}$	3643				
$^2P_{3/2}$	$^2P_{3/2}$	3323	5.0	4.7	3.56 ± 0.18	3.65
$^2P_{1/2}$	$^2P_{3/2}$	3392				
$^2P_{1/2}$	$^2P_{1/2}$	3378	5.38	4.40	5.63 ± 0.28	5.45
$^2P_{3/2}$	$^2P_{1/2}$	3309				

TABLE I (to be continued)

$2s^2 2p^4 3s - 2s^2 2p^4 3p$ transitions in Ne II						
lower level	upper level	λ in Å	branching ratio			
			experiment			theory (chap. III)
			Koopman [1]	Hodges [2]	this work	
$^2P_{3/2}$	$^2S_{1/2}$	3481	5.4	5.58	7.01 ± 0.42	7.45
$^2P_{1/2}$	$^2S_{1/2}$	3557				
$'^2D_{3/2}$	$'^2F_{5/2}$	3574.6	14.0	10.0	10.3 ± 1.03	12.6
$'^2D_{5/2}$	$'^2F_{5/2}$	3574.2				
$'^2D_{5/2}$	$'^2P_{3/2}$	3345.5	8.8	6.03	6.19 ± 0.31	6.13
$'^2D_{3/2}$	$'^2P_{3/2}$	3345.8				

TABLE II

$3s^2 3p^4 nl - 3s^2 3p^4 4p$ transitions in Ar II

lower level	upper level	λ in Å	branching ratio		
			experiment		theory
			Shumaker [3]	this work	(Chap. IV)
$3d\ ^4D_{7/2}$	$^4D_{7/2}$	4014	8.44	8.20 ± 0.25	7.95
$3d\ ^4D_{5/2}$	$^4D_{7/2}$	4039			
$4s\ ^4P_{3/2}$	$^4D_{5/2}$	4426	8.52	8.80 ± 0.60	11.7
$4s\ ^2P_{3/2}$	$^4D_{5/2}$	5145			
$4s\ ^4P_{3/2}$	$^4D_{5/2}$	4426	17.7	16.4 ± 0.60	16.3
$3d\ ^4D_{5/2}$	$^4D_{5/2}$	3968			
$4s\ ^4P_{3/2}$	$^4D_{5/2}$	4426	20.6	19.9 ± 0.9	17.8
$3d\ ^4D_{7/2}$	$^4D_{5/2}$	3944			
$4s\ ^4P_{3/2}$	$^4D_{5/2}$	4426	54.4	44.0 ± 2.7	44.7
$3d\ ^4D_{3/2}$	$^4D_{5/2}$	3992			
$4s\ ^4P_{5/2}$	$^4P_{5/2}$	4806	5.35	5.39 ± 0.17	5.38
$4s\ ^4P_{3/2}$	$^4P_{5/2}$	5009			
$4s\ ^4P_{5/2}$	$^4P_{5/2}$	4806	7.15	7.24 ± 0.36	5.79
$3d\ ^4D_{5/2}$	$^4P_{5/2}$	4431			
$4s\ ^4P_{5/2}$	$^4P_{5/2}$	4806	2.44	2.44 ± 0.07	2.01
$3d\ ^4D_{7/2}$	$^4P_{5/2}$	4401			
$4s\ ^4P_{5/2}$	$^4P_{5/2}$	4806	50.4	49.8 ± 2.5	42.2
$3d\ ^4D_{3/2}$	$^4P_{5/2}$	4461			
$4s\ ^4P_{5/2}$	$^4P_{3/2}$	4736	4.11	4.05 ± 0.06	4.18
$4s\ ^4P_{3/2}$	$^4P_{3/2}$	4933			

TABLE II (to be continued)

$3s^2 3p^4 nl - 3s^2 3p^4 4p$ transitions in Ar II

lower level	upper level	λ in Å	branching ratio		
			experiment		theory
			Shumaker [3]	this work	(chap.IV)
$4s\ ^4P_{5/2}$	$^4P_{3/2}$	4736	2.65	2.71 ± 0.03	2.73
$4s\ ^4P_{1/2}$	$^4P_{3/2}$	5062			
$4s\ ^4P_{5/2}$	$^4P_{3/2}$	4735	3.57	3.62 ± 0.2	2.97
$3d\ ^4D_{3/2}$	$^4P_{3/2}$	4400			
$4s\ ^4P_{5/2}$	$^4P_{3/2}$	4736	18.0	17.0 ± 0.9	16.3
$3d\ ^4D_{1/2}$	$^4P_{3/2}$	4421			
$4s\ ^4P_{3/2}$	$^4P_{1/2}$	4848	8.79	8.8 ± 0.3	8.46
$4s\ ^4P_{1/2}$	$^4P_{1/2}$	4972			
$4s\ ^4P_{3/2}$	$^4P_{1/2}$	4848	3.72	3.76 ± 0.02	2.95
$3d\ ^4D_{1/2}$	$^4P_{1/2}$	4352			
$4s\ ^4P_{1/2}$	$^4D_{3/2}$	4430	0.94	1.03 ± 0.05	1.02
$4s\ ^4P_{3/2}$	$^4D_{3/2}$	4331			
$4s\ ^4P_{1/2}$	$^4D_{3/2}$	4430	7.28	6.93 ± 0.3	7.06
$3d\ ^4D_{5/2}$	$^4D_{3/2}$	3892			
$4s\ ^4P_{1/2}$	$^4D_{3/2}$	4430	26.8	27.3 ± 1.3	24.5
$3d\ ^4D_{1/2}$	$^4D_{3/2}$	3931			
$4s\ ^4P_{1/2}$	$^4D_{1/2}$	4380	8.65	8.48 ± 0.15	7.76
$4s\ ^4P_{3/2}$	$^4D_{1/2}$	4283			
$4s\ ^4P_{1/2}$	$^4D_{1/2}$	4380	14.4	14.0 ± 0.2	11.3
$3d\ ^4D_{3/2}$	$^4D_{1/2}$	3875			

TABLE II (to be continued)

$3s^2 3p^4 nl - 3s^2 3p^4 4p$ transitions in Ar II

lower level	upper level	λ in Å	branching ratio: experiment: Shumaker [3]	branching ratio: experiment: this work	branching ratio: theory (chap. IV)
$4s\ ^4P_{5/2}$	$^4S_{3/2}$	3729	1.25	1.20 ± 0.01	1.19
$4s\ ^4P_{3/2}$	$^4S_{3/2}$	3851			
$4s\ ^4P_{5/2}$	$^4S_{3/2}$	3729	2.00	1.85 ± 0.03	1.94
$4s\ ^4P_{1/2}$	$^4S_{3/2}$	3929			
$4s\ ^2P_{3/2}$	$^2D_{5/2}$	4880	29.0	24.3 ± 1.8	26.4
$4s\ ^4P_{5/2}$	$^2D_{5/2}$	4082			
$4s\ ^2P_{3/2}$	$^2D_{5/2}$	4880	6.04	6.49 ± 0.60	7.15
$4s\ ^4P_{3/2}$	$^2D_{5/2}$	4228			
$4s\ ^2P_{3/2}$	$^2D_{3/2}$	4727	1.45	1.50 ± 0.04	1.88
$4s\ ^2P_{1/2}$	$^2D_{3/2}$	4965			
$4s\ ^2P_{3/2}$	$^2D_{3/2}$	4727	31.1	18.0 ± 0.9	23.2
$4s\ ^4P_{1/2}$	$^2D_{3/2}$	4202			
$4s\ ^2P_{3/2}$	$^2D_{3/2}$	4727	61.5	56.8 ± 2.8	60.5
$4s\ ^4P_{3/2}$	$^2D_{3/2}$	4113			
$4s\ ^2P_{1/2}$	$^2P_{3/2}$	4765	1.39	1.32 ± 0.03	1.58
$4s\ ^2P_{3/2}$	$^2P_{3/2}$	4545			
$4s\ ^2P_{3/2}$	$^2P_{1/2}$	4658	5.06	4.82 ± 0.06	4.30
$4s\ ^2P_{1/2}$	$^2P_{1/2}$	4889			
$4s\ ^2P_{1/2}$	$^2S_{1/2}$	4579	4.07	3.97 ± 0.17	3.26
$4s\ ^2P_{3/2}$	$^2S_{1/2}$	4376			

TABLE II (to be continued)

$3s^2 3p^4 nl - 3s^2 3p^4 4p$ transitions in Ar II

lower level	upper level	λ in Å	branching ratio		
			experiment		theory
			Shumaker [3]	this work	(chap. IV)
$4s'\ ^2D_{3/2}$ -	$'^2F_{5/2}$	4590	--	9.17 ± 0.04	7.37
$4s'\ ^2D_{5/2}$ -	$'^2F_{5/2}$	4637			
$4s'\ ^2D_{5/2}$ -	$'^2P_{3/2}$	4278	--	7.35 ± 0.1	10.8
$4s'\ ^2D_{3/2}$ -	$'^2P_{3/2}$	4237			

4. *Error discussion.* The systematic errors in our branching ratios are mainly determined by the accuracy of our relative quantum yield determination. Because of the good agreement of the data with two different standards we estimate the accuracy of the relative quantum yield better than 2% (for some error considerations see also ref. 9). The random root mean square error follows from the reproducibility of the measurements and is indicated with our results. It varies between 1 and 10% and is the smallest for the relatively strongest lines. An additional error might arise for some transitions due to polarization, but is probably smaller than 5%.

5. *Discussion.* The above results indicate that our calculations for Ne II are in most cases in good agreement with experiment. Considering the difference between experimental and theoretical lifetimes as shown in chapter III, Table VIII and taking into account the apparent successful determination of the angular wavefunction for Ne II, this difference can only be due to either the inaccuracy of the theoretical radial matrix element or to the inaccuracy of the lifetime experiments.

From Table II it is clear that the calculations for Ar II transitions described in chapter IV are less accurate than the corresponding Ne II calculations. This because the measured branching ratios in most cases agree with those of Shumaker [3], and therefore must be considered as reliable. Consequently the general conclusions at the end of chapter IV are confirmed by these measurements. Due to the fact that the Ar II calculations have been done in the multi-configuration approximation, it is impossible to decide whether the inaccuracy comes from the radial or from the angular parts of the wave functions.

ACKNOWLEDGEMENTS

This work is part of the research program of the Stichting voor Fundamenteel Onderzoek der Materie (Foundation for Fundamental Research on Matter) and was made possible by financial support from the Nederlandse Organisatie voor Zuiver-Wetenschappelijk Onderzoek (Netherlands Organization for the Advancement of Pure Research).

REFERENCES

[1]) Koopman, D.W., J.Opt.Soc.Amer. 54 (1964) 1354.

[2]) Hodges, D., Marantz, H. and Tang, C.L., J.Opt.Soc.Amer. 60 (1970) 192.

[3]) Shumaker Jr., J.B. and Popenoe, C.H., J.Opt.Soc.Amer. 59, 8 (1969) 980.

[4]) Wiese, W.L., Smith, M.W. and Miles, B.M., "Atomic Transition Probabilities" Vol.II, NSRDS-NBS 22, oct.(1969).

[5]) Aymar, M., Feneuille, S. and Klapisch, M., Proceedings of the second international conference on Beam-Foil Spectroscopy, North-Holland Publishing Company - Amsterdam (1970), 137.

[6]) van Eck, J., de Heer, F.J. and Kistemaker, J., Physica 30 (1964) 1171.

[7]) van den Bos, J,, Winter, G.J. and de Heer, F.J., Physica 40 (1968) 357.

[8]) Stair, R., Schneider, W.E. and Jackson, J.K., Applied Optics 1963, vol. 2, no.11, 1151.

[9]) van den Bos, J., Thesis 1968, University of Amsterdam.

SUMMARY

In this thesis some investigations are described in the field of electron-atom collisions, leading to excited ions.

In chapter II an experiment is described, where electrons are shot into a target gas, consisting of Ne, Ar, Kr or Xe. The formation of the $nsnp^6\ ^2S_{\frac{1}{2}}$ state is studied by observing the decay to the ionic ground state $ns^2np^5\ ^2P$, which results in vacuum ultraviolet radiation. Cross sections are given for impact energies between threshold and 20 keV. Above 2 keV a Bethe behaviour of the energy dependent cross section is found. For Ne and Ar a comparison has been made between experimental and theoretical $M^2(ns)$-values. It is shown that for both gases there is agreement, however, in Ar only provided configuration interaction is taken into account with regards to the $nsnp^6$-configuration.

In chapter III and IV a theoretical study is described, where wave functions for the states of the lower configurations in Ne II and Ar II are calculated. With different methods the angular as well as the radial parts of the wave functions are found, taking into account configuration interaction. With these wave functions transition probabilities and lifetimes are calculated and the results are compared with earlier experimental and theoretical work.

Because in many cases the existing experimental transition probabilities are so far in disagreement with each other, that a useful test of the reliability of our calculations, described in chapter III and IV, was impossible, an experiment has been carried out, as described in chapter V, where measured branching ratios for the spectral-line intensities in Ne II and Ar II are given. It turns out that for Ne II the agreement between experimental and theoretical branching ratios is quite good, whereas for Ar II the need for an extension of the setup of the theoretical approach is demonstrated.

SAMENVATTING

In dit proefschrift worden enige onderzoekingen op het gebied van electron-atom botsingen, welke tot aangeslagen ionen leiden, beschreven.

In hoofdstuk II wordt een experiment beschreven waarbij electronen op een doelwit gas, bestaand uit Ne, Ar, Kr of Xe, worden geschoten. De aanslag van het $nsnp^6\ ^2S_{\frac{1}{2}}$ niveau wordt bestudeerd, door het verval naar de grondtoestand van het ion waar te nemen. Dit verval geeft aanleiding tot vacuüm ultraviolette straling. Werkzame doorsneden worden gegeven voor botsingsenergieën vanaf de drempel tot 20 keV. Voor energieën groter dan 2 keV wordt een Bethe-afhankelijkheid van de werkzame doorsnede als functie van de botsingsenergie gevonden. Voor Ne en Ar is een vergelijking gemaakt tussen experimentele en theoretische waarden van $M^2(ns)$. Er wordt aangetoond dat er voor beide gassen overeenstemming tussen theorie en experiment bestaat; voor Ar is er echter alleen overeenstemming wanneer configuratie interactie ten opzichte van de $nsnp^6$-configuratie in rekening wordt gebracht.

In hoofdstuk III en IV wordt een theoretische studie beschreven. Hier worden golffuncties voor de toestanden van de lagere configuraties in Ne II en Ar II berekend. Met verschillende methoden worden het hoekafhankelijke- en het radiële deel van de golffuncties gevonden, waarbij configuratie interactie in rekening wordt gebracht. Met behulp van deze golffuncties worden overgangswaarschijnlijkheden en levensduren berekend. De resultaten worden vergeleken met vroeger experimenteel en theoretisch werk.

Omdat in vele gevallen de vroeger langs experimentele weg gevonden overgangswaarschijnlijkheden van de diverse auteurs dermate veel verschillen dat het geen bruikbaar materiaal is om de betrouwbaarheid van onze berekeningen uit hoofdstuk III en IV te testen, is er een experiment gedaan, beschreven in hoofdstuk V, waarmee vertakkingsverhoudingen voor intensiteiten van spectraallijnen in Ne II en Ar II gevonden zijn. Er blijkt voor Ne II een goede overeenstemming tussen experimentele en theoretische vertakkingsverhoudingen te bestaan. In het geval van Ar II wordt aangetoond dat de opzet van de theoretische benadering verbreed dient te worden.

Volgens het gebruik in de Faculteit der Wiskunde en Natuurwetenschappen volgt hier een kort overzicht van mijn academische studie.

Na het behalen van het einddiploma Gymnasium-B aan het Coornhert Lyceum te Haarlem begon ik in september 1962 met de studie in de natuurkunde aan de Rijksuniversiteit te Leiden. Het candidaatsexamen, letter a', werd afgelegd in maart 1966, waarna de studie in de experimentele natuurkunde werd voortgezet.

In september 1966 ben ik in dienst getreden van het F.O.M.-Instituut voor Atoom- en Molecuulfysica te Amsterdam, onder leiding van Professor Dr. J. Kistemaker. Van meet af aan heb ik daarbij deel uitgemaakt van de groep Atomaire botsingen, welke onder leiding staat van Dr. F.J. de Heer. Het onderzoek dat ik daar verrichtte, betrof de ion-atoom botsingen en wel in het bijzonder de vangst van een electron door He^+ in een aangeslagen toestand. De daarbij optredende zichtbare en vacuüm-ultraviolette straling werd bestudeerd met behulp van monochromatoren. Later werd een onderzoek gedaan naar de mogelijkheden het quantum rendement van een vacuüm-ultraviolet monochromator te bepalen. In februari 1969 werd het doctoraalexamen met als bijvak klassieke mechanica afgelegd. Het aanvankelijke dienstverband als wetenschappelijk assistent werd toen veranderd in dat van wetenschappelijk medewerker. Het onderzoek werd voortgezet met de bestudering van aanslag der edelgassen door electronen. Daarbij bleek enige theoretische kennis onontbeerlijk. Uiteindelijk leidde dit werk tot dit proefschrift, waarin naast een tweetal hoofdstukken over experimentele onderwerpen ook een tweetal hoofdstukken met theoretisch werk vervat zijn.

Vanaf september 1971 ben ik in dienst van de Gemeente Haarlem als milieuconsulent, met als taak het coördineren en integreren van het beleid en de maatregelen ten aanzien van het milieubeheer.

De vijf jaren op het F.O.M.-Instituut voor Atoom- en Molecuulfysica zijn voor mij een voortreffelijke leerschool geweest en niet alleen op fysisch-technisch gebied. Met grote voldoening en dankbaarheid denk ik terug aan deze tijd. Professor Dr. J. Kistemaker dank ik voor de mij geboden gelegenheid op zijn Instituut te mogen leren en werken. De stimulerende bereidwilligheid van Dr. F.J. de Heer om te luisteren naar moeilijkheden, de helpende hand te bieden waar dat nodig was, en zijn nooit aflatende belangstelling heb ik steeds op hoge prijs gesteld. Zijn steun tijdens het werk en zijn steeds positieve kritiek zijn

onmisbaar geweest bij het tot stand komen van dit proefschrift. Dr. P.E. Noorman dank ik voor zijn bereidwilligheid dit werk kritisch te bezien en als co-referent op te treden. Drs. J. Schrijver ben ik zeer erkentelijk voor zijn geduld om een onwennige nieuwkomer op het gebied van de theoretische atoomfysica enige houvast te verschaffen. Het beschikbaar stellen van zijn versie van het computerprogramma "Mappac" heb ik hogelijk gewaardeerd. Bij de metingen ben ik op waardevolle wijze bijgestaan door Dr. H. Tawara en de heren R.Ch. Baas, H.J. Luyken, J.J. van Zeeland en J. Corsel. De gruwel van het schrijven en ponsen van computerprogramma's is mij op zeer aangename wijze verlicht voor de vakkennis en het geduld van de heren F. Vitalis en W. van der Kaay. Tenslotte dank ik de heren F. Monterie en Th. van Dijk voor het fotografisch werk en mevrouw C.J. Köke-van der Veer voor het typen van het manuscript.